

# A Comprehensive Examination of Heat Transfer Correlations Suitable for Reactor Safety Analysis

D. C. Groeneveld and C. W. Snoek  
Atomic Energy of Canada Ltd.,  
Chalk River Nuclear Laboratories, Chalk River,  
Ontario, Canada

## 1 INTRODUCTION

Fuel sheath temperatures in water-cooled nuclear reactors are usually near the saturation temperature of water. However, during an accidental increase in power, or a decrease in flow and pressure, deterioration in heat transfer is possible. It occurs when the surface temperature increases to such a high level that the heated surface can no longer support continuous liquid contact. This phenomenon is usually referred to as the boiling crisis (or dryout) and the corresponding heat flux as the critical heat flux (or CHF). The boiling crisis is characterized by either a sudden rise in surface temperature, caused by the heated surface being covered by a stable vapor film (film boiling), or by small surface temperature spikes, corresponding to the appearance and disappearance of dry patches (transition boiling).

Due to the vapor's poor heat transport properties, high heated-surface temperatures are often encountered in the post-CHF or post-dryout region. Although nuclear reactors normally operate under conditions where dryout does not occur, accidents can be postulated where dryout occurrence is possible. The most serious of the postulated accidents is thought to be the loss-of-coolant accident (LOCA), caused by a rupture in the primary coolant system. Accurate prediction of the consequences of a LOCA requires precise calculation of fuel-coolant heat transfer during (i) the blowdown phase (when the fuel channel is voided) and (ii) the subsequent emergency-core-cooling (ECC) phase. A variety of prediction methods are currently used in accident analysis.

Heat transfer modes encountered during a LOCA, or any other incident where the fuel dries out, depend on the fuel sheath temperature. The boiling curve (Fig. 1) illustrates this departure for a given set of flow conditions. (Note that the shape of the boiling curve during flow boiling is similar but not identical to the pool boiling curve.) The flow conditions will change along the length of a heated channel, especially the fluid enthalpy. The resulting change in heat transfer mode is illustrated in Fig. 2.

A variety of heat transfer correlations have been recommended in the literature for each heat transfer mode. The choice of correlation frequently depends on the geometry of the heat transfer

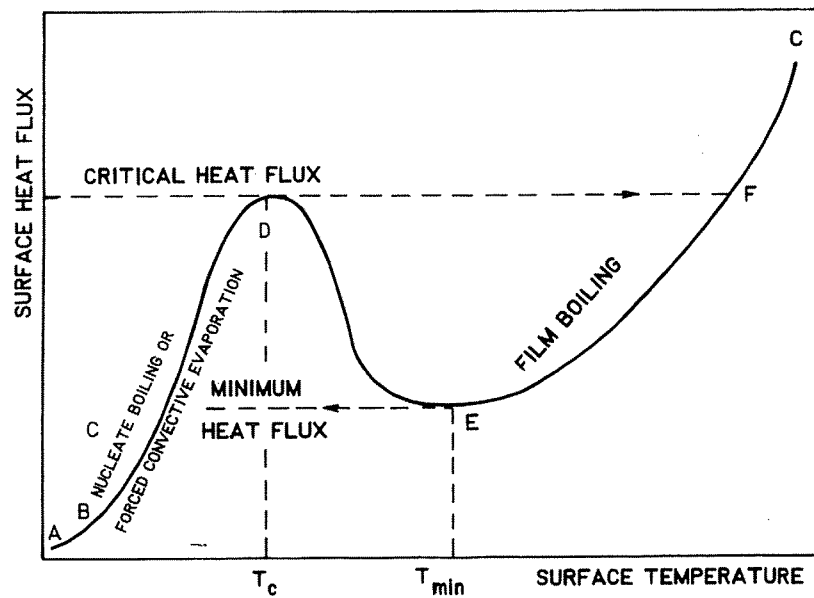


Fig. 1. Boiling curve.

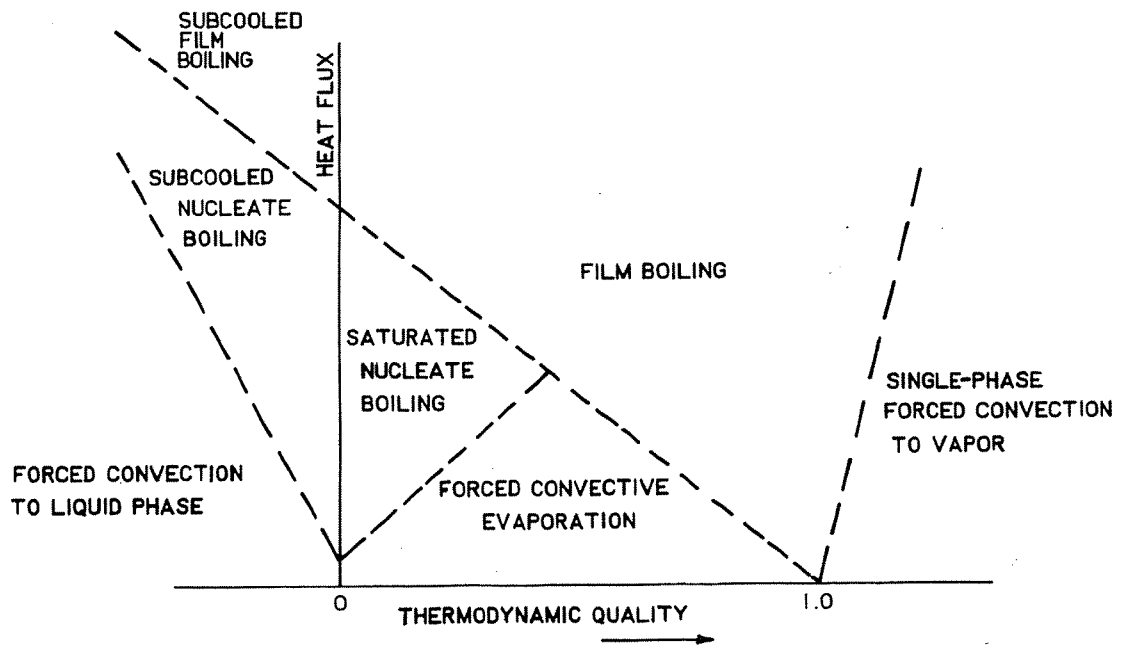


Fig. 2. Map of forced convective heat transfer modes. Collier (1980).

surface, the orientation of the surface, the direction of the flow velocity vector, and the local phase distribution. Common heat transfer configurations encountered in the in- and out-reactor components are shown in Fig. 3.

Due to the inadequate understanding of heat transfer mechanisms, an empirical approach is often necessary. This approach requires the derivation of empirical heat transfer correlations for

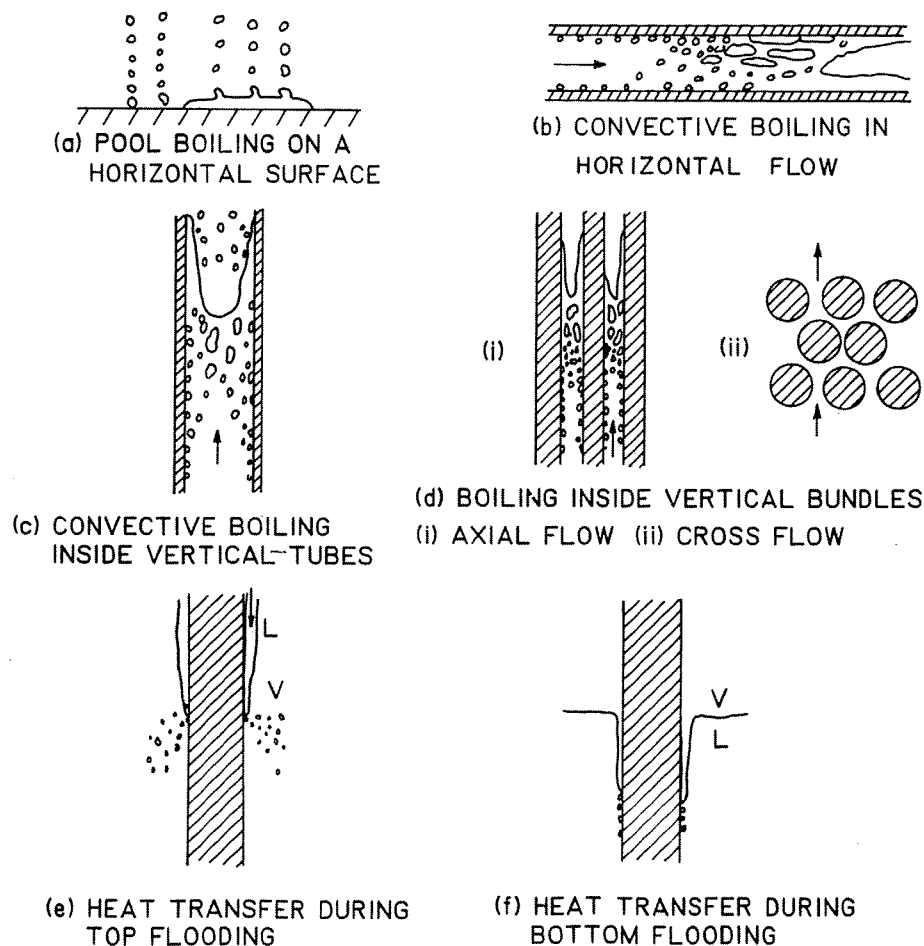


Fig. 3. Heat transfer configurations.

each heat transfer configuration, resulting in numerous correlations for each heat transfer mode. A simplification that is frequently used is to combine these heat transfer correlations (for one heat transfer mode) using some suitably defined local parameters (e.g.,  $X$ ,  $D_{hy}$ ,  $\alpha$ ) to characterize the heat transfer process. These local condition correlations, usually encountered in reactor safety codes, will be discussed in this chapter.

The prediction methods considered here include analytical models such as those currently used in modern reactor safety codes as well as frequently used empirical correlations. The correlations were examined with respect to (1) their applicability to the primary- and secondary-side heat transfer in in- and out-reactor components, (2) their parametric trends, (3) possible discontinuities or irregularities, and (4) behavior outside their recommended range. Other heat transfer evaluation methods such as the table look-up technique and graphical methods have also been considered.

Most heat transfer and fluid flow correlations are based on tube data, since the simplest test geometry is a heated tube. Extrapolation of tube correlations to other geometries (bundles, annuli) is common practice in reactor safety analysis, as is extrapolation outside the range of test conditions of the tube data

base. However, there is often no justification for these extrapolations. Improvements in the prediction accuracy may be made using suitably derived extrapolation factors. In this chapter, parametric and asymptotic trends of the data are discussed, and various correction factors used to extend the range of present correlations are examined.

## 2 SINGLE-PHASE HEAT TRANSFER

### 2.1 Introduction

In current power reactor systems a common mode of energy exchange between fuel and coolant is single-phase heat transfer, e.g., water-cooled reactors, upstream from the point of onset of nucleate boiling, and gas-cooled reactors. The heat transfer in nuclear steam generators and preheaters is also due primarily to single-phase heat transfer (except for the boiling and condensing regions). The prediction of the single-phase heat transfer coefficient was significantly improved when Dittus and Boelter (1930) published the now famous Dittus-Boelter correlation. In reactor safety analysis the availability of accurate single-phase correlations is imperative, especially downstream from a rewetting front where the fuel cooling may be due primarily to superheated steam.

### 2.2 Subcooled Water Heat Transfer

Commonly used correlations for single-phase liquid and vapor heat transfer are listed in Table 1. Most of the correlations have the same basic form as the original Dittus-Boelter correlation, which has been proven valid for many liquids and gases. Colburn's (1933) correlation differs from the Dittus-Boelter correlation only by the exponent of the Prandtl number, while Sieder and Tate (1936) included the influence of the thermal boundary layer. More recently, Nixon (unpublished Chalk River Nuclear Laboratories Report) derived a single-phase heat transfer correlation based on water data from many different sources. This correlation is recommended for use within the range of its data base ( $Re: 10,000-327,000$ ;  $Pr: 1.9-10.5$ ).

For free convective conditions, the theoretical relationship by Rohsenow and Choi (1961) or the empirical correlation of Collier (1980) is recommended.

### 2.3 Superheated Steam Heat Transfer

During certain accident conditions the coolant in the core or the steam generator (primary side) can be superheated steam. If the steam does not contain entrained droplets, most of the correlations of Table 1 will be applicable. Some of the correlations are derived specifically for gases where the temperature difference between wall and fluid may be significant and where the effect must be included. For low wall superheats the correlations derived for liquids may also be used. In safety analysis the heated surface temperature is usually the unknown quantity; hence, the correlations often require an iterative procedure.

The correlations of Heineman (1960), Bishop et al. (1964), and Hadaller and Banerjee (1969) were specifically derived for

Table 1. Correlations for Subcooled Water and Superheated Steam in Tubes<sup>a</sup>

References	Correlation	Comments
Dittus and Boelter (1930)	$Nu_b = 0.023 (Re_b)^{0.8} (Pr_b)^{0.4}$	Circular geometry, $Re > 10,000, L/D > 50$
Colburn (1933)	$Nu_b = 0.023 (Re_b)^{0.8} (Pr_b)^{1/3}$	Similar to Dittus-Boelter (1930)
Sieder and Tate (1936)	$Nu_b = 0.027 Re_b^{0.8} Pr_b^{1/3} (\mu_b/\mu_w)^{0.14}$	Valid for many fluids
Heineman (1960)	$Nu_f = 0.0157 Re_f^{0.84} Pr_f^{1/3} (D/L)^{0.04}$ (for $L/D > 60$ , $Nu_f = 0.0133 Re_f^{0.84} Pr_f^{1/3}$ )	$\left\{ \begin{array}{l} 20,000 < Re < 370,000 \\ 2 < P < 10 \text{ MPa} \end{array} \right.$ Steam only
Rohsenow and Choi (1961)	$Nu_b = 4.36 + \frac{0.036 Re_b Pr_b^{D/L}}{1 + 0.0011 Re_b Pr_b^{D/L}}$	Laminar flow in vertical tubes, $q = \text{const}$ ; developing velocity and temperature distribution
Bishop et al. (1964)	$Nu_f = 0.0073 Re_f^{0.886} Pr_f^{0.61} \left( 1 + \frac{2.76}{L/D} \right)$	High-pressure steam only
Kutateladze and Borishanskii (1966)	$Nu_b = 0.027 Re_b^{0.8} Pr_b^{0.4} \left( \frac{T_b}{T_w} \right)^{0.55}$	$1 < T_w^*/T_b^* < 3.5$ , valid for gases, $T^*$ in K
Nixon (unpublished Chalk River Nuclear Laboratories Report)	$Nu_f = 0.024 Re_f^{0.77} Pr_f^{0.057}$	$10,000 < Re < 327,000$ $1.9 < Pr < 10.5$ Based only on water data
Hadaller and Banerjee (1969)	(i) $Nu_f = 0.0101 Re_f^{0.8774} Pr_f^{0.6112} \left( \frac{D}{L} \right)^{0.0328}$ (ii) $Nu_f = 0.0170 Re_f^{0.8216} Pr_f^{0.625} (1 + 0.9842 \frac{D}{L})$	$\left\{ \begin{array}{l} 6.10^4 < Re < 6.10^5 \\ 295 < T_f < 580^\circ\text{C} \\ 2 < P < 21.4 \text{ MPa} \end{array} \right.$ Steam only
Collier (1980)	$Nu_b = 0.17 Re_b^{0.33} Pr_b^{0.43} \left( \frac{Pr_b}{Pr_w} \right)^{0.25} Gr_{Dhy}^{0.1}$	$Re < 2000, L/D > 50$ Heating in upflow; cooling in downflow

<sup>a</sup>For definition and units of all symbols, see Nomenclature.

superheated steam; they also include an  $L/D$  term to account for entrance effects. Hadaller and Banerjee's (1969) correlation has the widest range of application and is tentatively recommended within its data base range. Outside this range, Kutateladze and Borishanskii's (1966) correlation may be preferable.

## 2.4 Bundle Geometry

The correlations of Table 1 are all based on experiments inside tubular geometries. To characterize nontubular geometries, both heated and hydraulic equivalent diameters ( $D_{he}$  and  $D_{hy}$ ) have been used in the Nusselt number. Groeneveld (1973) concluded that the  $D_{hy}$  was preferable since it resulted in less scatter in the data.

To predict the heat transfer coefficients in a bundle from tube correlations (or data), Groeneveld (1973) recommended two correction factors

$$I \triangleq \frac{h_{\text{bundle,avg}}}{h_{\text{tube}}} \quad J \triangleq \frac{h_{\text{bundle,min}}}{h_{\text{bundle,avg}}}$$

where  $h_{\text{bundle,min}}$  is the minimum value of  $h_{\text{bundle}}$  encountered around the heated perimeter, and  $h_{\text{tube}}$  is evaluated from Halaller and Banerjee's correlation (1969) for the same bundle-cross-section average conditions and  $D_{hy}$ . Graphical representations of  $I$  and  $J$  are given in Figs. 4 and 5. Note that both factors become sensitive to the rod spacing at low  $p/d$  values. In addition, the higher degree of turbulence at higher  $Re$  appears to reduce the nonuniformity in surface temperatures (i.e.,  $J$  values closer to unity).

Tong and Weisman (1979) suggested that the constant 0.023 in the Dittus-Boelter equation is too general for rod bundles and recommended the following constants:

- for triangular-pitch lattice:  $C = 0.026 \, p/d - 0.006$
- for square-pitch lattice:  $C = 0.042 \, p/d - 0.024$

Variations in  $h$  around the circumference were found to be negligible for  $p/d > 1.2$ .

## 2.5 Entrance and Spacer Effects

A change in upstream geometry can have a strong effect on the local heat transfer coefficient, especially if the change in configuration is located less than 20 diameters upstream. McAdams (1954) suggested a development factor  $k_d$  that accounts for the entrance region effect

$$k_d \triangleq \frac{Nu_{\text{entrance}}}{Nu_{\infty}} = 1 + a \, Re^b \left( \frac{L}{D_{hy}} \right)^c$$

The coefficients  $a$ ,  $b$ , and  $c$  depend on the wall boundary conditions (e.g., constant heat flux or temperature) as well as on upstream conditions (developing thermal boundary layer and/or

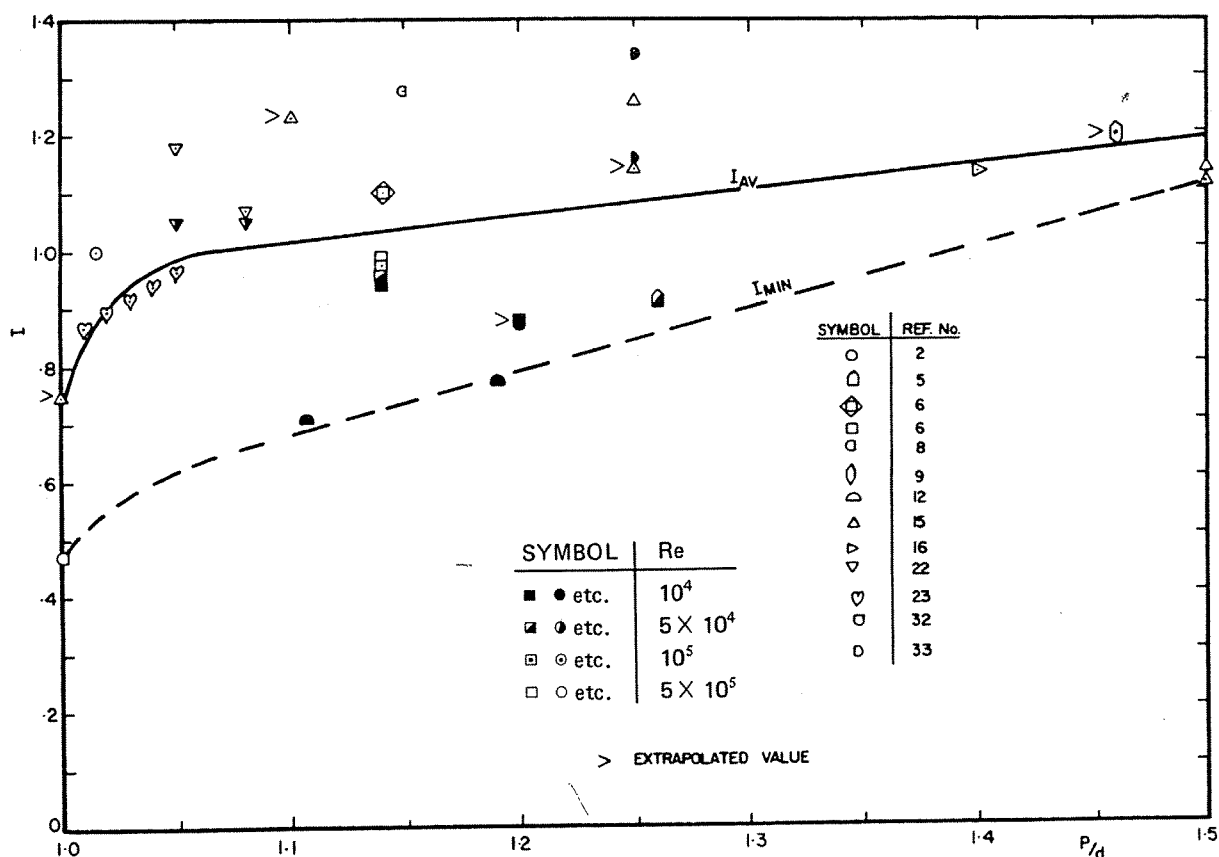


Fig. 4. Effect of pitch/diameter ratio on dimensionless bundle heat transfer. Coefficient  $I$  (based on hydraulic equivalent diameter). For reference numbers, see Groeneveld (1973).

hydrodynamic layer; shape of upstream flow area change). Table 1 contains several forms of the entrance effect.

The effect of spacing devices on heat transfer depends also on the radial location of the spacing device with respect to the heated surface. At locations where the spacing device is in contact with the heated surface, boundary-layer separation usually takes place. This results in a significant increase in downstream heat transfer felt over a considerable length [ $L/De > 30$ ; Koram and Sparrow (1978)]. Krall and Sparrow (1966) have shown that the increase in heat transfer due to flow separation and reattachment is much greater than that associated with a thermal entrance region and is felt over a much longer distance downstream. At locations around the rod periphery where no spacer-rod contact exists, the increase in heat transfer is small (Koram and Sparrow, 1978); this increase will probably depend on the shape of the leading and trailing edge and on the fraction of the flow area being blocked.

Spacers may cause considerable flow disturbances, depending on how much they block the flow. Kidd et al. (1968) reported that, in general, bundle-spacing devices do not cause much subchannel mixing but improve the local heat transfer by tripping the boundary layer, thus starting a new entry length; similar observations were

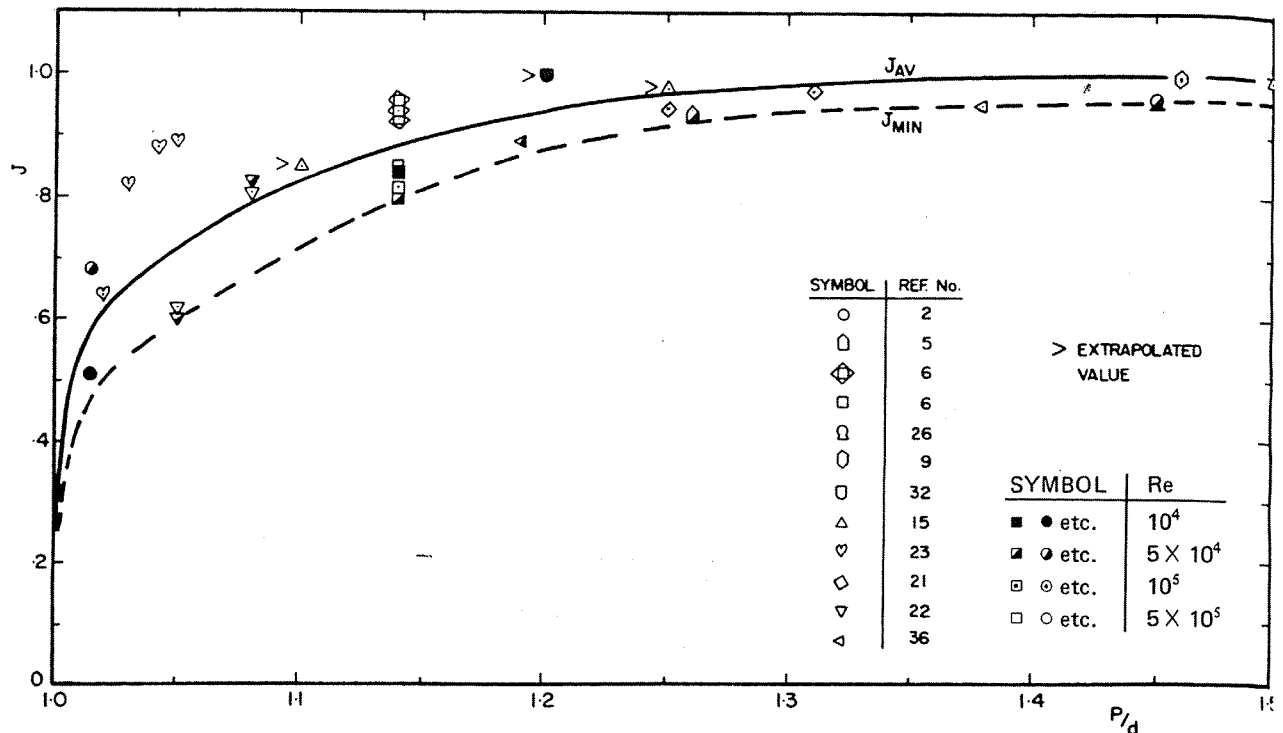


Fig. 5. Effect of pitch/diameter ratio on reduced minimum heat transfer. Coefficient  $J$  ( $= h_{\min}/h_{\text{avg}}$ ). For reference numbers, see Groeneveld (1973).

made by Gasc (1966) and Hoffman (1970). Yao et al. (1982), after examining the effect of spacers on the downstream heat transfer in tubes and bundles, recommended the following spacer correction factor:

$$\frac{\text{Nu}_{Ld}}{\text{Nu}_{\text{ref}}} = 1 + 5.55 \epsilon^2 \exp \left( -0.13 \frac{L_d}{D_e} \right)$$

In the spacer region the equation reduces to  $1 + 5.55 \epsilon^2$  and should be used as such over the length of the spacer.

### 3 NUCLEATE BOILING AND CONVECTIVE EVAPORATION

#### 3.1 Introduction

The transition from single-phase liquid heat transfer to nucleate boiling takes place once the wall temperature exceeds the  $T_{\text{ONB}}$ . The  $T_{\text{ONB}}$  can be predicted by many correlations (e.g., Collier, 1980; Tong, 1965; Ginoux, 1978). The same references also contain correlations for partial nucleate boiling, an intermediate heat transfer mode where both single-phase heat transfer and nucleate boiling are important. In general, however, little accuracy is lost by replacing correlations for the ONB and for partial nucleate boiling by the simple condition

$$h = \max(h_{\ell}, h_{\text{NB}}) \quad \text{for } T_w > T_{\text{sat}}$$



where both  $h_\ell$  and  $h_{NB}$  must be based on  $T_w - T_\ell$ .

In the saturated boiling region, at high void fractions, the flow regime may be annular, characterized by a high vapor core velocity and a turbulent liquid film. A highly turbulent liquid film will result in a suppression of the nucleate boiling mechanism, and the heat transfer will take place by evaporation at the liquid-vapor interface. This heat transfer mode is usually referred to as forced convective evaporation.

### 3.2 Prediction Methods

The prediction methods are summarized in Table 2. They may be subdivided into two groups: Nucleate boiling only and saturated boiling.

#### 3.2.1 Nucleate Boiling Only

Correlations for nucleate boiling frequently have the general form  $q_{NB} = a \Delta T_s^b f(P)$ , the most popular being those of Thom et al. (1966) and Jens and Lottes (1951). Note that these correlations, although valid for subcooled as well as saturated nucleate boiling, are all based on  $T_w - T_{sat}$  instead of on  $T_w - T_\ell$ .

Guglielmini et al. (1978, 1980) surveyed the relevant correlations for nucleate boiling heat transfer in forced convective flow. They found that most partial nucleate boiling and fully developed nucleate boiling correlations had a limited range of application. After testing the correlations in five pressure regimes, from 0.1 to 18.0 MPa, they concluded that for pressures up to 7.0 MPa the correlation by Jens and Lottes (1951) was among those giving the lowest discrepancies between predicted and measured values by seven other authors. The Thom et al. (1966) correlation was recommended at higher pressures.

More recently, Shah (1977, 1982) developed a general correlation for nucleate boiling valid for a large number of fluids. This correlation compares well with data obtained with Freons, water, and organic fluids for a wide range of flow conditions ( $Re > 10,000$ ) and pressures ( $0.005 < p^+ < 0.76$ ).

For nucleate pool boiling, correlations have been suggested by Rohsenow and Choi (1961) and Forster and Greif (1959). These correlations indicate a sensitivity to the fluid-surface combination and generally predict lower heat transfer coefficients because of the lower bubble removal rates (compared with forced convective nucleate boiling).

#### 3.2.2 Saturated Boiling: Nucleate Boiling and Forced Convective Evaporation

In the saturated boiling regime the heat transfer correlations often have the form

$$h_{TP} = h_{NB} + h_{conv}$$

where  $h_{NB} = f(P, Bo)$  and  $h_{conv} = f(X_{tt}, h_\ell^*)$ .

Table 2. Nucleate Boiling and Forced Convective Vaporization<sup>a</sup>

References	Correlation	Comments
Chen (1963)	$h = 0.023 k/D (Re_l^*)^{0.8} (Pr_l)^{0.4} F$ $+ 0.00122 \frac{k_l^{0.79} c_{pl}^{0.45} \rho_l^{0.49}}{\sigma^{0.5} \mu_l^{0.29} h_{fg}^{0.24} \rho_g^{0.24}} (T_w - T_{sat})^{0.24} (P_w - P)^{0.75} S$ <p> <math>P_w = P_{sat}</math> evaluated at <math>T_w</math>  <math>F = 1.0</math> for <math>X_{TT}^{-1} \leq 0.10</math>  <math>F = 2.35 (X_{TT}^{-1} + 0.213)^{0.736}</math> for <math>X_{TT}^{-1} &gt; 0.10</math>  and  <math>S = [1 + 0.12 (Re_l^* F^{1.25})^{1.14}]^{-1}</math> for <math>Re_l^* F^{1.25} &lt; 32.5</math>  <math>S = [1 + 0.42 (Re_l^* F^{1.25})^{0.78}]^{-1}</math> for <math>32.5 \leq Re_l^* F^{1.25} &lt; 70.0</math>  <math>S = 0.1</math> for <math>Re_l^* F^{1.25} \geq 70</math>  where  <math display="block">Re_l^* = \frac{G(1-X)Dh_y}{\mu_l}</math> </p>	<p>Large range of diameter, length, mass flux</p> <p> <math>50 &lt; P &lt; 3400</math> kPa  <math>6.3 &lt; q &lt; 2400</math> kW m<sup>-2</sup>  <math>0 &lt; X &lt; 0.71</math> </p> <p>Upflow and downflow; circular and annular; water, methanol, cyclohexane, pentane, heptane, benzene</p> <p>Estimates of <math>F</math> and <math>S</math> by Bjornard (1977); other approximations for <math>F</math> and <math>S</math> given by Butterworth and Shock (1975)</p>
Jens and Lottes (1951)	$h = 0.00254 \left[ (T_w - T_{sat})^{\frac{3}{4}} e^{(1.61 \times 10^{-4} P)} \right]^4$	For nucleate boiling of water only
Thom et al. (1966)	$h = 1.9712 e^{(2P/8687)} (T_w - T_{sat})$	For nucleate boiling of water only

Schrock and  
Grossman (1959)

$$h = 170 k_l / D h_y (Re_l^*)^{0.8} (Pr_l)^{1/3} F$$

$$[Bo + 1.5 \times 10^{-4} X_{tt}^{-2/3}]$$

Wright's (1961)  
modification of  
Schrock and  
Grossman

$$h = \frac{2.35}{X_{tt}^{2/3}} \left[ \frac{1}{h_L^*} - \frac{6.70 \times 10^3 (T_w - T_s)}{G \lambda} \right]^{-1}$$

$$h_L^* = 0.023 k_f / D h_y [Re_l^*]^{0.8} [Pr_l]^{0.4}$$

Dengler and  
Addoms (1956)

$$h_{TP} / h_{fo} = 3.5 (1/X_{tt})^{0.5}$$

Shah (1976)

$$h_{TP} / h_l^* = f[Bo, ((1-X)/X)^{0.8} (\rho_g / \rho_l)^{0.5}];$$

for graphical approach, see Fig. 6

$$h_l^* = 0.023 (Re_l^*)^{0.8} Pr_l^{0.4} k_l / D h_y$$

McAdams et al.  
(1949)

$$h = 2.257 (T_w - T_{sat})^{2.86}$$

Experiments with upflow of  
water in circular geometries

$$0.3 < D < 1.1 \text{ (cm)}$$

$$39.5 < L < 100 \text{ (cm)}$$

$$286 < P < 3435 \text{ (kPa)}$$

$$238 < G < 4447 \text{ (kg m}^{-2} \text{ s}^{-1}\text{)}$$

$$289 < q < 4574 \text{ (kW m}^{-2}\text{)}$$

$$0 < X < 0.57$$

Experiments with downflow of  
water in circular geometries

$$D h_y = 1.83, 1.4 \text{ (cm)}$$

$$L = 1.72, 1.43 \text{ (m)}$$

$$107 < P < 464 \text{ (kPa)}$$

$$536 < G < 3417 \text{ (kg m}^{-2} \text{ s}^{-1}\text{)}$$

$$43.5 < q < 277.6 \text{ (kW m}^{-2}\text{)}$$

$$0 < X < 0.19$$

$fo$  = total flow assumed to  
be liquid

This graphical correlation  
smoothly converges with  
Shah's (1977) correlation  
for large values of the  
quality-density parameter.

For nucleate boiling of  
water only

Table 2 continued

References	Correlation	Comments
Shah (1977)	<p>If <math>\frac{T_s - T_l}{T_w - T_s} &lt; \min [2, 6.3 \times 10^{-4} Bo^{1.25}]</math>, then <math>\frac{h_{TP}}{h_l^*} = \psi_0</math></p> <p>If <math>\frac{T_s - T_l}{T_w - T_s} &gt; \min [2, 6.3 \times 10^{-4} Bo^{1.25}]</math>,</p> <p>then <math>\frac{h_{TP}}{h_l^*} = \psi_0 + \frac{T_s - T_l}{T_w - T_{sat}}</math></p> <p>If <math>Bo &gt; 0.3 \times 10^{-4}</math>, then <math>\psi_0 = 230 Bo^{0.5}</math></p> <p>If <math>Bo &lt; 0.3 \times 10^{-4}</math>, then <math>\psi_0 = 1 + 46 Bo^{0.5}</math></p>	Valid for subcooled nucleate boiling of water, refrigerants and organic fluids, $Re_l > 10,000$
Rohsenow (1952)	$\frac{C_{pl} (T_w - T_{sat})}{H_{fg} Pr_l^{1.7}} = C_{sf} \left[ \frac{q}{\mu_l H_{fg}} \left[ \frac{\sigma}{g(\rho_f - \rho_g)} \right]^{\frac{1}{2}} \right]^{1/3}$	Pool boiling only
		Fluid-heating surface combination $C_{sf}$
		Water-copper 0.013
		Water-platinum 0.013
		Water-brass 0.0060
		Water-ground and polished stainless steel 0.0080
		Water-chemically etched stainless steel 0.0133
		Water-mechanically polished stainless steel 0.0132

<sup>a</sup>For definition and units of all symbols see Nomenclature.

The correlation most widely used in modern thermohydraulic codes is that by Chen (1963). The value of his Reynold's number factor  $F$  and his suppression factor  $S$  were originally presented in graphical form. Since graphical representations are cumbersome to use in computer calculations, Bjornard and Griffith (1977) approximated  $F$  and  $S$  in mathematical form, as shown in Table 2. The Chen correlation predicts the heat transfer coefficients for many different fluids with a standard deviation of 11% (Rohsenow and Hartnett, 1973).

Recently, a graphical prediction method based on many fluid-wall combinations was proposed by Shah (1976, 1982). It is basically an extension of Shah's (1977) subcooled nucleate boiling correlation and is very easy to use for hand calculation. Figure 6 shows Shah's graphical correlation, where

$$\frac{h_{TP}}{h_l^*} = f \left[ \left( \frac{1-X}{X} \right)^{0.8} \left( \frac{\rho_g}{\rho_l} \right)^{0.5}, Bo \right]$$

Figure 7 shows various predictions of two-phase heat transfer correlations. Shah's prediction method is not shown, but it closely follows Chen's correlation.

Shah (1977) also developed a graphical method to predict the reduction in  $h_{TP}$  due to horizontal flow for liquid Froude numbers up to  $Fr_L = 0.04$ . Shah (1981) reported that downflow heat transfer data are lower than the corresponding upflow data.

Schrock and Grossman (1959), Dengler and Addoms (1956), and Wright (1961) also recommended correlations for saturated nucleate

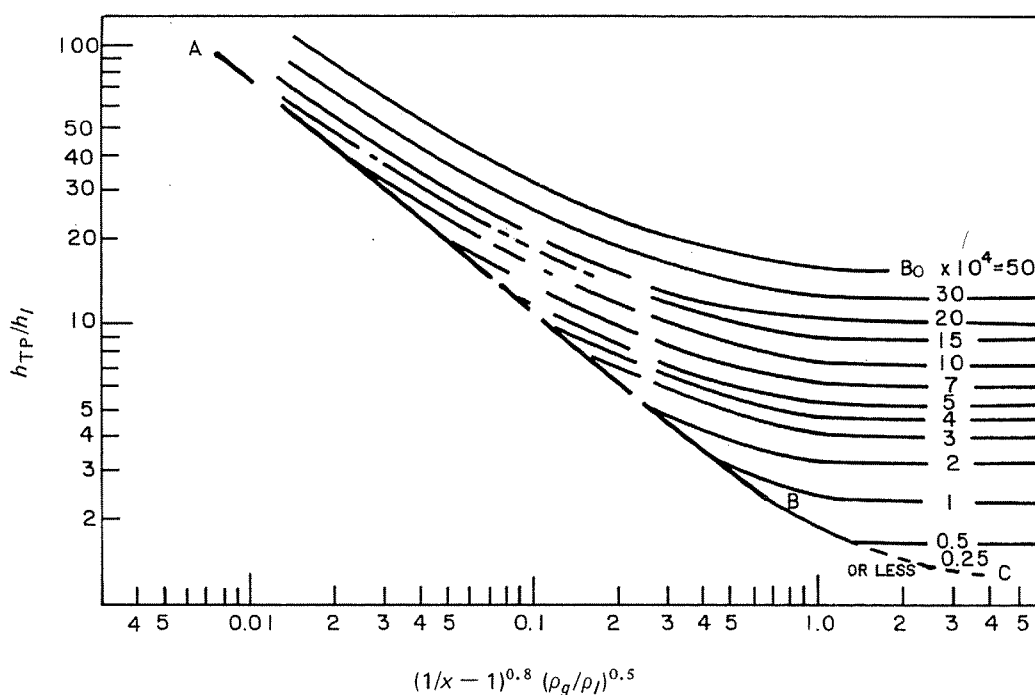


Fig. 6. Shah's graphical prediction method for  $h_{TP}$ . Shah (1976). Reprinted with permission.

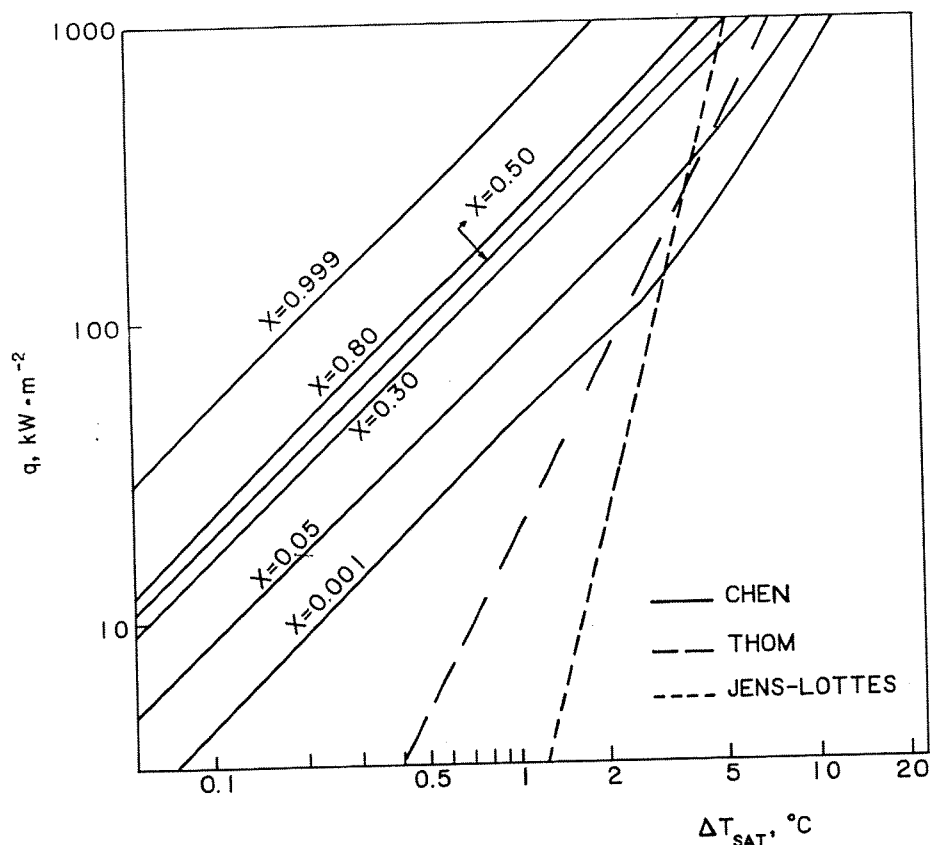


Fig. 7. Comparison of Chen's correlation with Thom's and Jens-Lottes's correlations.  $P = 10 \text{ MPa}$ ,  $G = 5.4 \text{ Mg m}^{-2} \text{ s}^{-1}$ ,  $De = 0.3 \text{ cm}$ . — Chen (1963), - - Thom et al. (1966), --- Jens-Lottes (1951).

boiling. However, their correlations appear to have a more limited data base and should be used with caution.

Cooper (1982) has shown that most thermodynamic properties used in nucleate boiling correlations can be replaced by a simple formulation using the reduced pressure  $P^+$  and reduced temperature  $T^+$ . The use of these reduced property terms significantly simplifies the analysis of boiling heat transfer data. Eventually more data are needed before the effect of the thermodynamic properties on the boiling curve can be established.

### 3.3 Conclusions and Final Remarks

The general consensus in the literature is that Chen's (1963) correlation will result in the most accurate prediction of forced convective boiling in the pre-CHF region. To obtain a quick first approximation, Shah's graphical method is recommended. Thom's correlation may also be used, but it applies only in the nucleate boiling region.

Due to small differences between wall and saturation temperatures, discrepancies between measured and predicted boiling heat transfer coefficients may appear quite large. These errors usually represent only a few degrees in heated surface temperatures

and are thus unlikely to have a large effect on the prediction of the maximum surface temperature. However, the error in predicted heat flux could be significant.

Subcooled nucleate boiling tends to be primarily a local phenomenon and does not appear to be affected by geometry. Flow direction will affect  $h_{TP}$  at lower flows.

No general cross-flow correlation has yet been derived for nucleate boiling since most experimenters have correlated only their own cross-flow data. However, it appears that the cross-flow heat transfer coefficient falls in between the corresponding upflow value and the pool boiling value.

#### 4 CRITICAL HEAT FLUX

##### 4.1 Introduction

The prediction of CHF in nuclear fuel bundles is complex since effects of radial and axial flux distribution, spacer location, rod spacing, etc., all have a significant effect on the magnitude and location of CHF. Even for a uniformly heated tube the results of different CHF prediction techniques are confusing. An early review by Clerici et al. (1965) covered 87 CHF correlations. As of 1982 there were over 400 CHF correlations available. This proliferation of correlations illustrates the sad state of the art in modeling the CHF phenomenon. It creates a particular concern when reliable CHF correlations are required for the evaluation of critical channel power in reactor operating conditions. The general approach has been to do ad hoc experiments - a feasible alternative since the range of operating conditions is limited.

For reactor accident conditions, however, it often becomes economically impossible to measure CHF using a representative simulation of a reactor core. Instead, empirical correlations based on tube CHF data (which can be obtained at a fraction of the cost of an equivalent bundle CHF experiment) are frequently employed. Unfortunately, even the range of conditions covered by experiments in tubes is inadequate, as is illustrated in Fig. 8. This limited coverage has resulted in empirical CHF correlations commonly being used well outside the range of their data base. Such practice leads to predictions that are often meaningless, for example, negative CHF predictions or high CHF values at steam qualities close to 100%.

A large number of terms have been used in the literature to denote the occurrence of CHF: burnout, dryout, boiling crisis, and departure from nucleate boiling (DNB). The term *DNB* is usually reserved for the CHF occurrence in the subcooling region caused by microlayer evaporation under a bubble. Dryout frequently refers to the CHF occurrence caused by evaporation of the wall liquid film in the annular flow regime. Detailed descriptions of the CHF mechanisms may be found in Collier (1980), Hewitt and Hall-Taylor (1970), Tong (1972a), and Tong and Hewitt (1972).

##### 4.2 Correlations

CHF correlations may be subdivided into two main groups:

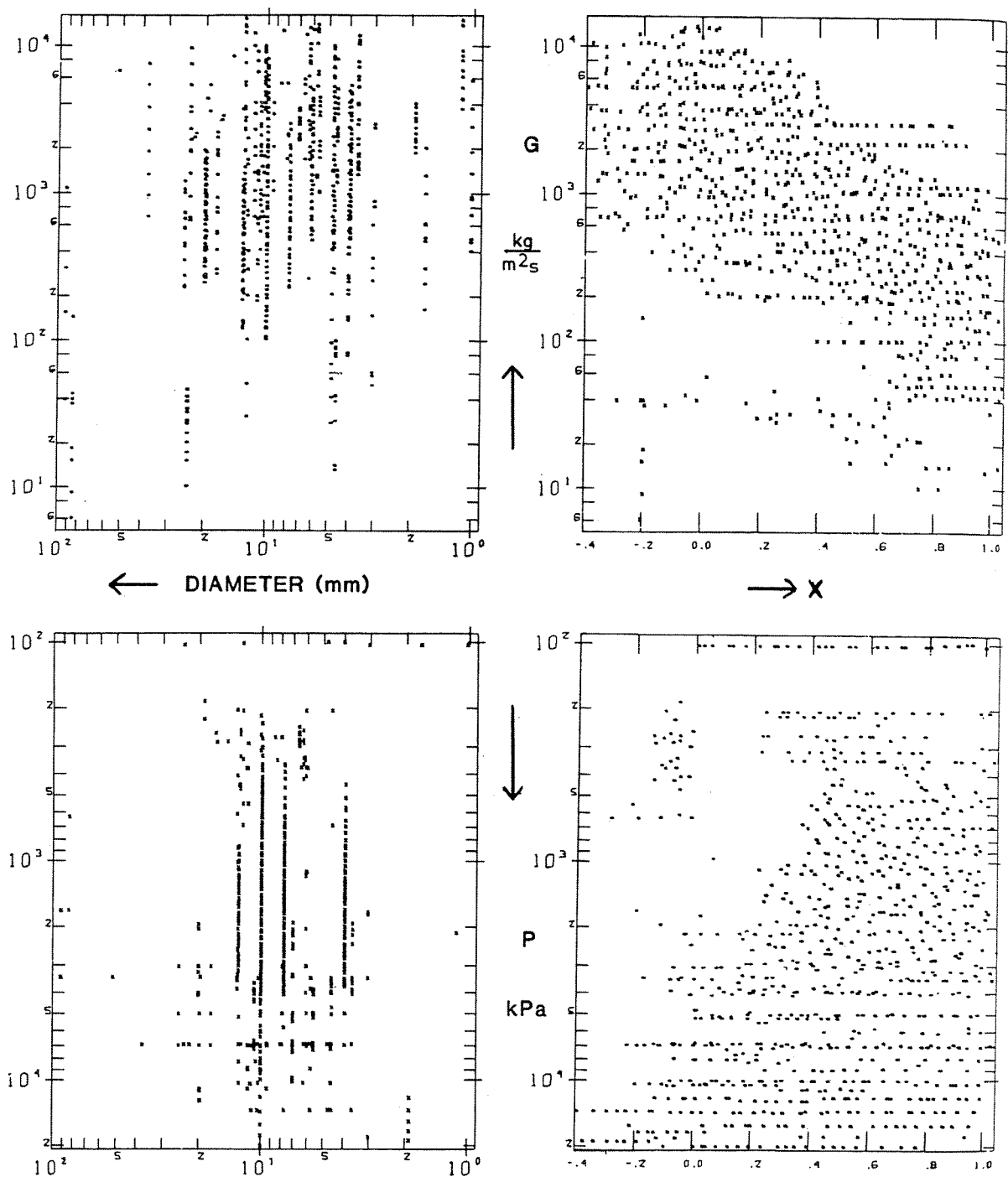


Fig. 8. Range of available CHF tube data.



Table 3. CHF Correlations<sup>a</sup>

Correlation	Comments
$\text{CHF} = [2.002 - 0.0000624 P + (0.1722 - 0.0000143 P) e^{(18.177 - 0.000599 P)X}]$ $[(0.1484 - 1.596 X + 0.1729 X  X ) 0.0007347 G + 1.037]$ $[1.157 - 0.869 X] [0.2664 + 0.8357 e^{-124.1 Dhy}] [0.8258 + 3.41 \times 10^{-4} \Delta H_{in}]$	<p>W-3 correlation (Tong, 1972a). Based on a large data base of tubes and rectangular cross sections. Data base range: <math>G</math>: 1356-6780 kg m<sup>-2</sup> s<sup>-1</sup> <math>P</math>: 6895-15860 kPa, <math>X</math>: -0.15 to +0.15 <math>Dhy</math>: 0.005-0.018 m, <math>L</math>: 0.25 - 3.66 m</p>
$\text{CHF} = (1 - \alpha) 0.131 \rho_g H_{fg} \left[ \frac{\sigma g (\rho_f - \rho_g)}{\rho_g^2} \right]^{0.25}$	<p>Zuber-Griffith correlation (Griffith et al., 1977). Recommended for <math>G &lt; 300</math> kg m<sup>-2</sup> s<sup>-1</sup> and up- or downflow. Underpredicts CHF at high <math>\alpha</math>-values.</p>
$\text{CHF} = \frac{1.155 - 16.03 Dhy}{4.03 \times 10^3 (2.25 \times 10^{-3} G)^A} [3.7 \times 10^7 (4.36 \times 10^{-4} G)^B - 48.22 \times H_{fg} G]$ <p>where <math>A = 0.712 + 3 \times 10^{-5} (P - 13,790)</math></p> <p><math>B = 0.834 + 9.9 \times 10^{-5} (P - 13,790)</math></p>	<p>B&amp;W-2 correlation (Gellerstedt et al., 1969). Based on 207 bundle CHF data. Data base range: <math>P</math>: 13,800-16,550 kPa <math>G</math>: 1020-5424 kg m<sup>-2</sup> s<sup>-1</sup> <math>X</math>: -0.03 - +0.20</p>
$\text{CHF} = \frac{8.585 H_{fg} (G/1356)^{0.51} (1 - X)}{1.444 Dhy^{0.1}}$	<p>Macbeth (1963). Only for low-flow tube CHF. Upper mass flux boundary depends on pressure and is defined graphically in original reference.</p>
$\text{CHF} = \frac{25,487 (G/1356)^{0.1775} \ln(X + 1)}{(X + 1)^{3.3906} 0.5356 P^{0.3234} \text{RPF}^{1.053}}$ <p>RPF = maximum radial power factor for bundle</p>	<p>RELAP 4-MOD-7 correlation (Condie and Bengston, 1978). Based on 5200 bundle CHF data covering following ranges: <math>P</math>: 690-15200 kPa <math>G</math>: 100-4100 kg m<sup>-2</sup> s<sup>-1</sup> <math>X</math>: -0.1 - +1.0, no. of rods: <math>\geq 9</math></p>

Table 3 continued

Correlation	Comments
$\text{CHF} = \text{CHF}_{W-3} \left[ 1.76 (0.96 - \alpha) \right]^{\frac{1}{2}} + q_{\text{dry}}$ <p><math>\text{CHF}_{W-3}</math> given by Tong (1972a), evaluated at <math>X = 0</math></p> $q_{\text{dry}} = h_{\text{Dittus-Boelter}} (T_{\text{CHF}} - T_{\text{SAT}})$	<p>Hsu and Beckner (1977). Recommended for transient CHF; predicts a 30% higher CHF than W-3 correlation at low voids.</p>
$\text{CHF} = \text{greater of } \left[ \frac{1.883 \times 10^4}{(100 D)^n (G/10)^{0.167}} \right] \left[ \frac{f_p}{(G/10)^{0.167}} - X \right] \quad (\text{low } X)$ $\left[ \frac{3.78 \times 10^4}{(100 D) (G/10)^{0.6}} \right] h_p (1 - X) \quad (\text{high } X)$	<p>Biasi et al., (1967). Data base range (tube data only): <math>D</math>: 0.003-0.0375 m <math>G</math>: 100-6000 <math>\text{kg m}^{-2} \text{s}^{-1}</math> <math>P</math>: 270-14,000 kPa, <math>X &lt; 1.0</math></p> $X_{\min} = \frac{1}{1 + \rho_l / \rho_g}$
<p>where <math>n = 0.4</math>, if <math>D \geq 0.01</math> <math>n = 0.6</math>, if <math>D &lt; 0.01</math></p> $f_p = 0.7249 + 0.99 \times 10^{-3} P \exp(-0.32 \times 10^{-3} P)$ $h_p = -1.159 + 1.49 \times 10^{-3} P \exp(0.19 \times 10^{-3} P) + \frac{0.09 P}{10 + [P/100]^2}$	
$\text{CHF} = 10^3 \left[ 10.3 - 17.5 \frac{P}{P_{cr}} + 8.0 \left( \frac{P}{P_{cr}} \right)^2 \right] \left( \frac{G}{1000} \right)^\alpha \left( \frac{0.008}{D} \right)^{\frac{1}{2}} e^{-1.5 X}$	<p>Doroshchuk et al. (1975). Based on large number of tube data obtained at:</p>
<p>where <math>\alpha = 0.68 \frac{P}{P_{cr}} - 1.2 X - 0.3</math></p>	<p><math>P</math>: 2900-15,600 kPa, <math>T_{\text{subc}} &lt; 50^\circ\text{C}</math> <math>G &lt; 2000 \text{ kg m}^{-2} \text{s}^{-1}</math>, <math>D</math>: 0.004-0.016 m</p>

$$\text{CHF} = 0.18 \text{ CHF}_{\text{PB}} G^{0.25} \left(1 - \frac{P}{P_{\text{cr}}}\right)^{0.1} \left(\frac{D_{\text{hy}}}{D_i}\right)^{0.2} \left[1 - 0.06 G^{0.5} \left(\frac{D_{\text{hy}}}{D_i}\right)^{0.2} X\right]$$

$$\text{where } \text{CHF}_{\text{PB}} = 0.14 H_{fg} \rho_g^{0.5} [\sigma g (\rho_l - \rho_g)]^{0.25}$$

$$\text{CHF} = \frac{A-B H_{fg} X}{C}$$

$$\text{where } A = \frac{2.317 (0.25 H_{fg}^{DG}) F_1}{(1 + 0.0143 F_2 D^{\frac{1}{2}} G)} \quad C = \frac{0.077 F_3^{DG}}{[1 + 0.347 F (G/1356)^n]}$$

$$n = 2.0 - 0.5 \text{ Pr}$$

$$B = 0.25 DG$$

$$\text{Pr} = 0.145 \times 10^{-3} P$$

$P < 6895$	$P > 6895$
$F_1 = \frac{\text{Pr}^{18.942} e^{20.89(1 - \text{Pr})} + 0.917}{1.917}$	$F_1 = \text{Pr}^{-0.368} e^{0.648(1 - \text{Pr})}$
$F_1/F_2 = \frac{\text{Pr}^{1.316} e^{2.444(1 - \text{Pr})} + 0.309}{1.309}$	$F_1/F_2 = \text{Pr}^{-0.448} e^{0.245(1 - \text{Pr})}$
$F_3 = \frac{\text{Pr}^{17.023} e^{16.658(1 - \text{Pr})} + 0.6671}{1.667}$	$F_3 = \text{Pr}^{0.219}$
$F_4 = F_3 \text{Pr}^{1.649}$	$F_4 = F_3 \text{Pr}^{1.649}$

Levitan and Lantsman (1977);  
Tolubinskiy et al. (1977). Based  
on a large number (>>1000) of  
annuli data obtained at:  
 $L$ : 0.5,  $D$ : 0.006-0.1 m  
 $D_{\text{hy}}$ : 0.002-0.006 m  
 $P$ : 5000-20,000 kPa  
 $G$ : 250-5000 kg m<sup>-2</sup> s<sup>-1</sup>,  $X < 0.3$

Bowring (1972). Empirical  
correlation of 3800 tube CHF data.  
RMS error for system parameter  
form of the correlation: 7%

Data base range:  
 $G$ : 136-18,600 kg m<sup>-2</sup> s<sup>-1</sup>  
 $D$ : 0.002-0.045 m  
 $L$ : 0.15-3.70 m  
 $P$ : 200-19,000 kPa

Table 3 continued

Correlation	Comments
$\text{CHF} = \left[ \frac{A - B H_{fg}^X}{C + Z Y \left( 1 - \frac{12,620 B}{G D_{he}} \right)} \right] 3154.6$	Bowring's (1977) mixed-flow correlation based on bundle CHF data covering the following ranges: $P$ : 600-15,500 kPa $G$ : 50-4000 kg m <sup>-2</sup> s <sup>-1</sup> $D_{he}$ : 0.0076-0.0366 m $L$ : 1.5-4.6 m $F_p$ : 1.0-1.32
where $A = \frac{7.063 F_1 G D_{he}}{1 + G F_p^2 D_{he}^2 \left\{ 68.22 F_2 D_{hy}^{1.3} \left[ 1 + 0.0007373 G \left( 0.8 F_p D_{he}/D_{hy} - 1 \right) \right] \right\}^{-1}}$	Geometry: pressure-tube cluster NB: for square lattice clusters the same correlation is recommended if $p < 8620$
$B = 0.00312 G D_{he} e^{-1.375 \times 10^{-4} G}$	
$C = 69.448 D_{hy}^{0.57} G^{0.27} \left[ 1 + \frac{Y - 1}{0.0007373 G + 1} \right]$	
$Z$ = heated length to dryout point	for $p > 8620$ kPa:
$F_p$ = radial heat flux peaking factor = $q_{\max}/q_{\text{avg}}$	$A = A_2 + (2.250 - 0.000145 P)$
	$(A_1 - A_2)$
$Y = \frac{\text{average flux from entry to } Z}{\text{local radially averaged flux at } Z}$	$A_1$ = value of $A$ as calculated for the tube clusters at $P = 8620$ kPa

$$F_1 = [1 - 5.8028 \times 10^{-6} P (1 + 9.8913 \times 10^{-9} P^2)^{\frac{1}{2}}]^2$$

$$\text{if } P < 2861 \quad F_2 = 0.45 + 1.8134 \times 10^{-4} P$$

$$2861 < P < 4482 \quad F_2 = 0.424 + 2.8419 \times 10^{-4} P - 3.2746 \times 10^{-8} P^2$$

$$P > 4482 \quad F_2 = (3.2 - 0.14507 \times 10^{-3} P) (0.32 + 1.958 \times 10^{-5} P)$$

$$\text{CHF} = f(D) = (b H_{fg} / B v_{fg} G^{\frac{1}{2}})$$

$$\text{where } B = \frac{-\ln(1 - X) + \ln \left( 0.98 - \frac{\epsilon v B^{\frac{1}{2}}}{X^{\frac{1}{4}} (B + 1)} \right) - \ln \left( 1 - \frac{\epsilon (X + v) B^{\frac{1}{2}}}{(1 - X) X^{\frac{1}{4}} (B + 1)} \right)}{\ln [(X + v)/v]}$$

$\epsilon, b$  are functions of pressure

$$v = v_f / v_{fg}$$

$D \text{ (mm)}$	4	6	8	10	12	16	20	25
$f(D)$	1.18	1.176	1.085	1.00	0.973	0.951	0.928	0.900

a) For definition and units of all symbols see nomenclature.

$$A = 0.0132 G + \frac{0.276 G D h_e}{0.1 + 0.0007373 G}$$

Becker et al. (1967)

Agreed with tube data within the following ranges:

$P$ : 270-10,000 kPa,  $D$ : 0.004-0.025 m

$L$ : 0.4-3.5 m,  $X_c$ : 0-0.50,

$G$ : 120-5400 kg m<sup>-2</sup> s<sup>-1</sup>

For  $X_c > 0.6$  the mass flux effect decreases.

Agrees with large data base from eight different laboratories (Becker et al., 1972)

1. *Local conditions-type CHF correlations* where  $CHF = f(P, G, X, \text{ or } \alpha, \text{ cross-section geometry})$ . These correlations are convenient to use for predicting the location of dryout and the magnitude of the CHF. Effects of axial flux distribution, spacers, flux spikes, and flow transients (e.g., flow stagnation) often require a modified local conditions approach, i.e., a local conditions approach combined with techniques that consider the upstream flow history (e.g., boiling length,  $F$ -factor method).
2. *Global conditions correlations* where the burnout power  $= f(P, G, H_{in}, L_h, \text{ cross-section geometry})$ . These correlations predict only the burnout power. They cannot be used to predict the location of dryout or the magnitude of the CHF. These correlations are also incapable of accounting for the effect of axial flux distribution or flow transients. They are primarily used to predict critical power during steady-state operation for a given geometry and axial flux distribution.

Due to the limitation of global conditions correlations in a LOCA analysis, local conditions correlations are emphasized in this review. Table 3 contains most of the currently popular CHF correlations.

A limited comparison of the CHF correlations with the AECL tube CHF data bank (containing 10,000 CHF data points) has been made. The results of the comparison are shown in Figs. 9 and 10. Figure 9 shows an error histogram. The fraction of the data with  $CHF_{pred}/CHF_{meas} < 0$  (below range) or  $CHF_{pred}/CHF_{meas} > 2.0$  (above range) is also indicated. Of all the correlations tested, that of Biasi et al. (1967) appears to be the most promising. Its parametric and asymptotic trends are shown in Fig. 10. Even this correlation has significant shortcomings when compared with the experimentally observed parametric and asymptotic trends, e.g., increasing the flow always decreases the CHF according to Biasi's correlation. The experimentally observed trends are shown in Table 5 and will be discussed in detail in Sec. 4.4.

### 4.3 Alternative Prediction Methods

#### 4.3.1 Analytical Methods

During the past 20 years, several analytical approaches to predict the CHF have been developed. Two popular models are those by Hewitt and Hall-Taylor (1970) and Tong (1965). Hewitt and Hall-Taylor's model is a three-fluid model (vapor, liquid film, entrained droplets). It is based on the commonly accepted hypothesis that the boiling crisis in annular flow occurs when the liquid film is depleted by evaporation and entrainment. Many variations of this model may be found in the literature. The model has been improved and extended to annuli (Whalley, 1974; Whalley et al., 1975), to bundles (Whalley et al., 1978; Whalley, 1978) and to transient conditions (Whalley et al., 1975). Tong (1965) developed a two-fluid model for the prediction of CHF in the bubbly flow regime. This model has been successfully used to include the effect of upstream axial flux distribution. Zuber et al.'s (1961) CHF equation is derived from a two-fluid model for pool boiling on a horizontal surface. All these models are

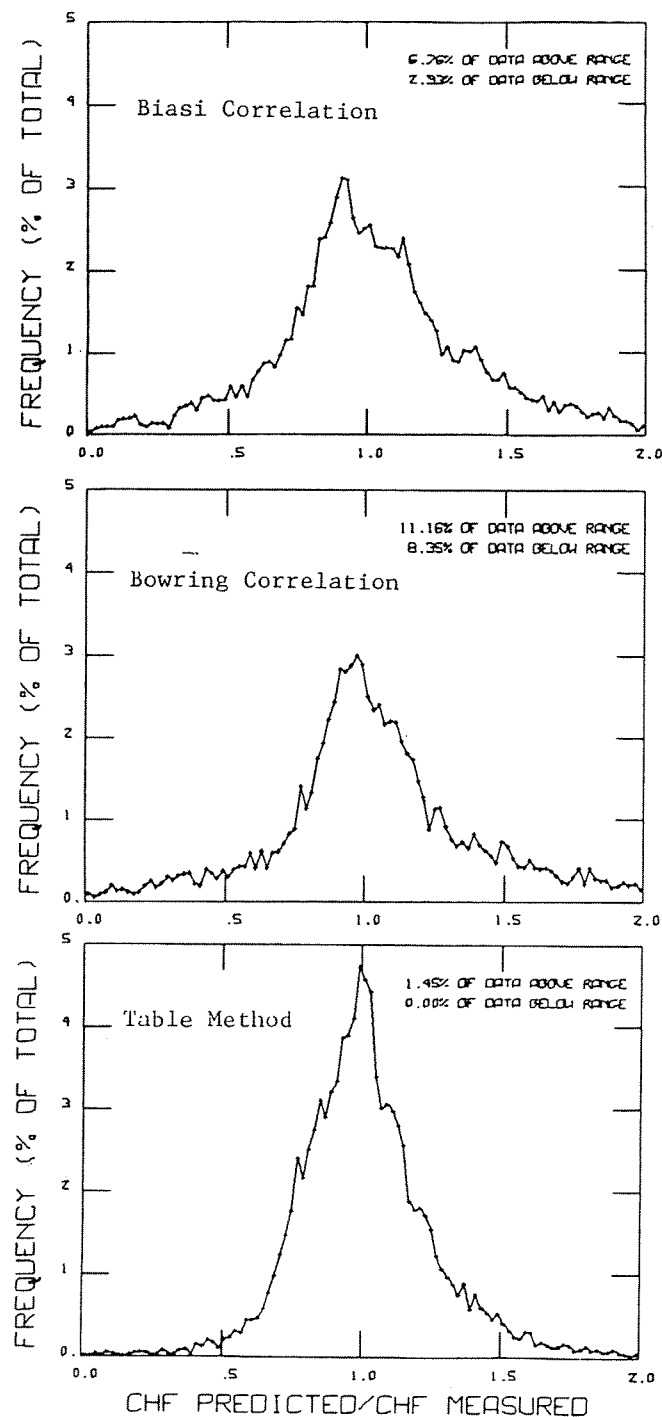


Fig. 9. Comparison of CHF error histograms.

basically valid for one flow regime and heat transfer configuration.

#### 4.3.2 Table Look-Up Technique

Since most empirical correlations and analytical models have a limited range of application, the need for a more general technique is obvious. Attempts have been made in the USSR to

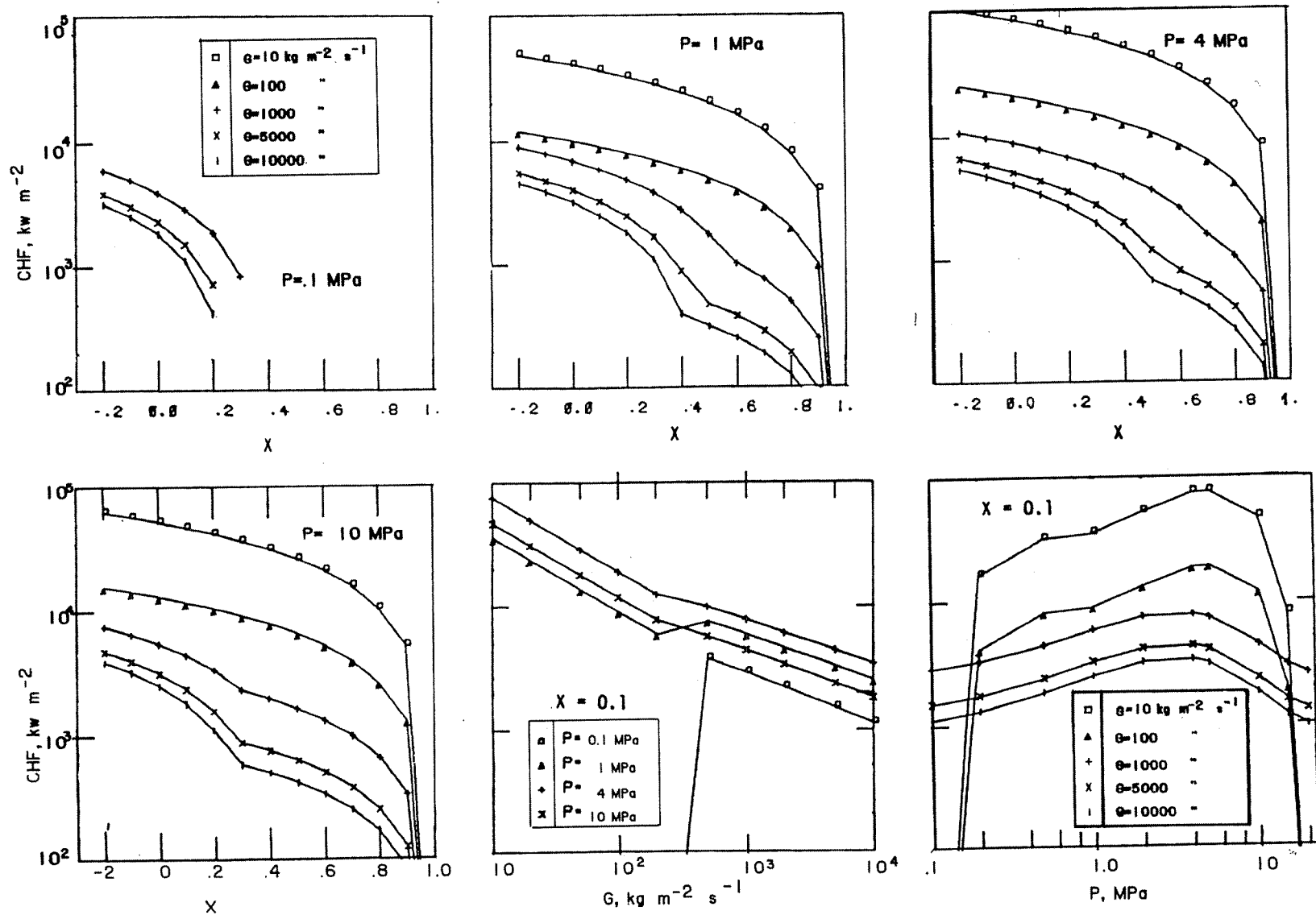


Fig. 10. Parametric and asymptotic trends for Biasi et al.'s (1960) CHF correlation.



Fig. 10. Parametric and asymptotic trends for Biasi et al.'s (1960) CHF correlation.

Table 4. Estimated CHF Values

Pressure (kPa)	G (kg m <sup>-2</sup> s <sup>-1</sup> )	Quality																
		-0.15	-0.10	-0.05	0.00	0.05	0.10	0.15	0.20	0.25	0.30	0.40	0.50	0.60	0.70	0.80	0.90	1.0
100	0	3930	3430	2045	1200	1000	980	800	750	740	733	500	500	450	356	212	89	0
100	50	4008	3500	2400	1700	1600	1500	1250	1200	1150	1108	873	756	710	506	386	350	0
100	100	4800	4200	3100	2200	2100	2000	1450	1000	850	820	750	727	700	667	493	330	0
100	200	5600	4900	3800	2600	2550	2500	1500	1400	1350	1300	1200	1160	1108	863	532	407	0
100	300	6400	5600	4500	3000	3000	3000	2200	2100	2000	1978	1900	1774	1443	827	620	450	0
100	500	7200	6300	5200	3600	3550	3500	3450	3350	3300	2486	2354	2318	1251	662	633	440	0
100	750	3000	7000	5900	5500	5000	4700	4572	4105	3186	2986	2687	2394	1308	905	700	400	0
100	1000	3800	7600	6600	4800	4600	4400	4200	3552	3536	3400	3319	2534	1514	1100	600	300	0
100	1500	9600	8200	7000	5500	4800	4200	4600	4500	4000	3823	3266	2200	1100	600	300	0	0
100	2000	10000	8800	7700	5900	5400	5300	5260	5100	5050	5000	4900	4840	2900	1100	600	300	0
100	3000	10500	9400	8400	7300	6500	6000	5992	5400	5300	5200	5017	3500	2700	1100	600	300	0
100	4000	11000	10000	9000	6800	6683	6500	6100	5300	5000	4600	4000	3000	2000	1000	500	300	0
100	5000	11500	10600	9500	8358	7951	7600	7400	5200	4400	3800	3000	2500	1500	900	500	300	0
100	7500	12000	11000	10000	9500	9200	9000	7500	5000	4000	3000	2200	2000	1200	800	400	300	0
150	0	4000	3500	2400	1350	1200	1100	950	947	900	887	680	600	560	377	236	111	0
150	50	4100	3600	2700	1900	1800	1700	1500	1400	1390	1285	984	793	600	521	403	300	0
150	100	4800	4200	3200	2400	2200	2000	1900	1800	1400	1072	944	920	900	890	680	450	0
150	200	5400	4800	3800	2700	3600	2500	2100	1600	1500	1400	1325	1304	1200	1100	1000	500	0
150	300	6000	5400	4400	3000	3000	3000	2700	2400	2200	1700	1650	1600	1500	1400	800	500	0
150	500	6600	6000	5000	3700	3600	3500	3100	2700	2227	1800	1668	1500	1300	1100	670	450	0
150	750	7200	6600	5600	4300	4150	4000	3500	2200	2000	1900	1800	1700	1500	1170	650	400	0
150	1000	7800	7200	6200	5000	4700	4400	3700	3400	3100	2900	2700	2300	2200	1100	600	350	0
150	1500	8400	7600	6800	5500	5200	4800	3800	3600	3400	3100	3000	2800	2500	1100	550	300	0
150	2000	9000	8200	6000	5500	4988	4529	4135	4000	3900	3700	3500	3400	3000	1000	550	300	0
150	3000	9600	8240	5800	5600	5400	5200	4600	4100	3800	3300	3250	3200	2500	1000	500	300	0
150	4000	10000	6636	6000	5766	5214	5000	4700	4200	3600	2800	2800	2600	2000	1000	450	300	0
150	5000	10500	9900	9100	8901	7254	6500	5700	4000	3100	2600	2300	2000	1500	900	450	300	0
150	7500	11000	10400	9700	9000	8600	8000	6500	5000	3000	2200	1800	1600	1000	600	400	300	0
200	0	4820	3700	2774	1450	277	262	248	233	219	204	175	146	117	87	58	29	0
200	50	4955	4000	3094	2313	1794	1641	1562	1483	1405	1326	1244	1044	700	600	593	468	0
200	100	5000	4100	3200	2600	2300	2100	2000	1900	1300	1200	1085	900	751	700	650	315	0
200	200	5200	4300	3400	2800	2500	2300	2150	1400	1350	1325	1300	1250	1200	1142	800	315	0
200	300	5400	4450	3500	3000	2700	2400	2200	2150	2100	2000	1810	1461	1000	700	600	350	0
200	500	5600	4650	3700	3150	2900	2500	2250	2100	2000	1800	1649	1500	1100	800	450	300	0
200	750	5800	4850	3900	3300	3000	2650	2350	2118	2066	1826	1767	1600	1000	600	450	300	0
200	1000	6000	5000	4000	3400	3000	2600	2350	2140	1958	1800	1700	1600	1000	600	450	300	0
200	1500	6200	4600	3800	3300	3000	2600	2350	2284	2119	1800	1700	1500	1000	600	450	300	0
200	2000	6400	4500	4000	3500	3000	2600	2350	2150	2050	1800	1700	1400	1000	600	450	300	0
200	3000	7000	5742	4287	3900	3000	2600	2350	2150	2050	1800	1700	1400	1000	600	450	300	0
200	4000	8500	6411	4800	4500	3000	2600	2350	2150	2050	1800	1700	1400	1000	600	450	300	0
200	5000	6607	6120	5267	4845	3000	2600	2350	2150	2050	1800	1700	1400	1000	600	450	300	0
200	7500	5990	6465	5581	5077	3000	2600	2350	2150	2050	1800	1700	1400	1000	600	450	300	0

Table 4 (cont'd)

Pressure (kPa)	G (kg m <sup>-2</sup> s <sup>-1</sup> )	Quality																
		-0.15	-0.10	-0.05	0.00	0.05	0.10	0.15	0.20	0.25	0.30	0.40	0.50	0.60	0.70	0.80	0.90	1.0
300	0	4650	3667	2683	1700	325	308	291	274	257	240	205	171	137	103	68	34	0
300	50	5063	4292	3296	2975	2481	2327	2248	2168	2014	1860	1551	1067	637	592	549	500	0
300	100	5200	4500	3500	3400	3200	3000	2900	2800	2600	2400	1212	900	856	825	800	700	0
300	200	5600	4700	3600	3500	3200	2900	2800	1760	1717	1301	1209	1200	1170	1140	849	600	0
300	300	4592	3324	3300	3250	3200	2800	2700	2600	2500	2400	2091	1746	1084	511	287	250	0
300	500	4634	3367	3300	3250	3200	2700	2600	2575	2550	2500	1988	1373	945	400	250	200	0
300	750	6000	5000	3900	3800	3200	2600	2500	2400	2337	2100	1687	1400	1396	386	281	200	0
300	1000	6200	5200	4000	3900	3200	2600	2500	2400	2229	2100	1800	1500	1200	700	400	200	0
300	1500	6400	4154	4100	4000	3200	2600	2500	2456	2301	2100	1800	1500	1200	700	400	200	0
300	2000	6600	4300	4200	4100	3200	2600	2500	2294	2200	2100	1800	1500	1200	700	400	200	0
300	3000	7778	5690	4800	4706	3200	2600	2500	2294	2200	2100	1800	1500	1200	700	400	200	0
300	4000	3443	6302	4518	4400	3200	2600	2500	2294	2200	2100	1800	1500	1200	700	400	200	0
300	5000	3419	4851	3967	3525	3200	2600	2500	2294	2200	2100	1800	1500	1200	700	400	200	0
300	7500	5316	5198	4236	3630	3200	2600	2500	2300	2200	2100	1800	1500	1200	700	400	200	0
450	0	4540	4222	1900	1968	380	360	340	320	300	280	240	200	160	156	93	90	0
450	50	5035	4627	2330	2250	2195	2115	2035	1993	1950	1870	1860	1625	896	633	567	500	0
450	100	5200	4100	3400	2900	2800	2700	2600	2550	2500	2400	1500	1234	1217	1090	949	585	0
450	200	5600	4150	3400	3000	2800	2600	2550	2500	2200	1700	1650	1600	1500	1243	841	572	0
450	300	4145	2896	2850	2825	2800	2600	2500	2450	2400	2375	2358	1841	1677	744	447	414	0
450	500	4187	2939	2900	2850	2800	2600	2400	2400	2400	2200	2200	1738	1240	435	275	254	0
450	750	6000	4300	3400	3100	2800	2600	2300	2150	2000	2785	1439	1024	876	395	300	256	0
450	1000	6200	4400	3400	3200	2800	2600	2100	1976	1821	1500	1300	1000	564	500	300	200	0
450	1500	6400	4145	3060	3200	2800	2600	2000	2004	1849	1500	1250	673	450	500	300	200	0
450	2000	6600	3521	3400	3300	2800	2600	2100	1800	1500	1300	1200	1000	700	500	300	200	0
450	3000	9216	5752	4146	3716	2800	2600	2200	1800	1500	1300	1200	1000	700	500	300	200	0
450	4000	9594	6210	4292	4076	2800	2600	2200	1800	1500	1300	1200	1000	700	500	300	200	0
450	5000	6619	6002	5440	3500	2800	2600	2200	1900	1500	1300	1200	1000	700	500	300	200	0
450	7500	6878	6271	5707	3600	2800	2600	2200	2000	1600	1300	1200	1000	700	500	300	200	0
700	0	4482	4264	2059	1488	448	424	401	377	354	330	283	236	189	97	72	47	0
700	50	5021	4669	2488	1971	2212	2056	1825	1594	1363	1133	971	809	496	363	424	472	0
700	100	5200	4200	3500	3000	2800	2600	2300	2000	1700	1400	1200	1000	842	764	691	572	0
700	200	5600	4250	3600	3200	3000	2900	2700	2600	2500	1900	1650	1589	1500	1450	947	647	0
700	300	5800	4300	3700	3400	3000	2900	2700	2600	2550	2500	2461	2404	1600	1140	662	529	0
700	500	5900	4400	3800	3500	3000	2900	2800	2700	2650	2600	2500	2396	1376	645	419	359	0
700	750	6000	4600	3900	3600	3000	2700	2600	2500	2400	2300	2229	1419	717	412	410	376	0
700	1000	6200	5060	4094	3600	3000	2800	2700	2690	2133	1593	1306	888	484	269	250	200	0
700	1500	6400	4991	4025	3600	3000	2500	2400	2380	1837	1022	1138	722	274	199	175	150	0
700	2000	6600	5200	4400	3600	3000	2500	2200	1800	1500	1300	1300	900	250	200	200	150	0
700	3000	6800	5400	4600	3600	3000	2500	2200	1800	1500	1300	1200	900	250	200	200	150	0
700	4000	7000	5600	4800	3600	3000	2500	2200	1800	1500	1300	1200	900	250	200	200	150	0
700	5000	7200	5800	4900	3600	3000	2500	2200	1900	1500	1300	1200	900	250	200	200	150	0
700	7500	7400	6000	5000	3600	3000	2500	2200	2000	1600	1300	1200	900	250	200	200	150	0

700	4000	7000	5600	4800	3600	3000	2500	2200	1900	1500	1300	1200	900	250	200	200	150	0
700	5000	7200	5800	4900	3600	3000	2500	2200	2000	1600	1300	1200	900	250	200	200	150	0
700	7500	7400	6000	5000	3600	3000	2500	2200	2000	1600	1300	1200	900	250	200	200	150	0

1000	0	4480	3866	3240	2620	509	483	456	429	402	375	322	268	214	161	107	54	0
1000	50	5620	5092	4560	4105	3427	3271	3114	3032	2801	2569	2330	1942	1104	875	814	426	0
1000	100	6000	5500	5000	4600	4400	4200	4000	3900	3600	3300	3000	2500	1400	1113	1050	550	0
1000	200	8000	7500	7000	6000	5800	5600	5400	5100	4700	4300	4000	4200	2327	1697	1139	702	0
1000	300	3000	7500	7000	6500	6300	5600	5400	5100	4700	4400	4250	3914	2202	1544	918	683	0
1000	500	8000	7500	7000	6500	6200	5600	5400	5100	4800	4663	4500	3726	2083	1095	609	437	0
1000	750	8000	7500	7000	6500	6100	5600	5400	5000	4900	4785	3936	2297	1134	683	549	500	0
1000	1000	8000	7500	7000	6500	6000	5600	5300	5100	4845	4193	2934	1613	867	575	376	250	0
1000	1500	8000	7500	7000	6500	5900	5300	5000	4800	4459	3354	2366	1307	624	276	188	100	0
1000	2000	8000	7500	7000	6500	5700	5200	4800	4400	3354	3300	3226	2493	800	250	150	100	0
1000	3000	8000	7500	7000	6500	5500	5100	4700	4200	3573	3400	3326	1300	750	250	150	100	0
1000	4000	8000	7500	7000	6500	5300	5000	4500	4000	3400	2800	1850	1150	700	250	150	100	0
1000	5000	8000	7500	7000	6500	5400	4900	4400	3800	3300	2600	1650	1000	650	250	150	100	0
1000	7500	8000	7500	7000	6500	5500	4800	4300	3600	3200	2300	1500	900	600	250	150	100	0
1500	0	4525	4007	3488	2970	584	553	523	492	461	430	369	307	246	184	123	61	0
1500	50	5781	5100	4922	4493	3596	3513	3356	3273	3115	2883	2567	2327	1149	1021	879	426	0
1500	100	6200	5500	5400	5000	4600	4500	4300	4200	4000	3700	3300	3000	1450	1300	1131	548	0
1500	200	7100	6900	6600	6400	6200	6000	5700	5400	5000	4100	3600	3100	2131	2062	1314	779	0
1500	300	7400	7100	6700	6500	6300	6000	5700	5300	5200	4400	3800	3294	3000	2122	1334	843	0
1500	500	7700	7200	6700	6400	6100	5800	5500	5300	5000	4649	4500	4297	3152	1859	997	608	0
1500	750	8000	7200	6700	6300	5900	5600	5400	5200	5150	5100	4551	2990	1765	1087	681	443	0
1500	1000	8000	7200	6700	6250	5700	5600	5550	5500	5450	5169	3733	2116	1125	793	450	366	0
1500	1500	8000	7200	6700	6250	5500	5300	5275	5271	4969	4591	2913	1511	873	455	236	200	0
1500	2000	8000	7200	6700	6200	5500	5200	4900	4100	4000	3977	2505	1418	1000	800	400	200	0
1500	3000	7529	6720	6700	6100	5600	5100	4800	4813	4200	3700	2300	2100	1000	800	400	200	0
1500	4000	7645	6836	6700	6100	5600	5000	4700	3800	3800	3100	1900	1800	1000	800	400	200	0
1500	5000	3500	7500	6900	6300	5600	4800	4400	3600	3500	2600	1700	1500	1000	800	400	200	0
1500	7500	9000	8000	7100	6300	5500	4700	4100	3600	3300	2350	1600	1200	1000	800	400	200	0
2000	0	4581	4130	3680	3230	643	609	575	541	507	474	406	338	271	203	135	68	0
2000	50	5870	5420	4970	4708	3836	3752	3594	3510	3352	3118	2601	2710	1193	941	927	434	0
2000	100	6300	5850	5400	5200	4900	4800	4600	4500	4300	4000	3600	3500	1500	1287	1191	556	0
2000	200	7000	6900	6800	6700	6600	6300	6000	5600	5300	4800	4400	4000	2151	2020	1311	824	0
2000	300	7600	7350	7200	6900	6600	6600	5900	5700	5500	5200	4950	4181	4313	2749	1500	869	0
2000	500	8200	7800	7500	7200	6600	6600	6200	5964	5514	5183	4750	4457	3688	2222	1274	777	0
2000	750	3400	8000	7600	7200	7000	6981	6361	6200	6100	6096	5129	3590	2319	1281	954	586	0
2000	1000	8700	8400	7800	7762	7061	6718	6301	6047	5573	5581	4234	2769	1713	1029	607	479	0
2000	1500	3800	8400	7800	7144	6867	6459	5649	5000	4900	4870	3239	1909	1041	704	316	300	0
2000	2000	9200	8500	7800	7000	6500	5078	4650	4395	4111	3955	3218	1073	481	415	400	300	0
2000	3000	3944	8135	7800	7000	6200	5600	5506	4918	4717	4508	3217	1600	1200	1000	400	300	0
2000	4000	9060	8251	7800	6900	5900	5500	5080	4900	4889	4415	2816	1400	1200	900	400	300	0
2000	5000	10000	8500	7000	6500	5800	5500	5200	4600	4500	4202	2400	1400	1200	900	600	500	0
2000	7500	10300	8500	7200	6100	5500	5200	4900	4500	4324	2800	1700	1500	1300	1100	800	600	0

Table 4 (cont'd)

Pressure (kPa)	G (kg m <sup>-2</sup> s <sup>-1</sup> )	Quality																
		-0.15	-0.10	-0.05	0.00	0.05	0.10	0.15	0.20	0.25	0.30	0.40	0.50	0.60	0.70	0.80	0.90	1.0
3000	0	4650	4290	3930	3570	919	690	651	613	575	536	460	383	306	230	149	147	0
3000	50	6038	5573	5108	4868	4130	3997	3913	3753	3594	3359	3040	2721	2327	882	391	323	0
3000	100	6500	6000	5500	5300	5200	5100	5000	4800	4600	4300	3900	3500	3000	1223	831	726	0
3000	200	8000	7500	7000	6600	7000	6700	6300	6000	5700	5400	4800	4000	3503	2055	1425	837	0
3000	300	9000	8500	7352	7029	7900	7700	7300	6970	6600	6260	5500	4233	4200	2614	1664	884	0
3000	500	9600	9300	7968	7645	8000	7700	6734	6479	6272	5902	5589	4064	3719	2522	1769	1035	0
3000	750	9800	9300	8700	8410	7227	6948	6945	6388	6175	6133	5519	3637	2825	1996	1281	663	0
3000	1000	9800	8000	7187	7679	7010	6648	6500	6380	5755	5239	4174	3246	2257	1823	1074	1006	0
3000	1500	9800	7552	7184	7000	6749	6548	5690	5200	4771	4486	3410	2545	1787	1623	1500	1275	0
3000	2000	9900	9000	8500	8000	7500	6975	5878	5125	4374	4107	2795	2099	1288	1000	1000	600	0
3000	3000	10000	9000	7600	8400	7482	5986	5401	4973	4443	3043	1943	2109	1133	1050	1000	600	0
3000	4000	10500	9000	7500	6517	5754	5409	5014	4629	3915	2134	2000	1900	1750	1350	1000	600	0
3000	5000	10800	8342	7171	6020	5367	5164	4685	4117	3564	2100	1900	1900	1750	1350	1000	600	0
3000	7500	11200	8608	7200	5504	4590	4117	3779	3600	3424	2200	2150	2000	1800	1500	1200	700	0
4500	0	4676	4400	4125	3850	1362	793	730	687	644	601	515	429	344	240	134	100	0
4500	50	5669	5300	5006	4713	3941	3573	3482	3247	2711	2175	1629	1232	836	372	338	300	0
4500	100	6000	5600	5300	5000	4800	4500	4400	4100	3400	2700	2000	1500	1000	800	746	666	0
4500	200	7900	7300	6700	6000	5800	4900	4700	4600	4200	3700	3200	2800	2500	1600	1419	954	0
4500	300	8100	7600	6490	6367	6300	5400	5300	5200	4700	4600	4440	3627	3480	2240	1620	1049	0
4500	500	8200	7800	7106	6783	5900	5516	5035	4500	4181	3852	3480	3067	2500	2358	1691	1103	0
4500	750	8300	8000	7500	6600	5593	5121	4802	4500	4300	4200	3923	2704	2602	2301	1631	965	0
4500	1000	8700	6500	6244	6067	5803	4800	4622	4385	4350	4336	3731	3032	2554	2552	1400	875	0
4500	1500	8900	6138	5724	5600	5500	5407	4846	4511	4083	3974	3178	2663	1976	1713	1200	800	0
4500	2000	6239	6484	5422	5422	5400	5233	4754	4204	3906	3821	2762	2064	1415	1300	1000	200	0
4500	3000	6580	6177	5453	5100	5054	4818	4606	4161	3743	3156	2013	1324	639	391	300	224	0
4500	4000	3901	6682	6034	5248	4849	4506	4248	3849	3251	2446	1700	1600	1500	393	309	200	0
4500	5000	3200	7836	6453	4917	4528	4273	4018	3671	2975	2263	1700	1600	1500	1300	1100	900	0
4500	7500	9400	8354	6800	4923	4375	3415	3613	3600	3214	2770	2600	2200	1800	1500	1300	1000	0
7000	0	4538	4348	4160	3970	1921	1221	868	761	713	666	570	475	380	195	121	100	0
7000	50	5485	5137	4790	4443	3780	3380	3142	2965	2578	1966	1493	1169	920	525	288	200	0
7000	100	5800	5400	5000	4600	4400	4100	3900	3700	3200	2400	1800	1400	1100	900	668	660	0
7000	200	6500	6000	5500	5093	4800	4600	4500	4400	4000	3500	3000	2300	1600	1450	1300	1165	0
7000	300	7000	6300	5600	5122	5000	4800	4700	4400	4100	4000	3500	2630	2568	1914	1521	1236	0
7000	500	7250	6500	5800	5500	5300	5200	5000	4414	4293	3224	2662	2438	2235	2069	1587	1083	0
7000	750	7500	7000	6200	5700	5600	5557	5044	3907	3692	3272	2839	2618	2292	1937	1497	1046	0
7000	1000	7700	5802	5626	5122	5100	4416	4170	3575	3400	3215	2853	2557	2243	1431	1009	800	0
7000	1500	7900	5453	4966	4800	4747	4392	3915	3469	3206	3016	2505	1538	1482	721	600	400	0
7000	2000	5966	5889	4956	4638	4349	3680	3170	3167	2878	2659	1712	1013	634	313	176	115	0
7000	3000	6286	5858	5138	4213	3787	3205	3028	3078	2823	2178	1088	465	262	213	171	124	0
7000	4000	8217	6382	5757	4604	3737	2942	2687	2437	2075	1668	1068	600	255	234	175	110	0
7000	5000	8600	7814	6357	4465	3603	2857	2453	2428	2298	1770	1136	600	400	300	250	150	0
7000	7500	9100	8400	6903	4857	4046	3169	2478	2300	2200	1953	1700	700	500	400	300	200	0

7000	4000	8217	8382	7127	7007	3727	2857	2453	2428	2298	1770	1136	600	400	300	250	200	0
7000	5000	8600	7814	6357	4465	3603	2857	2453	2428	2298	1770	1136	600	400	300	250	200	0
7000	7500	9100	8400	6903	4857	4046	3169	2478	2300	2200	1953	1700	700	500	400	300	200	0

100000	0	4144	4019	3894	3770	2280	1584	1181	918	748	698	598	498	399	300	250	200	0
100000	50	4486	4230	4000	4018	3495	2946	2545	2180	1837	1524	1200	950	700	450	400	397	0
100000	100	4600	4300	4200	4100	3500	2731	2680	2636	2469	1807	1716	1659	1590	1067	800	754	0
100000	200	5000	4600	4450	4400	2861	2700	2600	2538	2398	2100	1800	1650	1550	1327	1280	1150	0
100000	300	5100	4311	4300	4197	3938	3600	3575	3299	3139	2799	2396	1989	1698	1391	1120	844	0
100000	500	5873	5089	4460	4000	3700	3682	3426	2956	2803	2513	2259	1849	1371	1027	735	598	0
100000	750	5076	4815	4465	3635	3500	3475	3265	2910	2680	2227	1897	1443	1023	680	443	301	0
100000	1000	4500	4400	4385	4035	3671	3388	3329	3150	2731	2163	1556	1164	803	600	550	400	0
100000	1500	4859	4606	4445	3919	3652	3393	3087	2596	2114	1678	1050	678	623	500	400	300	0
100000	2000	5900	5023	4783	4070	3602	2962	2233	1899	1670	1346	761	390	362	275	230	166	0
100000	3000	6400	5472	5174	3650	3256	2561	2024	1837	1811	1428	866	277	223	220	209	168	0
100000	4000	7100	6120	5200	3659	3061	2539	1826	1600	1564	1182	768	700	500	400	177	160	0
100000	5000	8322	7155	5532	4080	3113	2586	1967	1879	1700	1545	1262	800	500	400	177	160	0
100000	7500	8835	7355	6052	4555	3681	2872	2262	2200	2100	1800	1554	1000	500	400	170	160	0
150000	0	3103	3046	2987	2930	2206	1731	1395	1145	952	798	577	481	385	300	250	199	0
150000	50	3176	3087	2997	2908	2501	2158	1999	1786	1663	1549	1419	795	696	500	450	404	0
150000	100	3200	3100	3000	2900	2400	2200	1900	1800	1700	1615	1513	1308	1173	772	578	550	0
150000	200	3200	3200	3000	2500	1800	1600	1500	1417	1400	1350	1300	1200	1125	863	654	650	0
150000	300	3300	2728	2700	2632	2573	2300	2284	2000	1878	1600	1500	1083	795	548	370	379	0
150000	500	3300	3200	2946	2400	2200	2124	2090	1706	1578	1434	1163	796	465	289	211	173	0
150000	750	3400	3400	3004	2447	2149	2214	2041	1560	1362	1127	744	460	312	222	200	173	0
150000	1000	3100	3000	2978	2576	2257	1893	1646	1420	1299	1037	523	311	250	225	200	173	0
150000	1500	3272	3089	2855	2340	2009	1666	1414	1193	893	748	395	283	250	225	200	173	0
150000	2000	3819	3595	3107	2421	2171	1816	1439	1009	726	694	565	586	530	225	200	173	0
150000	3000	4400	3847	3573	2661	2241	1813	1457	1176	1150	954	885	800	530	225	200	173	0
150000	4000	5100	4200	3154	2860	2437	2031	1491	1362	1592	1102	1033	900	700	225	200	173	0
150000	5000	5583	4658	4056	3694	2976	2438	2100	1983	1800	1495	1291	1000	750	710	400	200	0
150000	7500	5791	5301	4387	4480	3773	2822	2400	2274	2100	1877	1669	1100	950	910	400	200	0
200000	0	1107	1087	1066	1045	907	791	692	607	533	467	357	269	200	150	100	50	0
200000	50	1133	1101	1069	1037	922	813	762	687	642	598	544	308	264	199	170	146	0
200000	100	1142	1106	1070	1034	927	820	785	713	678	642	606	321	285	563	368	399	0
200000	200	1142	1142	1070	1034	927	820	785	700	640	606	571	560	496	488	420	404	0
200000	300	1177	1150	1100	1000	900	850	785	713	650	571	535	440	334	260	184	150	0
200000	500	1177	1142	1013	1097	903	820	813	722	652	547	415	290	211	122	100	98	0
200000	750	1213	1213	1000	963	907	895	755	636	475	401	361	250	158	110	100	98	0
200000	1000	1280	1268	1251	999	901	875	853	634	510	500	350	253	161	110	100	98	0
200000	1500	1296	1260	1100	1050	1000	998	968	682	590	564	412	340	189	110	100	98	0
200000	2000	1560	1408	1200	1190	1144	1143	1141	857	747	679	595	507	189	110	100	98	0
200000	3000	1882	1700	1606	1550	1450	1400	1343	1267	1131	986	833	639	189	110	100	98	0
200000	4000	2500	2400	2300	2200	2100	2000	1800	1517	1410	1248	983	649	189	182	178	143	0
200000	5000	3085	2831	2771	2561	2373	2350	2180	1927	1689	1405	940	700	268	253	250	214	0
200000	7500	3268	2969	2900	2800	2758	2500	2412	2164	1950	1557	1016	750	339	325	321	250	0

construct a standard table of CHF values for a given geometry (Doroshchuk et al., 1975). The table approach has been continued at the CENG in Grenoble and at the University of Ottawa using a much more extensive data base (10,000-tube CHF data). The table was completed at the Chalk River Nuclear Laboratories. The CHF table for an 8-mm tube is shown in Table 4. It was derived by statistically averaging experimentally obtained CHF values within each  $P$ ,  $G$ , and  $X$  interval. At conditions where the data were scarce or unavailable, CHF values were obtained from extrapolations using the factors and parametric trends described in Table 5. CHF values for a tube of  $D \neq 8$  mm may be obtained from  $\text{CHF}_D = \text{CHF}_8 (8/D)^{1/3}$  for  $4 < D < 16$  mm. Table look-up techniques are accurate (e.g., see Fig. 9), simple to use, and can easily be given the correct parametric and asymptotic trends. They normally do not require extrapolations since the range of conditions covered is sufficiently wide. They do, however, require interpolation to evaluate CHF at nonmatrix conditions. For very low flows and downflow, the approach suggested by Groeneveld and Rousseau (1983) is recommended.

#### 4.3.3 Graphical Techniques

A number of graphical techniques for predicting CHF have been developed by Katto and Shah. Katto's (1978, 1979a,b) method is based on distinguishing between various flow regimes. For each flow regime, graphs were presented to find the CHF as a function of flow and fluid properties. More recently, Katto (1980) presented correlations for each graph. Shah (1979) also presented the CHF in graphical form using a parameter  $Y$ , which depends both on flow and fluid properties. For low  $Y$  values, local as well as inlet conditions were required to evaluate the CHF. These graphic techniques are valid for a wide range of fluids. They are considered excellent for handbook applications and for obtaining a first estimate of the CHF value, especially for fluids for which no CHF data are available.

#### 4.4 Parametric Trends

##### 4.4.1 General

The correlations presented in Table 3 all have limited ranges of application. Extrapolations are, therefore, frequently necessary because of a mismatch of the data base range and the range of reactor accident conditions.

Frequently, effects such as flux distribution, subcooling, or spacer effects have been incorporated in CHF correlations using the parametric trends suggested in Table 5. In addition, the correlations are sometimes modified to satisfy the following commonly observed asymptotic trends:

- CHF approaches pool boiling CHF at low flows;
- CHF approaches zero for  $X$  and  $\alpha$  approaching 1.0;
- CHF cannot be less than zero, not even for negative flow (downflow);

TABLE 5. Parametric Trends<sup>a</sup>

Effect	Correction factor	References	Comments																				
Spacing device	$\frac{\text{CHF with grids}}{\text{CHF without grids}} = 1 + 0.1 \exp \left( - \frac{L_{sp}}{40 Dh_y} \right)$	Smolin and Polyakov (1978)	Constants 0.1 and 40 must be dependent on spacer geometry.																				
	$\frac{\text{CHF with grids}}{\text{CHF without grids}} = 1 + \phi K \left( \frac{G}{1 - \alpha} \right)^{0.6} D_{he}^{0.28} \exp \left( - \frac{\psi L_{sp}}{Dh_y} \right)$	Tong (1975)	Based on experiments using PWR-type bundles and grids.																				
	$\phi, \psi$ are spacer and flow regime constants																						
	$K$ = pressure loss coefficient of spacer		N.B. Increases in CHF of over 200% have been observed for short spacer pitch. Spacers also improve post CHF heat transfer																				
	$L_{sp}$ = spacer pitch																						
Diameter	$\frac{\text{CHF}(D)}{\text{CHF}(D_o)} = \left( \frac{D_o}{D} \right)^{1/2}$	Doroshchuk et al. (1975)	Valid for $4 \leq D < 16$ mm, for $\Delta T_{sub} < 75^\circ\text{C}$ and burnout of the first kind (not for very high qualities). Valid for positive qualities only; $q_o = f(P)$ .																				
	$\frac{\text{CHF}(D)}{\text{CHF}(D = 0.008)} = 1 + \frac{q_o}{\text{CHF}(D = 0.008)} \left( \frac{0.008}{D} \right)^{1/3} - 1$	Doroshchuk and Lantsman (1970)																					
	$\frac{\text{CHF}(D)}{\text{CHF}(D_o)} = \left( \frac{D_o}{D} \right)^n$ $n = 0.4, \text{ if } D > 10 \text{ mm}$ $n = 0.6, \text{ if } D < 10 \text{ mm}$	Biasi et al. (1967)	From Biasi's correlation. Ranges: $D = 0.003$ - $0.0375$ m, $P = 270$ - $14,000$ kPa,																				
	$\frac{\text{CHF}(D)}{\text{CHF}(D = 0.01)} = f(D)$	Becker (1967)	$G = 100$ - $6000 \text{ kg m}^{-2} \text{ s}^{-1}$ , $\frac{1}{1 + \rho_g/\rho_l} < \chi < 1.0$																				
	<table><tr><td><math>D(\text{mm})</math></td><td>4</td><td>6</td><td>8</td><td>10</td><td>12</td><td>14</td><td>18</td><td>24</td><td>25</td></tr><tr><td><math>f(D)</math></td><td>1.18</td><td>1.176</td><td>1.085</td><td>1.00</td><td>0.973</td><td>0.962</td><td>0.94</td><td>0.917</td><td>0.90</td></tr></table>	$D(\text{mm})$	4	6	8	10	12	14	18	24	25	$f(D)$	1.18	1.176	1.085	1.00	0.973	0.962	0.94	0.917	0.90		From Becker's correlation. Ranges: $D = 0.004$ - $0.025$ m, $P = 270$ - $10,000$ kPa, $G = 120$ - $5400 \text{ kg m}^{-2} \text{ s}^{-1}$ , $\chi = 0$ - $0.5$
	$D(\text{mm})$	4	6	8	10	12	14	18	24	25													
$f(D)$	1.18	1.176	1.085	1.00	0.973	0.962	0.94	0.917	0.90														
Flow	$\frac{\text{CHF}(G)}{\text{CHF}(G = 1000(\text{kg m}^{-2} \text{ s}^{-1}))} = \left( \frac{G}{1000} \right)^{0.68} \frac{P}{P_{cr}} - 1.2 \chi - 0.3$	Doroshchuk et al. (1975)	Derived from Doroshchuk's correlation. Large-tube data base. Ranges: $D = 0.004$ - $0.016$ m, $P = 290$ - $15,600$ kPa, $G < 2000 \text{ kg m}^{-2} \text{ s}^{-1}$ , $\Delta T_{sub} < 50^\circ\text{C}$																				
	$\frac{\text{CHF}(G)}{\text{CHF}(G_o)} = \left( \frac{G_o}{G} \right)^{1/2}$	Becker (1967)	From Becker's correlation. Large-tube data base. Ranges: $\chi = 0$ - $0.6$ , $G = 120$ - $5400 \text{ kg m}^{-2} \text{ s}^{-1}$ , $P = 270$ - $10,000$ kPa																				
	$\frac{\text{CHF}(G)}{\text{CHF}(G_o)} = \frac{1 + 1.06 \cdot 10^{-4} G}{1 + 1.06 \cdot 10^{-4} G_o}$	Griffel and Bonilla (1965)	Tube data covered: $368 < G < 10,000 \text{ kg m}^{-2} \text{ s}^{-1}$ , $3.5 < P < 10.5 \text{ MPa}$ , and negative $\chi$ ( $0 < \Delta T_{sub} < 65^\circ\text{C}$ ).																				

Table 5 (cont'd)

Effect	Correction factor	References	Comments
Pressure	$\frac{\text{CHF}(P)}{\text{CHF}(P_o)} = \left( \frac{1 - P/P_{cr}}{1 - P_o/P_{cr}} \right)^{0.1} \frac{\text{CHF}_{PB}(P)}{\text{CHF}_{PB}(P_o)}$ <p>where <math>\text{CHF}_{PB} = 0.14 h_{fg} \rho_g^{1/2} \left[ \sigma g (\rho_l - \rho_g) \right]^{1/4}</math></p> $\frac{\text{CHF}(P)}{\text{CHF}(P_o)} = \left( \frac{P_o}{P} \right)^{0.3234}$ $\frac{\text{CHF}(P)}{\text{CHF}(P_o)} = \frac{\text{CHF}_{PB}(P)}{\text{CHF}_{PB}(P_o)}$	<p>Tolubinsky et al. (1977)</p> <p>Levitan and Lantsman (1977)</p> <p>Condie and Bengston (1978)</p> <p>Griffith et al. (1977)</p>	<p>From Levitan's correlation based on a large number of annuli data.</p> <p>Ranges: <math>P = 5000-20,000</math> kPa, <math>\chi &lt; 0.3</math>  <math>G = 250-5000</math> kg m<sup>-2</sup> s<sup>-1</sup></p> <p>From RELAP 4-MOD 7 correlation. Based on large-bundle data base.</p> <p>Ranges: <math>P = 690-15,200</math> kPa, <math>\chi = -0.1-1.0</math>  <math>G = 100-4100</math> kg m<sup>-2</sup> s<sup>-1</sup></p> <p>From Griffith-Zuber correlation for same void fraction. Valid for low flows only.</p>
Adjacent Unheated Surface	$\frac{\text{CHF}_{\text{adj unh surf}}}{\text{CHF}_{\text{ref}}} = f(D_{he}, D_{hy}, \chi, G, P)$	Tong (1972a)	Adjacent unheated surface robs liquid that would otherwise be available for cooling of the heated surface
Void and transients (low flow)	$\frac{\text{CHF}}{\text{CHF}_{PB}} = (1 - \alpha)$	Griffith et al. (1977)	At low flow (also during CCF) flow quality becomes meaningless: $\alpha$ becomes a much better parameter to describe the vapor presence.
Void and transients (blowdown)	$\frac{\text{CHF}}{\text{CHF}_{W-3}(\chi = 0)} = 1.33(0.96 - \alpha)^{1/2} + \frac{q_{\text{steam}}}{\text{CHF}_{W-3}(\chi = 0)}$	Hsu and Beckner (1977)	From Hsu-Beckner correlation. Increases CHF due to transient effect. Reference CHF (CHF at $\chi = 0$ , W-3 correlation) is fairly arbitrary. Recommended for high pressure, blowdown transients.
Axial flux distribution	$\frac{\text{CHF}_{\text{non-UN}}}{\text{CHF}_{\text{UN}}} = F = \hat{f}(\text{AFD}, G, \chi)$ <p>CHF occurs when <math>q_{\text{BLA}} &gt; \text{CHF}_{\text{UN}}</math></p>	<p>Tong (1972a)</p> <p>Groeneveld (1981a)</p>	<p>Upstream AFD has a weak effect at highly subcooled conditions (local conditions dominate) but becomes important at higher enthalpies.</p> <p>In the annular flow regime, use boiling length average heat flux instead of local heat flux.</p>
Flux spike	$\frac{\text{CHF}_{\text{with spike}}}{\text{CHF}_{\text{ref}}} = f(G, \chi, \frac{q_{sp}}{q_{\text{avg}}}, \frac{L_{sp}}{D})$	Groeneveld (1975)	Short flux spikes can significantly affect CHF in the subcooled region but usually have negligible effect in annular flow regime.



Local enthalpy  
( $\chi < 0$ )

$$\frac{\text{CHF}(\Delta T_{\text{sub}})}{\text{CHF}(\Delta T_{\text{sub}} = 0)} = 1 + B \Delta T_{\text{sub}}$$

$$B = 0.1 \left( \frac{\rho_l}{\rho_g} \right)^{0.75} \left( \frac{C_p}{h_{fg}} \right)$$

$P(\text{MPa})$	20	35-70	100	150
$B(\frac{1}{^\circ\text{C}})$	0.058	0.055	0.053	0.050

Local enthalpy  
( $\chi > 0$ )

$$\frac{\text{CHF}(\chi)}{\text{CHF}(\chi_o)} = \frac{\chi_{\text{max}} - \chi}{\chi_{\text{max}} - \chi_o} \quad \chi_{\text{max}} = 1.0$$

$$\text{For very low } G: \chi_{\text{max}} = 1 - \frac{4 \text{ MWR}}{G D h_{fg}}$$

MWR = minimum wetting rate

$$\frac{\text{CHF}(\chi)}{\text{CHF}(\chi = 0)} = e^{-1.5\chi} \left( \frac{G}{1000} \right)^{-1.2\chi}$$

Cross section  
geometry

$$\frac{\text{CHF}_{\text{annulus}}}{\text{CHF}_{\text{tube}} (D = 8\text{mm})} = K_\chi K_F K_D$$

$P(\text{MPa})$	$< 6.9$	$> 6.9$	$D h_{fg}(\text{mm})$	$\leq 8$	$> 8$
$K_P$	1	$1.2\sqrt{P/9.8}$	$K_D$	$\left( \frac{D h_{fg}}{D_i} \right) 0.2$	$\left( \frac{64}{D_i D h_{fg}} \right) 0.2$

$$K_\chi = \min(1, e^{-2\chi})$$

CHF bundle = CHF annulus having equivalent  $D_i, D_o$

equiv.  $D_i = d$  (= rod diameter)

$$\text{equiv. } D_o = [d(d + D h e^*)]^{1/2}, D h e^* = \frac{4A}{n \pi d} \frac{q_{\text{max}}}{q_{\text{avg}}}$$

Ivey and Morris  
(1962)

Ivey's correction is based only on pool boiling results and agrees with water data at  $P < 1800$  kPa.

Povarnin  
(see Tong, 1972a)

Povarnin's correction is based on small-diameter tubing (2-3 mm) and  $P = 2000 = 20,000$  kPa.

Groeneveld  
(1981b)

Only for high-quality.  $\chi_o$  is highest quality where CHF is known. MWR value reported by Norman and McIntyre (1960).

Doroshchuk  
et al. (1975)

From Doroshchuk's correlation.

Ranges:  $P = 2900-15,600$  kPa,  $\Delta T_{\text{sub}} < 50^\circ\text{C}$ ,  
 $G < 2000 \text{ kg m}^{-2} \text{ s}^{-1}$ ,  $D = 0.004-0.016$  m,  
Burnout of the first kind only.

Levitan and  
Lantsman  
(1977)

Based on large number of annuli data and on tube CHF correlation from Doroshchuk et al. (1975) which was equally based on a large-tube data bank.

Barnett (1968)

Barnett obtained excellent agreement using the equivalent annulus and his annulus CHF correlation.

<sup>a</sup>For definition and units of all symbols, see Nomenclature.

- CHF reaches a maximum within the approximate pressure range of 3-4 MPa; and
- CHF approaches zero when  $P$  approaches  $P_{crit}$ .

The various parametric trends of CHF are discussed in detail in the following sections.

#### 4.4.2 Cross-Section Geometry

Most correlations of Table 3 are based on tube data. The correlations of Bowring, B & W-2 and RELAP4-MOD7 were derived from bundle data, whereas Griffith-Zuber's correlation is based on pool boiling and low flow annulus data. In general, the CHF in tubes is greater than the corresponding value (at the same cross-section average conditions and  $D_{hy}$ ) in bundles because

1. The subchannel with the highest enthalpy usually reaches the boiling crisis before a subchannel at cross-section average conditions.
2. Of the cold wall effect: a cold wall reduces liquid available for cooling heated rods (Tong and Hewitt, 1972).
3. Inside a subchannel, significant variation in velocities and near-wall void fraction may occur (Groeneveld, 1973). This is particularly evident in the gap between adjacent rods of tightly spaced rod bundles. One can thus expect preferential CHF locations within a single subchannel.
4. Upstream or fluid memory effects can become very important, especially in the net quality region. Large differences in subchannel enthalpy rise rates can result in significant asymmetric CHF patterns (McPherson, 1971).

Some of the above effects can be partially incorporated in subchannel codes. An excellent review of subchannel-type analyses has been presented by Weisman and Bowring (1975). Caution must be exercised when using subchannel codes since verification data frequently are lacking. Subchannel CHF correlations, based on bundle CHF data and predicted subchannel conditions, are especially unreliable. Their application should be limited to the narrow range of their data base. Subchannel codes currently under development are based on 2- or 3-fluid models (e.g., Tahir and Carver, 1982); they are expected to be capable of predicting the bundle CHF with a much better accuracy than their predecessors.

Tube and annuli CHF correlations may be useful in predicting the CHF behavior of bundles, especially for well-balanced bundles having wide rod spacings. Correction factors should then be used to include specific bundle characteristics. Barnett (1966, 1968) expressed the bundle cross-section parameters in terms of an equivalent annular geometry. Levitan and Lantsman (1977) used a correction factor based on quality, pressure, and diameter to convert a tube correlation into an annulus CHF correlation.

McPherson (1971) accounted for the differences in enthalpy rise rates and hydraulic resistances of subchannels in various bundle geometries by using a bundle enthalpy imbalance factor.

#### 4.4.3 Effect of Rod-Spacing Devices

A number of researchers have investigated the effect of various types of spacing devices on CHF. Groeneveld and Yousef (1980) presented a summary of these studies. Although these studies do not always agree with each other, the following trends may be observed:

1. In general, a significant increase in local CHF was observed just downstream of the spacers. This increase decayed slowly with distance downstream.
2. A minimum effect on critical power was observed for ferrule-type spacer grids made up of concentric rings fitting tightly around the heater rods. This type of spacer will result in two opposing effects: (1) the rings will strip the liquid film off the heated rods, thus lowering the critical power; and (2) the reduction in flow area at the spacer will generate turbulence and crossflow downstream. This mixing will reduce the subchannel enthalpy and flow imbalance in neighboring subchannels and hence increase the critical power. Gaspari et al. (1968) used spacers of this type and observed small effects on CHF.
3. The largest increase in critical power does not necessarily correspond to the grid spacer producing the largest flow blockage. This is clearly illustrated by the results of Gaspari et al. (1968, 1970). Their plate-type spacers with a flow blockage of 50% resulted in an 8% lower critical power than their ferrule-type spacers with a flow blockage of only 10%.
4. The maximum increase in CHF due to grid spacers usually occurs at high flows, high qualities, and short axial grid spacings. The majority of the studies (Groeneveld and Yousef, 1970) support this argument. Kobori's results (1976) show an opposing trend: a maximum increase in CHF was observed at low flows and low qualities. Most studies show that at low flows the effect of spacers on critical power is minimal (e.g., Becker and Hernborg, 1964; Groeneveld and Yousef, 1980).
5. Although an increase in CHF due to rod spacing devices was observed in most studies, detrimental effects can also be present. Both Ginoux (1978) and Janssen et al. (1969) reported up to 20% reduction in CHF in a 16-rod bundle due to egg crate-type spacers. In most studies the detrimental effect of spacers, etc.) is usually overshadowed by the much larger beneficial effect (due to improved mixing and phase distribution downstream of the spacer).
6. In the majority of experimental studies, the CHF was found to occur preferentially just upstream of a rod spacer. Only Ginoux (1978) reported preferential CHF occurrence just downstream of a rod-spacing device.

Table 5 presents correction factors that have been used to incorporate the spacer effect into existing CHF correlations.

#### 4.4.4 Effect of Heat Flux Distribution

Many experimenters have studied the effect of axial flux distribution (AFD) on critical heat flux (e.g., Tong, 1967, 1972a; Todreas and Rohsenow, 1965; Groeneveld, 1975). The common observation in these studies was that the AFD effect is strongly dependent on the boiling crisis mechanisms, as indicated in Table 6.

Table 6. Axial Flux Distribution Effect on CHF and Critical Power

Quality	Boiling crisis mechanisms	AFD Effect
Negative (subcooled dryout)	DNB, microlayer evaporation	CHF occurs when heat flux exceeds CHF for uniform heating on CHF versus $X$ plot.  No effect of upstream AFD on local CHF.  Strong effect of AFD on critical power for constant inlet subcooling.
High quality	Film dryout	Strong effect of upstream flux distribution on local CHF.  Magnitude and location of CHF difficult to predict.  Weak effect of AFD on critical power for constant inlet subcooling.
Zero-low quality	Bubble clouding	In between above effects.

Four prediction techniques are currently popular in predicting the CHF or burnout power for a heated section having a nonuniform AFD:

1. *Overall power hypothesis*: This hypothesis states that the critical power is a function only of inlet conditions and geometry. This technique does not permit the prediction of location or magnitude of the CHF and hence is not useful for accident analysis.
2. *Local conditions hypothesis*: This hypothesis states that the CHF is a function only of local conditions ( $P$ ,  $G$ ,  $X$ ,  $C/S$ ) and does not consider the effect of non-uniform upstream AFD.
3. *Boiling length average heat flux hypothesis*, or  $X_c$  versus  $q_{BLA}$  approach: This method assumes that for a given  $P$ ,  $G$ , and test

section  $C/S$  there is a unique relationship between the boiling length average heat flux and the critical quality, i.e., averaging the heat flux over the boiling length properly accounts for the effect of nonuniformity in upstream AFD.

4. *F-factor approach*: This approach corrects the CHF for nonuniform heating using the correction factor shown in Table 5.

These methods may be applied in bundle geometries using either a mixed flow or a subchannel-type correlation.

In a bundle having an optimum radial flux distribution (RFD), the CHF occurs simultaneously on all elements. Experiments by Gaspari et al. (1969) and Becker et al. (1967) suggest that the preferential location of initial dryout occurrence in a rod cluster having a uniform RFD is near the center of the bundle. The presence of a flux depression across the rod cluster tends to shift the location of initial dryout outward and increases the critical power (Gaspari et al., 1968). This increase in critical power is strongly dependent on the radial form factor ( $q_{\max}/q_{\text{avg}}$ ) and rod spacing, both of which affect the subchannel enthalpy imbalance. Both the Bowring (1977) and the RELAP4-MOD7 CHF correlations contain a radial form factor.

#### 4.4.5 Transient Effects

Leung (1978, 1980) presented an excellent assessment of current predictions for transient CHF. He noted that times to dryout, measured in bundles, were predicted reasonably well with local conditions-type correlations, especially for early CHF's (i.e., dryout within 1 s).

For annular flow, CHF predictions based on complete vaporization ( $X = 1.0$ ) also performed reasonably well. For delayed CHF (times to dryout greater than 2 s), correlations based on void fractions (Griffith-Zuber) usually resulted in better predictions, especially at low flows. This was expected since the quality at low flow transients no longer expresses the presence of the liquid phase, i.e., a 100% quality could refer to a continuous stream of vapor emerging from a tube filled with stagnant water. None of the prediction methods in the codes surveyed include a parameter describing the speed of the transient.

Very little work has been carried out in predicting the maximum heat flux during rewetting. This partially reflects the confusion with respect to the choice of a rewetting model, heat transfer coefficient, and quench temperature during rewetting. For very slow rewetting rates, no hysteresis effect is present. Cheng et al. (1978) found that the maximum heat flux during rewetting appeared to be in reasonable agreement with steady-state CHF correlations, while Bennett et al. (1967) in his steady state experiments did not notice any significant hysteresis effect on CHF during return to nucleate boiling.

#### 4.4.6 Other Effects

The discussion in this chapter has been limited to the most common parametric effects. Other effects, which may be significant, include flow direction, surface properties, and type of heating.

Their significance depends on the heat transfer configuration and accident scenario. Further details on parametric effects may be found in CHF reviews by Tong (1972), Tong and Hewitt (1972), Collier (1980), Hewitt (1978), Hewitt and Hall-Taylor (1970), and Bergles (1977, 1979).

#### 4.5 Final Remarks

CHF measurements are usually less accurate at high  $G$ ,  $X$ , and  $P$  because of the absence of a significant temperature excursion. At these conditions, post-dryout heat transfer is excellent, and the consequences of exceeding CHF are insignificant.

The local conditions approach is reasonable for most CHF conditions provided the AFD is nearly uniform. However, for  $L/D < 100$ , especially when combined with two-phase inlet conditions, the CHF can become strongly dependent on length. The length effect is least important at highly subcooled conditions.

The CHF table approach described in this chapter may be useful to reactor safety analysts in two ways: (1) the standard table may be incorporated directly into the reactor safety codes, thus replacing CHF correlations, or (2) the table may be used to check predictions of a CHF correlation, especially when the correlation is used outside its range of applicability.

Zuber-Griffith's CHF correlation  $[= CHF_{PB} (1 - \alpha)]$  appears reasonable for up- and downflow for mass velocities less than  $300 \text{ kg m}^{-2} \text{ s}^{-1}$  and  $\alpha < 0.8$ . However, for  $\alpha > 0.8$  this correlation significantly underpredicts the CHF. At these conditions the  $(1 - \alpha)$  correction is no longer recommended by the authors (Griffith et al., 1977).

Caution should be exercised when using empirical CHF correlations even within the range of their data base. For example, the highest flow CHF data are usually obtained only at low qualities and the lowest flow CHF data only at high qualities, because of experimental equipment limitations. Our analysis indicates that CHF correlations, used within their data base, can have prediction errors between -66% and +200%.

## 5 TRANSITION BOILING

### 5.1 Introduction

Transition boiling is a rather unique heat transfer mode because here the heat flux generally decreases with an increase in surface temperature. It is basically a combination of unstable film boiling and unstable nucleate boiling alternately existing at any given location on a heating surface.

The transition boiling section of the boiling curve is bounded by the critical heat flux and the minimum heat flux (Fig. 1). The critical heat flux has been extensively studied, but, as was shown in the previous chapter, there are still wide ranges of conditions where data are virtually nonexistent. The minimum heat flux has undergone less study; it is known to be affected by flow conditions, fluid properties, and heated surface properties.

In pool boiling, at surface temperatures just above the boiling crisis temperature, the heated surface is partially covered with unstable vapor patches, varying with space and time. The formation of such dry patches is accompanied by a drastic reduction in heat transfer coefficient corresponding to the change from nucleate boiling to film boiling; the corresponding reduction in local vapor generation permits the liquid to momentarily rewet the heated surface. Liquid contact with the heated surface is frequent at low wall superheats but becomes less frequent at higher wall superheats. A similar heat transfer process takes place during low-quality convective transition boiling, but here the convective velocities improve the heat transfer coefficient both in film and nucleate boiling.

In the high-quality region, most of the heat transferred during transition boiling is due to convection to the vapor and to droplet-wall interaction. Initially, at surface temperatures just in excess of the boiling crisis temperature, a significant fraction of the droplets deposit on the heated surface, but at higher wall superheats the vapor repulsion forces become significant and repel most of the droplets before they can contact the heated surface. The repelled droplets can contribute to the heat transfer by disturbing the boundary layer sufficiently to enhance the local heat transfer coefficient.

## 5.2 Data Trends

A thorough review of the transition boiling literature was conducted by Groeneveld and co-workers (1976, 1977) and Fung (1978). Since then, additional data have been reported by Ragheb et al. (1981). The data suffer from serious shortcomings and cover only narrow ranges of conditions; they are not considered sufficiently accurate and plentiful to serve as a basis for deriving a correlation. Parametric trends have been deduced from the data (Groeneveld and Fung, 1976). In general, an increase in mass flux increases the transition boiling heat flux, especially at higher wall superheats because of its strong positive effects on film boiling heat transfer. The effect of an increase in subcooling is similar, but the effect of quality is less clear. The data suggest that at low wall superheats an increase in quality will have a negative effect on the transition boiling heat flux (similar to its effect on CHF). At higher wall superheats, the film boiling mode dominates, and hence the reverse is true. Figure 11 illustrates the above trends. Note also the change in slope of the transition boiling curve from a negative value to a positive value at high flows and qualities. This trend is discussed in greater detail by Groeneveld and Borodin (1980).

## 5.3 Correlations

Despite the scarcity of transition boiling data, a large number of correlations have been proposed (Table 7). They may be divided into three groups:

1. *Correlations containing boiling and convective components*, e.g., Ramu and Weisman (1974), Mattson et al. (1974), and Tong (1972b). These correlations usually have the form

TABLE 7. Transition Boiling Correlations for Water<sup>a</sup>

Equations and References	Range of Applicability for Water				Comments
	$P$ (kPa)	$G \times 10^3$ (kg m <sup>-2</sup> s <sup>-1</sup> )	Subcooling (°C) or Quality	$T_w$ (°C)	Geometry (De)
$\phi = 3.51 \times 10^8 \times \Delta T_s^{-2.4}$ Ellion (1954)	110-413	0.33-1.49	28-56°C		Annulus (5.72 cm)
$\frac{CHF - \phi}{T_w - T_{CHF}} = 4.15 e^{3970/P}$ McDonough et al. (1961)	5510- 13,790	0.2-2.04	0-0.64	$T_{CHF-554}$	Tube (0.38 cm)
$\frac{\phi}{CHF} = \left( \frac{\Delta T_s}{T_{CHF} - T_s} \right)^n$ Berenson (1960)					Based on data obtained in steady-state tests with 7.5 cm heated length and a secondary stabilising fluid $30 \leq L/D \leq 62$ . Based on data from a heat flux-controlled system
$h_{FB} \text{ or } h_{FB} = 7000 \exp(-0.008 \Delta T_s)$ $+ 0.023 \frac{k_v}{De} \exp \left[ -\frac{190}{\Delta T_s} \left( \frac{Cp_l}{k} \right)_f^{0.4} \right]$ $\left\{ \frac{DeG}{u_f} \left[ X_e \frac{\rho_f}{\rho_g} + (1 - X_e) \frac{\rho_f}{\rho_l} \right] \right\}^{0.8}$	6890	0.38-5.23		321-832	Pool boiling correlations: $n = -3$ (Peterson, 1973) $n = -1$ (Groeneveld, 1976)  Agrees with data from Quinn (1965) and Bennett (1967) with rms error = 18%
Tong (1972a) <sup>b</sup>	103-620	0.05-0.25	9-105°C		49, 100-rod
$h_{FB} = 9000 \exp(-0.0054 \Delta T_s) + h_{FB} + h_{rad}$ $h_{FB} = 0.023 \left( \frac{k_v}{De} \right) \frac{GDe}{u_f} \left[ X_e \frac{\rho_f}{\rho_g} + (1 - X_e) \frac{\rho_f}{\rho_l} \right]^{0.8} \left( \frac{Cp_l}{k} \right)_f^{0.4}$					Correlation of bottom flooding data (FLECHT); extrapolation outside range is tentatively permitted



$$h_{\text{rad}} = 1.73 \times 10^{-9} \frac{1 - 0.6 \alpha}{1.25 - 0.15 \alpha} \frac{T_b^4 - T_s^4}{T_b - T_s}$$

Tong (1972b)<sup>b</sup>

$$n_{\text{TB}} = h_b + h_c$$

$$h_b = 0.55 h_m \left\{ \exp[-0.014 (T - T_{\text{CHF}})] + \exp[-0.1256 (T - T_{\text{CHF}})] \right\}$$

$$h_c = 0.023 \frac{k_g}{De} \left( \frac{\mu_g}{\mu_b} \right)^{0.14} \left( \frac{Cp_{\text{H}}}{k} \right)^{1/3} \left( \frac{GDeX_e}{\mu_g} \right)^{0.8} \left( 1 + \frac{1 - X_e}{X_e} \frac{\rho_g}{\rho_l} \right)^{0.8}$$

$$h_c = 0.023 \frac{k_g}{De} \left( \frac{\mu_g}{\mu_b} \right)^{0.14} \left( \frac{Cp_{\text{H}}}{k} \right)^{1/3} \left( \frac{GDeX_e}{\mu_g} \right)^{0.8} \left[ 1 + \frac{1 - X_e}{X_e} \left( \frac{\rho_g}{\rho_l} \right)^{2/3} \right]$$

$$h_c = 0.023 \frac{k_g}{De} \left( \frac{\mu_g}{\mu_b} \right)^{0.14} \left( \frac{Cp_{\text{H}}}{k} \right)^{1/3} \left( \frac{GDeX_e}{\mu_g} \right)^{0.8} \left[ \frac{0.15 + 0.86 X_e}{X_e^{0.8}} \right]$$

Ramu and Weisman (1974)

$$h_{\text{TB}} \text{ and } h_{\text{FB}} = 9.09 \times 10^4 \exp(-0.5/\sqrt{\Delta T})$$

$$+ 20.8 \left( \frac{GDe}{\mu_g} \right)^{0.269} \left( \frac{\mu_{\text{CP}}}{k} \right)^{3.67} De^{-0.319} k_g^{0.306} X_e^{-0.091}$$

$$h_{\text{TB}} \text{ and } h_{\text{FB}} = 2.93 \times 10^4 \exp(-0.5/\sqrt{\Delta T})$$

$$+ 1.22 \left( \frac{GDe}{\mu_g} \right)^{0.505} \left( \frac{\mu_{\text{CP}}}{k} \right)^{4.56} De^{-0.16} k_g^{0.189} X_e^{-0.113}$$

Mattson et al. (1974)<sup>b</sup>

$$q_{\text{TB}} = A \text{ CHF} + (1 - A) q_{\text{min}}$$

$$A = \left( \frac{T_{\text{min}} - T_b}{T_{\text{min}} - T_{\text{CHF}}} \right)^2$$

Bjornard and Griffith (1977)

Up to critical  
0.31-3.49

≥ 0.2

≥ 0.2

0 ≤ X<sub>e</sub> < 0.2

0.1-0.99

4130-  
21,530

Tube and  
annulus

Rod  
bundle

25.8% rms error

Reported to agree with  
Ramu's (1974) data  
(Bjornard, 1977)

Convective component  
correlation due to Quinn  
(1966); boiling component  
fitted to data of Hensch  
(1964), Polomik (1967), Cumo  
(1971), and Nobel (1970)  
with suppression factor S  
(due to Chen, 1963); h<sub>m</sub> based  
on critical heat flux data of  
Addoms (1948) (pool boiling)

At low flow and high quality,  
they replaced S h<sub>m</sub> with  
φ<sub>CHF</sub>/ΔT<sub>max</sub>; φ<sub>CHF</sub> is assumed  
to be a function of the void  
fraction only

Correlations obtained from  
regression analysis; 28% rms  
error

Table 7 (cont'd)

Equations and References	Range of Applicability for Water				Comments
	$P$ (kPa)	$G \times 10^3$ (kg m <sup>-2</sup> s <sup>-1</sup> )	Subcooling (°C) or Quality	$T_b$ (°C)	Geometry ( $D_e$ )
$\phi = C \frac{R \sigma C_p \rho_s T_s^2}{P \lambda h_{fg}} \frac{1 - X_e}{X_e} \frac{U \sqrt{f}}{\delta} \exp\left(-\frac{\Delta T_s}{\Delta T_m}\right)$ $+ \lambda(1 - \alpha) \left[ 1 - \exp\left(-\frac{T_s}{T_m}\right) \right] \frac{4k_f}{\delta} \left[ \left( 1 + \frac{2U_{mb}}{\delta} \right) \ln\left( 1 + \frac{\delta}{2U_{mb}} \right) - 1 \right] \frac{\Delta T_s}{\delta}$ $+ 0.023 \frac{k}{D_e} \left[ X_e + (1 - X_e) \frac{\rho_g}{\rho_l} \right]^{0.8} \left( \frac{\mu C_p}{k} \right) \frac{\Delta T_s}{\rho_l}$ $U_{mb} = \epsilon \left\{ \frac{\Delta T_s}{\Delta T_m} \right\} / \left[ 1 - \exp\left(-\frac{\Delta T_s}{\Delta T_m}\right) \left( 1 + \frac{\Delta T_s}{\Delta T_m} \right) \right]^{1/3}$ $\Delta T_m \text{ given by}$ $\frac{k_v \Delta T_m}{G D_e h_{fg}} = 3.274 \times 10^{-5} \left[ 2.93 + 4.44 X_e + 0.084 \left( \frac{G X_e}{125,000} \right)^2 \right]$ $- 7.361 \left( \frac{G X_e}{125,000} \right)^3 \left/ \left( \frac{G D_e}{\mu_v} \right)^{0.477} \right.$	6890	0.41-1.70	0.1-0.7		Tube
<p><math>C</math> = correlation constant; evaluated using data in transition boiling region, where the first term dominates.</p> <p><math>\lambda</math> = geometric parameter; can be evaluated from data at high wall superheat and low quality, where the second term dominates.</p> <p>Illoeje et al. (1974)<sup>b</sup></p> $\phi = \frac{\phi_{FB}}{1 - \phi_{TB}}$	6890	0.41-5.16	0.2-1.45	5.56 ≤ $\Delta T_s$ < 556	Tube
Based on data of Bennett et al. (1967) and Era et al. (1967); rms error = 13.8%					

$$\phi_{FB} = 0.023 \left( \frac{T_w - T_v}{T_v} \right) \left\{ \frac{k_v}{De} \left( \frac{GDe}{\mu} \right)^{0.8} \left[ \frac{nX_e \rho_v / \rho_g + S(1 - nX_e) \rho_v / \rho_l}{nX_e + S(1 - nX_e)} \right] \right\}^{0.8}$$

$$\times \left( \frac{10CP}{k} \right)^{0.4} \left( \frac{T_w}{T_v} \right)^{0.4}$$

$$n = 1.0 + \left( \frac{dn}{dX_e} \right) (X_e - X_1)$$

$$n = 1.0 \text{ for } \Delta T_g < 200^\circ\text{F or } \frac{G}{10^6} > 2.5$$

$$X_1 = \exp \left[ C_3 \left( 0.05 + \frac{G}{10^6} \right)^{0.8} \right]$$

$$\frac{dn}{dX_e} = C_4 \left( 0.05 + \frac{G}{10^6} \right)^{-0.12}$$

$$\text{for } G/10^6 \leq 0.7 \quad C_3 = -0.26 \quad C_4 = 0.49$$

$$0.8 \leq G/10^6 \leq 2.5 \quad C_3 = -0.57 \quad C_4 = -0.29$$

$$0.7 < G/10^6 < 0.8 \quad X_1 \text{ and } \frac{dn}{dX_e} \text{ obtained by linear interpolation}$$

$$\psi_B^T = \exp \left[ -0.012 \frac{X_e^{2/3}}{dX_e} \frac{\Delta T_g}{dL} \left( \frac{\Delta T_g}{100} \right)^{1 + 0.0016 \Delta T_g} \right]$$

Tong and Young (1974)<sup>b</sup>

$$h_{FB} = 0.62 \left[ \frac{g^{1/3} \rho_v (\rho_l - \rho_v) h_{fg}}{\Delta T_g \mu_v} \frac{1}{2\pi} \left( \frac{g(\rho_l - \rho_v)}{\sigma} \right)^{1/4} \right]$$

$$+ A \exp(-B \Delta T_g)$$

$$A = 1456 \text{ } P^{0.558}$$

$$B = 3.758 \times 10^{-3} \text{ } P^{0.1733}$$

$$\text{Hsu (1975)}^b$$

<sup>a</sup>For definition and units of all symbols, see Nomenclature.

<sup>b</sup>British engineering units.

Based on data of Groeneveld (1969), Polomik (1967), and Bennett et al. (1964); rms error = 29.2%

Annulus and rod bundle

$$5.56 < \Delta T_g < 556$$

$$0.15-1.10$$

$$0.68-4.21$$

$$3450-9650$$

Correlation based on FLECHT data; development of  $h_{FB}$  based on Taylor's instability; relations of  $A$  and  $B$  were plotted by Hsu and correlated by Groeneveld and Fung (1976)

100 rod

$$12-83$$

$$0.05-0.25$$

$$103-620$$

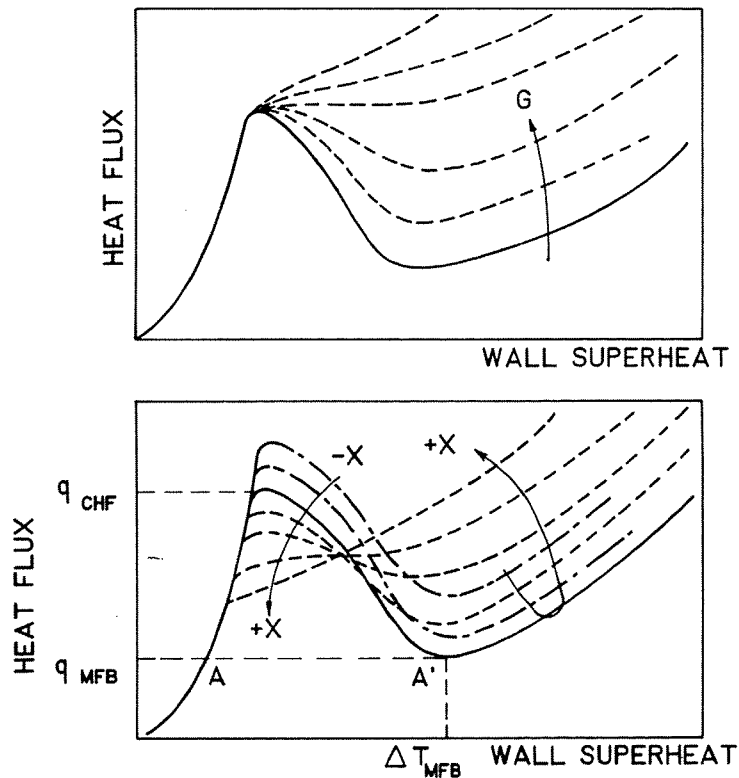


Fig. 11. Parametric trends of convective boiling curve.

$$h = A \exp(-B \Delta T_w) + \frac{k_v}{D_e} a \text{Re}_v^b \text{Pr}_v^c$$

where the first term on the right-hand side represents the boiling component (which becomes insignificant at high wall superheats) and the second term represents the convective component. These correlations are often claimed to be valid both in the transition boiling and film boiling regions.

2. *Phenomenological correlations*, e.g., Iloeje et al. (1974) and Tong and Young (1974). These correlations are based on a physical model of heat transfer in the transition boiling region. Because of an inadequate physical understanding, they still contain many empirical constants.

3. *Empirical correlations*, e.g., Ellion (1954), Berenson (1960), and McDonough et al. (1961). These correlations all have a very simple form and generally cannot be extrapolated outside the range of data on which they are based. Some of these correlations are based on the conditions at the boiling crisis (CHF and  $T_{CHF}$ ).

Frequently, when comparing correlations with one another, order-of-magnitude differences have been observed. Figure 12 illustrates some of the observed differences. More detailed comparisons have been shown by Groeneveld and Fung (1976).

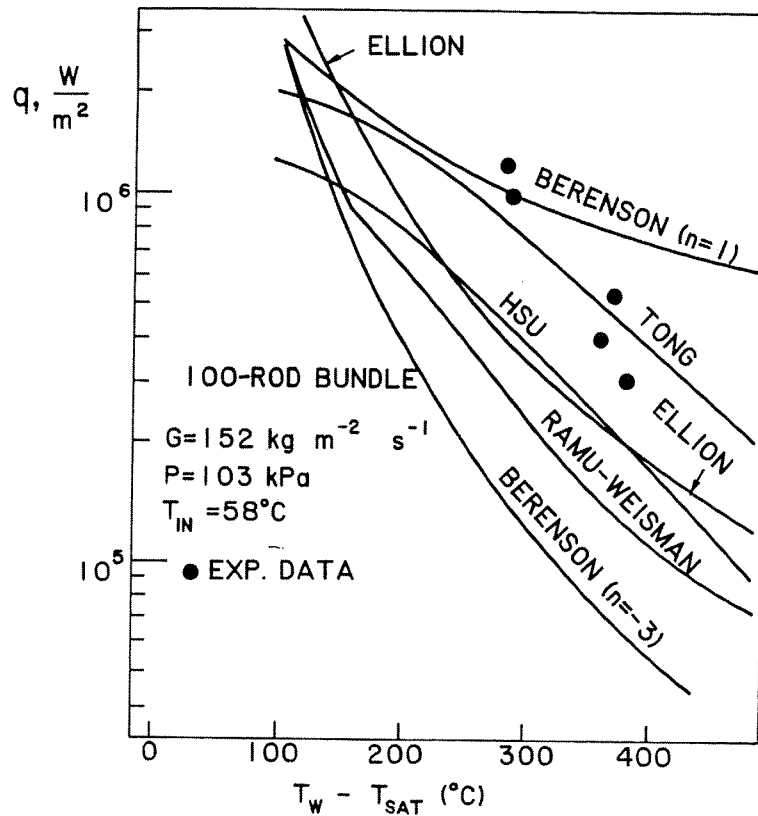


Fig. 12. Comparison of transition boiling correlations with "FLECHT" data. From Ellion (1954), Berenson (1960), Tong (1972b), Hsu (1975), Ramu-Weisman (1974).

#### 5.4 Prediction of the Critical Heat Flux Temperature

Many of the transition boiling correlations of Table 7 require a value for the CHF and the wall superheat at CHF,  $\Delta T_{\text{CHF}}$ , as a starting point. Traditionally,  $\Delta T_{\text{CHF}}$  has been evaluated from  $\text{CHF}/h$ , where  $h$  is either the nucleate boiling or forced convective evaporation heat transfer coefficient discussed in Sec. 3. A shortcoming of using the correlations of Table 2 for predicting  $\Delta T_{\text{CHF}}$  is the assumption that these correlations are valid up to the initiation of transition boiling. Experimental data usually shows a leveling off of the  $q$  versus  $\Delta T$  slope when the CHF point is reached (Ragheb et al., 1981), while the correlations predict a continuing steep slope. This is to be expected since the CHF is usually beyond the range of the data base used for developing the nucleate boiling correlation.

At least one author (Howard, 1976; Howard et al., 1975) has suggested that the CHF temperature corresponds to the sputtering temperature during top flooding. Sputtering temperature predictions are required for predicting the rewetting velocity (e.g., Thompson, 1974), and it would appear that the CHF temperature represents at least a lower bound to the sputtering temperature. Usually, however, the sputtering temperature is assumed to be equal to the minimum film boiling temperature (Sec. 6).

### 5.5 Discussion

When using the correlations of Table 7, it must be kept in mind that the correlations often do not agree with each other and that their data base is questionable. A limited comparison of some of the correlations with the data was carried out by Groeneveld and Fung (1976) and Fung (1977). Aside from ad hoc applications, such as using Hsu's correlation (1975) to predict FLECHT data (Fig. 12), none of the current correlations can be fully recommended. The most reasonable prediction was obtained by connecting the experimentally determined CHF and minimum film boiling points by a straight line on a log-log plot of  $q$  versus  $\Delta T_w$

$$\frac{q_{TB}}{q_{min}} = \left[ \frac{CHF}{q_{min}} \right]^{n_1} \quad \text{where } n_1 \triangleq \frac{\ln(\Delta T_{min}/\Delta T_w)}{\ln(\Delta T_{min}/\Delta T_{CHF})}$$

or

$$\frac{\Delta T_w}{\Delta T_{min}} = \left[ \frac{\Delta T_{CHF}}{\Delta T_{min}} \right]^{n_2} \quad \text{where } n_2 \triangleq \frac{\ln(q_{TB}/q_{min})}{\ln(CHF/q_{min})}$$

If experimental values or predictions for  $q_{min}$  (to be obtained from  $h_{FB} \Delta T_{min}$ ),  $\Delta T_{CHF}$ , and  $\Delta T_{min}$  are questionable or unavailable, the following correlation is tentatively suggested

$$q_{TB} = \max \left[ q_{FB}, CHF \left[ \frac{\Delta T_{CHF}}{\Delta T_w} \right] \right]$$

where  $\Delta T_{CHF}$  is obtained from  $\Delta T_{CHF} = CHF/h_{CHEN}$  (Chen, 1963) and  $q_{FB}$  is obtained from an appropriate film boiling model or correlation (Sec. 7).

### 5.6 Final Remarks

Few experimental studies on forced convective transition boiling have been done. The available studies suffer from serious shortcomings and cover only narrow ranges of conditions. They are not considered sufficiently accurate and plentiful to serve as a basis for deriving a correlation.

Present transition boiling correlations are valid only for the narrow range of conditions of the data on which they are based. A transition boiling correlation having a wider range of applications was suggested in the preceding section. It provides adequate predictions if CHF and  $\Delta T_{CHF}$  or  $q_{min}$  and  $\Delta T_{min}$  can be predicted with confidence. The present state of the art permits a reasonable prediction of CHF; predictions of  $\Delta T_{CHF}$ ,  $q_{min}$ , and  $\Delta T_{CHF}$  are still subject to a large degree of uncertainty.

The physical mechanisms governing forced convective transition boiling are poorly understood. This hinders the development of an analytical heat transfer model.

## 6 MINIMUM FILM BOILING

### 6.1 Introduction

The minimum film boiling temperature separates the high-temperature region, where inefficient film boiling or vapor cooling takes place, from the lower-temperature region, where the much more efficient transition boiling occurs. It thus provides a limit to the application of transition boiling and film boiling correlations. Knowledge of the minimum film boiling temperature is particularly important in reactor safety assessments.

In the literature a large number of terms have been used to describe the phenomenon at the boundary between transition boiling and film boiling, e.g., sputtering, DFFB (departure from film boiling), rewetting, film boiling collapse, Leidenfrost point, minimum film boiling. Frequently it is assumed that the temperature at the minimum of the boiling curve is equal to the minimum film boiling temperature (e.g., Nelson, 1980). It was shown in Fig. 11 that the boiling curve does not necessarily have a minimum, but it does always have a minimum film boiling temperature,  $T_{\min}$ . It is the latter that has a physical meaning and that is discussed in this chapter. We distinguish between six different types of film boiling terminations, which are shown schematically in Fig. 13 and discussed in Sec. 6.2.

The following two mechanisms for the minimum film boiling have been proposed and have been used to develop theoretical equations:

1. *Hydrodynamic Mechanism.* The separation of the liquid-vapor interface from the wall can be maintained only as long as the vapor generation rate exceeds the vapor removal rate (by trains of bubbles leaving from the tips of standing waves in the case of pool film boiling; Taylor's instability).
2. *Thermodynamic Mechanism.* Here it is assumed that liquid can never exist beyond a "maximum liquid temperature," which depends only on the liquid properties and hence is a unique function of pressure. Thus, a heated surface whose temperature is beyond the maximum liquid temperature cannot support liquid contact.

The above mechanisms do not include forced convective effects (flow rate, flow geometry, quality, or liquid subcooling), which may affect  $T_{\min}$ . Heated surface properties may also affect  $T_{\min}$ .

### 6.2 Minimum Film Boiling Types

The minimum film boiling phenomenon is usually encountered in one of the following fluid-wall configurations (Fig. 13):

- *Type I: Collapse of Vapor Film.* In this type, liquid contact with the heated surface is established as a result of a spontaneous collapse of a vapor film following a reduction in surface temperature. The preceding flow regime is the inverted-annular flow regime. This heat transfer configuration has been studied by Cheng et al. (1981), Groeneveld and Stewart (1982), and Stewart (1981).

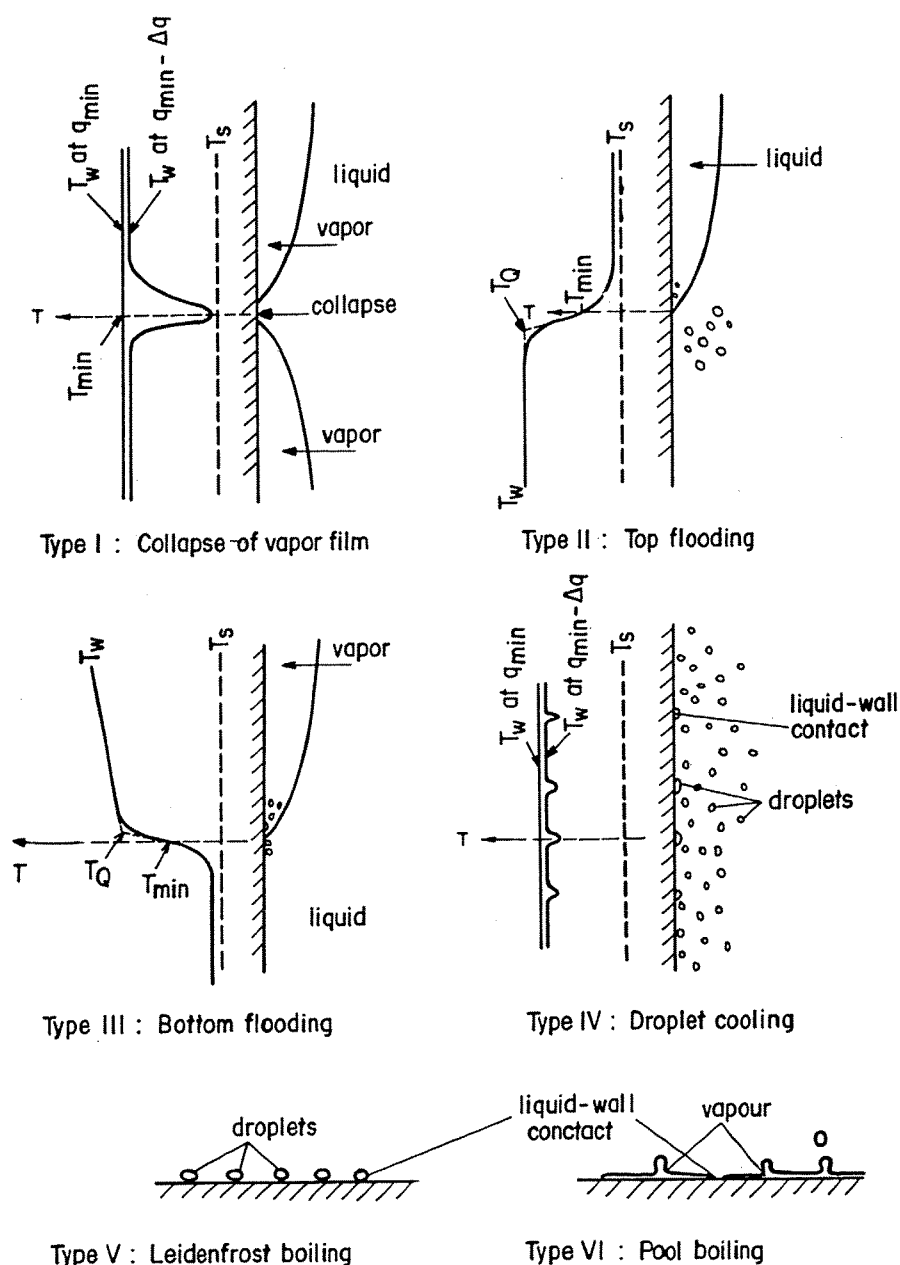


Fig. 13. Film boiling termination types.

- Type II: Top Flooding.** In top flooding, liquid contact with the heated surface is established by means of an axially propagating liquid film. Axial conduction is usually the main mechanism of reducing the surface temperatures just ahead of the quench front. Precooling effects can become important just ahead of the quench front at higher vapor flow rates. Direct measurement of  $T_{min}$  is difficult since the temperature drops rapidly near the quench front. Bennett et al. (1966), Butterworth and Owen (1975), and others have reported a linear relationship between the inverse rewetting front velocity and the wall superheat downstream of the quench front. Eventually, after lowering the surface temperature, the rewetting velocity becomes



equal to the liquid front velocity and independent of the surface temperature, i.e., the propagation of the quench front is no longer impeded by a high dry-side temperature. The temperature at which the rewetting velocity first becomes independent of the dry-side surface temperature is usually referred to as the sputtering temperature, and is thought to correspond to the triple interface (liquid-vapor-wall) temperature.

- *Type III: Bottom Flooding.* Prior to rewetting, the heated surface is precooled by film boiling (inverted annular, dispersed, or slug flow). Near the quench front, axial conduction becomes effective. Rewetting is due to an axially propagating rewetting front. Compared with top flooding, the precooling effect is usually much more significant for bottom flooding, except for low flow rates and high subcoolings, where the quench front velocity may be equal to the liquid level velocity. Thompson (1973) suggested that the sputtering temperature for bottom flooding is the same as in top flooding, while Howard and co-workers (1975, 1976) believe the bottom flooding sputtering temperature to be higher.
- *Type IV: Rewetting Following Dispersed Droplet Cooling.* The heated surface is precooled by a spray of droplets, which eventually may lead to the droplets rewetting the surface. A review of droplet-wall interaction for this configuration has been made by Groeneveld and McPherson (1973); it suggests the existence of a  $T_{min}$  at which the heat transfer efficiency changes drastically. Note that this type of minimum film boiling is characterized by the absence of a propagating rewetting front; thus, it is similar to the type I film boiling, except for the liquid phase being dispersed in the vapor instead of being continuous.
- *Type V: Rewetting of a Horizontal Surface by Leidenfrost Cooling.* Prior to rewetting, the heated surface is cooled by stationary discrete droplets separated from the heated surface by a vapor blanket. A reduction in the heated surface will eventually lead to an insufficient vapor generation rate to maintain droplet-wall separation. The temperature corresponding to the first contact of the droplets with the wall is usually referred to as the Leidenfrost temperature. This type of film boiling termination has been extensively studied (e.g., Bell, 1967; Snoek, 1972; Henry, 1974), and several correlations for this configuration are presented in Table 8.
- *Type VI: Collapse of Vapor Film on a Horizontal Surface During Pool Boiling.* This heat transfer configuration is similar to that of type V, except for the liquid phase being continuous rather than dispersed. Pool film boiling is terminated due to the vapor generation rate becoming smaller than the vapor removal rate. The corresponding temperature and heat flux may be predicted theoretically from Taylor's instability theory (Berenson, 1961; Table 8).

There appears to exist some confusion regarding the term *quench temperature* in the presence of a propagating rewetting front.

TABLE 8. Equations for the Minimum Film Boiling Temperature<sup>a</sup>

Equations	Comments
For $P < 9000$ kPa:	Empirical correlations based on convective water data
$T_{\min} = 284.7 + 0.0441 P - 3.72 \times 10^{-6} P^2$ $+ \frac{\Delta H \times 10^4}{(2.82 + 0.00122 P) H_{fg}}$	$P = 0.1 - 9$ MPa, $G = 50-2750$ kg m <sup>-2</sup> s <sup>-1</sup> , and $X = -0.10$ to $+0.13$
For $P > 9000$ kPa:	Type I or type IV (no quench front present)
$T_{\min} = (\Delta T_{\min}, 9000 \text{ kPa}) \left[ \frac{P_{\text{crit}} - P}{P_{\text{crit}} - 9000} \right] + T_{\text{sat}}$	
Groeneveld and Stewart (1982)	
$P < 689$ kPa; $\Delta T_{\min} = 0.0948 P + 29.1$ $689 \leq P \leq 4200$ kPa; $\Delta T_{\min} = 0.00765 P + 89.1$ $P > 4200$ ; $T_{\min} = T_C = 374.15$	Empirical correlation based on Bennett et al.'s (1966) and Shires et al.'s (1964) top flooding data; predict sputtering temperature. Type II quench
Groeneveld (1975)	
$\Delta T_{\min} = 0.127 \left[ \frac{\rho_v^2 f g}{k_v} \right] f \left[ \frac{g(\rho_l - \rho_v)}{\rho_l + \rho_v} \right]^{2/3} \left[ \frac{\sigma}{g(\rho_l - \rho_v)} \right]^{1/2}$ $\times \left[ \frac{\mu_f}{(\rho_l - \rho_v)} \right]^{1/3}$	Theoretical equation based on Taylor instability criterion; derived for pool boiling on a horizontal surface
Berenson (1960)	

$$\frac{T_{\min}^*}{T_c^*} = 0.13 \frac{P}{P_c} + 0.84 \quad (*\text{absolute temperature (K)})$$

Spiegler et al. (1963)

$$\frac{T_{\min} - T_{\text{sat}}}{T_{\text{crit}} - T_{\text{sat}}} = 1.65 \left[ 0.1 + 0.6 \frac{(\rho c k)_l}{(\rho c k)_w} + 1.5 \left( \frac{(\rho c k)_l}{(\rho c k)_w} \right)^{\frac{1}{2}} \right]$$

Kalinin et al. (1969)

$$T_{\min}^* = T_{\text{HN}}^* + (T_{\text{HN}}^* - T_l^*) \left[ \frac{(\rho c k)_l}{(\rho c k)_w} \right]^{\frac{1}{2}}$$

$T_{\text{HN}}$  = homogeneous nucleation temperature

\* absolute temperature (K)

Bjornard and Griffith (1977)

Derivation based on Van der Waal's equation of state; constant term corrected to 0.872 based on Merte and Clark's (1961) nitrogen data; also reported to be 0.916 by Simon and Simoneau (1969)

Applicable in the following ranges of parameters:

$$10^{-3} < \frac{(\rho c k)_l}{(\rho c k)_w} < 1; \text{ angle of wetting} = 0^\circ;$$

$$\frac{\Delta T_{\text{sub}}}{T_{\text{crit}} - T_{\text{sat}}} \leq 1.5; 0.02 \leq P/P_c \leq 0.63$$

$$De \geq 10 \left( \frac{g_\sigma}{g(\rho_l - \rho_v)} \right)^{\frac{1}{2}}; \frac{\rho_l v_l De}{\mu_l} \leq 1.4 \times 10^5;$$

$$U_l \left[ \frac{\rho_l - \rho_v}{g_\sigma} \right]^{\frac{1}{4}} \leq 160$$

$T_{\text{HN}}$  may be evaluated from classical nucleation theory; this equation agrees with some of the FLECHT and semiscale results: recommended in TRAC code for high pressures; similar form used in THOR code where

$$T_{\text{HN}}^* = 642 \left( 0.92 + 0.08 \frac{P}{P_{\text{crit}}} \right)$$

Table 8 (cont'd)

Equations	Comments
$\frac{\Delta T_{\min} - \Delta T_{\text{Ber}}}{T_{\text{Ber}} - T_{\ell}} = 0.42 \left\{ \left[ \frac{(\rho c k)_{\ell}}{(\rho c k)_w} \right]^{\frac{1}{2}} \frac{i_{fg}}{C p_{\ell} \Delta T_{\text{Ber}}} \right\}^{0.6}$	Modification of Berenson's correlation incorporating effects of surface and liquid thermal properties. Correlations based on pool boiling data of water, organic liquids, and liquid metals (Type V and VI quench). Recommended in TRAC code for low pressures.
$\Delta T_{\text{Ber}} = \Delta T_{\min} \text{ as predicted by Berenson (see equation above)}$	
Henry (1974)	
$\Delta T_Q = 0.29 \Delta T_{\text{Ber}} (1 - 0.295 X_e^{2.45}) F_G$	Modification of Berenson's correlation based on forced convective transient data at: $G = 67.8 - 135 \text{ kg m}^{-2} \text{ s}^{-1}$ , $P = 6900 \text{ kPa}$ , $X = 0.3, 0.6$ , and $0.8$ . Predicts apparent quench temperature (type III quench for high $G$ and $\alpha$ ).
$G < 67.8 \text{ kg m}^{-2} \text{ s}^{-1}, F_G = 2.41$	
$G > 135.6 \text{ kg m}^{-2} \text{ s}^{-1}, F_G = 3.24$	
$67.8 < G < 135.6, F_G = (1 + G/13.56)^{0.49}$	
Plummer et al. (1973)	
$T_{\min}^* = \frac{0.84 T_C^* \left( 1 - \exp \left\{ -0.52 \left[ 10^4 (\rho/A)^{4/3} / \sigma_{lv} \right]^{1/3} \right\} - T_{\ell}^* \right)}{\exp(0.00175 \beta) \text{erfc}(0.042 \sqrt{\beta})} + T_{\ell}^*$	Correlation based on Spiegler's theory, taking into account the effects of solid-liquid surface energy ratio and thermal properties of the solid. Type V or VI quench.
*Absolute temperature (K)	$\beta = (1/k\rho C p)_w$ ; $A$ = atomic number
Baumeister and Simon (1973)	
$\Delta T_Q = 19.51 \Delta T_w \left( \frac{\Delta T_{\text{sub}}}{\Delta T_w} \right)^{0.107} \left( \frac{k}{C p G t} \right)^{0.162} \left( \frac{t G^3}{k \rho^2 \Delta T_w} \right)^{0.0989} \left( \frac{t}{Z} \right)^{0.163}$	Empirical correlation derived from dimensional analysis. Constants obtained from bottom flooding tests.
$t$ = wall thickness	$100 < G < 400 \text{ kg m}^{-2} \text{ s}^{-1}$ , $10 < \Delta T_{\text{sub}} < 80^\circ \text{C}$
Kim and Lee (1979)	Predicts apparent quench temperature. Properties in correlations are wall material properties.
$\Delta T_{\min} = 3.146 \Delta T_{\text{sub}} + 197.2$	Based on Bradfield's (1967) data obtained at 100 kPa.
Tong (1972)	Type IV quench on sphere.

In accordance with previous papers (e.g., Lee et al., 1978; Yamanouchi, 1968), we find it more prudent to use the term *apparent quench temperature* for the upstream surface temperature, below which axial conduction becomes effective in reducing the dry-side wall temperature. This temperature,  $T_Q$ , for which several correlations have been developed (e.g., Kim and Lee, 1979; Dhir et al., 1981), is higher than the minimum film boiling temperature or sputtering temperature but can easily be determined from temperature-time charts. Since  $T_Q$  depends strongly on the upstream and downstream temperature distribution as well as the prior surface temperature, it cannot be used to predict the minimum film boiling temperature  $T_{min}$ .

### 6.3 Prediction Methods

An extensive review of the literature on minimum film boiling resulted in the selection of the correlations of Table 8 for possible use in reactor safety analysis. The correlations may be divided into the following groups:

- *Equations based on the Taylor-Helmholtz hydrodynamic instability theory.* Berenson (1961) combined his theoretically derived equation for  $h_{FB}$  with a theoretical equation for  $q_{min}$  to obtain an expression for  $T_{min}$ . This expression is applicable only to a type VI film boiling termination. Berenson's equation in its original form depends only on fluid properties; it was modified by Henry (1974) to include the surface properties for a nonisothermal surface.
- *Equations based on the maximum liquid superheat concept.* These correlations are based on the theory that the surface cannot support any liquid contact when its temperature is higher than the maximum liquid temperature. This temperature can be predicted from an equation of state or the heterogeneous nucleation theory, as was done by Spiegler et al. (1963) and Nishio and Hirata (1978). The correlations by Bjornard and Griffith (1977), Kalinin et al. (1969), and Baumeister and Simon (1973) are of the same type but include corrections for nonisothermal surfaces.
- *Empirical correlations for minimum flow film boiling.* These correlations are based directly on minimum flow film boiling data. Experimental data are unfortunately very scarce and different, depending on whether they are obtained during spontaneous film boiling collapse (types I and IV) or during a propagating rewetting front (types II and III). Groeneveld and Stewart (1982) proposed a minimum film boiling correlation based on quench types I and IV, while the correlations of Kim and Lee (1979) and Plummer et al. (1973) are based on the apparent quench temperature.

The theoretically derived equations for  $T_{min}$ , such as Berenson's (1960, 1961) and Spiegler et al.'s (1963), are based on the assumption that the heated surface is isothermal. During the rewetting process, large temperature gradients are present. If liquid-wall contacts are intermittent (e.g., at the initiation of transition boiling during cooling down of a surface), they will be

of very short duration. These contacts are usually not immediately noticeable at the thermocouple junction, which is normally embedded in the heated surface and hence measures an average temperature. The difference between the thermocouple junction temperature and the true liquid-wall temperature can be significant and has been analyzed by Henry (1974), Baumeister and Simon (1973), and others. It depends on the ratio  $(k\rho C_p)_l / (k\rho C_p)_w$  and can only be ignored for high conducting surfaces such as copper and aluminium. The temperature difference becomes particularly significant for surfaces covered with an oxide layer and appears to be independent of the oxide layer thickness.

## 6.4 Correlation Assessments

### 6.4.1 Data Trends

True minimum film boiling temperatures during simulated reactor accident conditions are very difficult to measure because of the very large temperature gradients over the short ( $\approx 10$  mm) quench front region. The recently developed hot-patch technique, however, permits the measurement of minimum flow film boiling temperatures over a wide range of steady-state conditions.

Experimental data have been obtained for all heat transfer configurations in Fig. 13. These data display some contradictions; nevertheless, the following trends can be identified:

- *Flowrate.* Plummer et al.'s (1973) results indicate an increasing  $T_Q$  with an increase in  $G$ , as do the results of Kim and Lee (1979) and Dhir et al. (1981). They all measured the apparent quench temperature (type II or III); however, their observation does not necessarily apply to  $T_{min}$ . No significant flow effect on  $T_{min}$  was observed by Bennett et al. (1966) (type II), Groeneveld and Stewart (1982) (type I and IV), Lauer and Hufschmidt (1976) (type III), or Laperrière (1983) (types I and IV).
- *Pressure.* Our literature survey has shown that the quench time always decreases with pressure; this is to be expected as the  $T_{min}$  normally increases with  $P$  (and  $T_{sat}$ ), as does the precooling heat transfer coefficient. When considering the  $\Delta T_{min}$  for types I and IV (Groeneveld and Stewart, 1982) or the sputtering superheat (type II) (Shires et al., 1964; Bennett et al., 1966) for the range 0.1 to 9 MPa, a maximum can be observed at approximately 4 MPa.
- *Quality.* The effect of this parameter is not well understood. The quality covered by Groeneveld and Stewart (1982) extended only up to 13% and showed no significant trend. Recent experiments by Laperrière (1983) covered a quality range of 0%-40% and again showed no effect. Bennett et al.'s (1966) and Shires et al.'s (1964) top flooding experiments covered only high void fractions. Their results are slightly (0-30%) below Groeneveld's. Plummer et al. (1973) obtained a very limited amount of data; he showed an increase in apparent quench temperature with a decrease in quality.

- *Subcooling.* All experimental studies have shown a  $T_{\min}$  or a  $T_Q$  increase with an increase in subcooling. Groeneveld and Stewart (1982) has shown that this increase is strongest for atmospheric pressure. Figure 16 displays the subcooling effect by showing Groeneveld and Stewart's (1982) correlation (based on a type I quench) and the data of Bradfield (1967) (type VI quench) and Lauer and Hufschmidt (1976) (type III quench).
- *Surface properties.* All experimental studies have shown that  $T_Q$  or  $T_{\min}$  increase with a decrease in  $kpC_p$  of the wall. Significant increases (50°-100°C) in  $T_{\min}$  and  $T_Q$  were also observed when the surface became oxidized (i.e., Dhir et al., 1981; Baumeister and Simon, 1973). The effect of a change in  $kpC_p$  has been theoretically derived (Henry, 1974; Baumeister and Simon, 1973) and is included in several of the correlations of Table 8. In the flow film boiling collapse studies (types I and IV), only one surface material was used, and hence no surface property term was included in the empirical correlation (Groeneveld and Stewart, 1982).

#### 6.4.2 Comparison with Data

Current reactor safety codes recommend a single correlation for  $T_{\min}$  covering all conditions. Figures 14 and 15 illustrate that most correlations do not predict data for different film boiling terminations adequately. The pressure was chosen as the independent variable since this effect was known to vary significantly for most correlations. Figure 14 also shows type II data (Bennett et al., 1966; Shires et al., 1964), while Fig. 15 is based on type VI data and shows a significant surface property

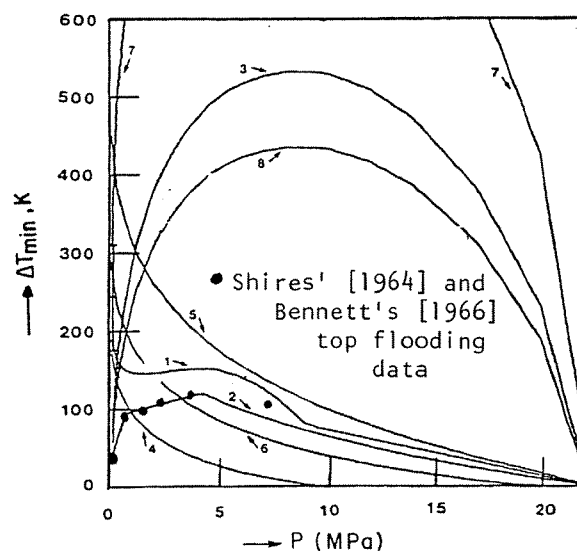


Fig. 14. Effect of pressure on measured and predicted  $T_{\min}$  for a Zircaloy surface. Numbers on curves refer to the first eight equations of Table 8. Only Eq. (8) (Plummer et al., 1973) has a mass flux and quality dependence and was evaluated at  $X = 0.2$  and  $G = 100 \text{ kg m}^{-2} \text{ s}^{-1}$ . All other equations were evaluated at saturated conditions.

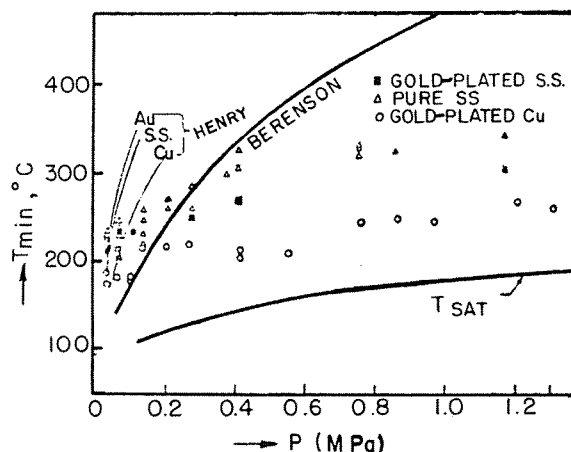


Fig. 15. Comparison of predicted and measured  $T_{\min}$  for type VI quench. From Yao and Henry (1978) and Berenson (1961). Reprinted with permission.

effect. A comparison of Groeneveld and Stewart's (1982) type I and IV data and the predictions of the correlation showed a significant overprediction of these high-pressure data by Berenson's (1961) and Henry's (1974) equations. This was expected since these equations are recommended only for low (near-atmospheric) pressures. The pressure trend of Plummer et al.'s (1973) correlation is the same as that of Berenson's equation since Plummer obtained apparent quench temperature data only at  $P = 7$  MPa. The large difference between Plummer's data and those of Bennett and Groeneveld is thought to be due to  $T_Q$  being much higher than  $T_{\min}$ . Spiegler's equation underpredicts the bulk of the data. The agreement between Groeneveld's and Bennett's data sets (and hence between the empirical correlations 1 and 2) is surprising considering their very different geometries and flow conditions. It suggests that the sputtering temperature (rather than  $T_Q$ ) properly represents film boiling termination and hence  $T_{\min}$  and that the effects of flow geometry, flow rate, and quality are not very significant, at least for the range of data.

Figure 16 shows the effect of subcooling on  $T_{\min}$ . Agreement between Groeneveld's correlation [based on the data of Stewart (1981) and Fung (1981)] and Bradfield's (1967) and Lauer's (1978) data is fortuitous. It suggests a wider applicability than originally visualized provided the surfaces have  $k\rho C_p$  values within the  $30\text{--}70 \text{ kJ}^2 \text{ m}^{-4} \text{ K}^{-2} \text{ s}^{-1}$  range (i.e., excluding such surfaces as glass, gold, copper, and heavily oxidized surfaces).

#### 6.4.3 Discussion

Because of the very different types of film boiling terminations and the scarcity of reliable data, not much confidence can be put into any correlation. Despite these qualifying remarks, the Groeneveld-Stewart (1982)  $T_{\min}$  correlation currently appears to be the most appropriate correlation for types I-IV film boiling terminations. This observation is based on the approximate agreement of this correlation with the data of Stewart (1981), Fung (1981), Shires et al. (1964), Bennett et al. (1965), Laperrière (1983), Bradfield (1967), and Lauer (1976) and on the



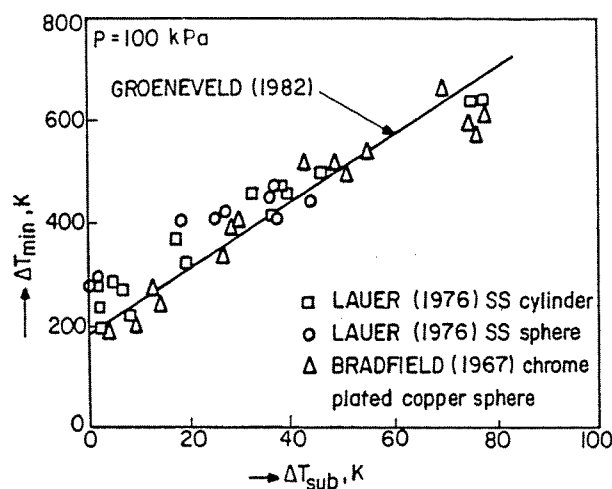


Fig. 16. Effect of subcooling on  $T_{min}$ . From Groeneveld and Stewart (1982).

correct asymptotic trend of pressure and subcooling. Although in these experiments thin oxide layers were present, no large correction in  $T_{min}$  due to oxide layers was needed, and consequently surface property corrections, such as those suggested by Henry and Kalinin, are thought to be of secondary importance for engineering surfaces (i.e., Inconel, steel, Zircaloy).

For types V and VI film boiling terminations, the surface condition has been found to play a significant role. Here the  $T_{min}$  correlations of Henry (1974) and Baumeister and Simon (1973) are recommended for low pressures. For higher pressures where the minimum film boiling is no longer hydrodynamically controlled, Henry's correlation no longer applies. The Groeneveld-Stewart (1982) correlation is recommended at these conditions.

## 6.5 Final Remarks

Strong effects of surface oxide layers on the minimum film boiling temperature have been observed for pool boiling conditions. This effect can be predicted using the surface property correction factor suggested by Henry.

Measurements of the minimum film boiling temperature during subcooled flow film boiling have shown a strong dependence of  $T_{min}$  on the local subcooling. This effect is usually absent in correlations for  $T_{min}$ .

Correlations have been proposed for the quench temperature during flooding conditions. This quench temperature, however, usually corresponds to a temperature significantly higher than the minimum film boiling temperature and is strongly affected by axial conduction in the heated surface.

The wall-vapor heat flux at the minimum could be strongly affected by the preceding heat transfer mode. In the case of a surface heating up after passing through the higher turbulent transition boiling regime, the vapor temperature is likely to be

near saturation. However, during a cooling down of an initially very hot surface, high vapor superheats may be present. Assuming that  $h_{w-v}$  and  $T_{\min}$  are identical during heating and cooling, one may write

$$\begin{aligned} q_{\min, \text{heat up}} &= h_{w-v} (T_{\min} - T_{\text{sat}}) > q_{\min, \text{cool down}} \\ &= h_{w-v} (T_{\min} - T_v) \end{aligned}$$

This inequality cautions against calculation procedures based on the minimum heat flux.

## 7 FILM BOILING

### 7.1 Introduction

During film boiling, the heated surface is cooled by radiation, by forced convection to the vapor, and by interaction of the liquid and the heated surface. The vapor can become highly superheated; its temperature is controlled both by wall-vapor and vapor-liquid heat exchange. The liquid is thought to be in the form of a dispersed spray of droplets usually encountered at void fractions in excess of 80% (liquid-deficient flow regime); a continuous liquid core (surrounded by a vapor annulus that may contain entrained droplets) usually encountered at void fractions below 30% (inverted annular flow regime); and a transition between the above two cases, usually in the form of slug flow.

Of the above post-dryout regimes, the liquid deficient regime is most commonly encountered and has been well studied. Its post-dryout temperature is moderate while for the latter two flow regimes, excessive surface temperatures are frequently encountered.

### 7.2 Prediction Methods

#### 7.2.1 Post-Dryout Models

The first semitheoretical models for the liquid deficient regime were developed by the United Kingdom Atomic Energy Authority (Bennett et al., 1967) and the Massachusetts Institute of Technology (Lavery and Rohsenow, 1967). In these models all parameters were initially evaluated at the dryout location. It was assumed that heat transfer takes place in two steps: from the heated surface to the vapor and from the vapor to the droplets. The models evaluated the axial gradients in droplet diameter, vapor, and droplet velocity, and pressure, from the conservation equations. Using a heat balance, the vapor superheat was then evaluated. The wall temperature was finally found from the vapor temperature using a superheated steam heat transfer correlation. Bailey (1972), Groeneveld (1972), and Plummer et al. (1976) have suggested improvements to the original model by including droplet-wall interaction, by permitting a gradual change in average droplet diameter due to the breakup of droplets, and by including vapor flashing for large pressure gradients. Additional expressions for the vapor generation rate have more recently been suggested by Saha (1980) and Jones and Zuber (1977).

Recently, models have also been developed for the inverted annular flow regime (Fung, 1981; Kaufman, 1976; Elias and Chambré, 1981; Chan and Yadigaroglu, 1980). They are basically unequal velocity, unequal temperature (UVUT) models that can account for nonequilibrium in both the liquid and the vapor phases.

Table 9 summarizes the salient features of the post-dryout models. Most of the models are based on empirical relationships to predict interfacial heat and momentum transfer. Advanced thermohydraulic codes employ similar models to simulate the post-CHF region. As with the models described above, their universal use is limited because of unresolved uncertainties in interfacial heat transfer, interfacial friction, and liquid-wall interactions.

### 7.2.2 Post-Dryout Correlations

Empirical post-dryout correlations may be subdivided as follows: thermal equilibrium correlations, empirical correlations, phenomenological correlations, pool film boiling correlations, and miscellaneous. Discussions of each follow.

#### Thermal Equilibrium Correlations

Thermal equilibrium correlations are correlations that assume the liquid is in thermal equilibrium with the vapor and that the heated surface is cooled by forced convection to the vapor only. These correlations are basically forced convective correlations where the vapor velocity is evaluated by assuming either homogeneous flow (Dougall and Rohsenow, 1963) or by using a suitable slip ratio correlation (e.g., Quinn, 1966).

Thermal equilibrium correlations usually have the form

$$\text{Nu}_v = \alpha \left( \frac{\rho_v U_v D_e}{\mu_v} \right)^b (\text{Pr}_v)^c$$

where

$$U_v = \frac{GX}{\rho_v \alpha} = \frac{G}{\rho_v} \left[ X + \frac{\rho_v}{\rho_l} S (1 - X) \right]$$

This type of correlation assumes that the liquid and the vapor are in equilibrium, i.e.,  $X = X_e$ . This assumption does not agree with experiments (Mueller, 1967; Clément et al., 1979; Polomik, 1967; Nijhawan et al., 1980) except at high mass flows and high void fractions where the liquid-vapor heat exchange is very efficient and near the dryout location where the vapor has had insufficient time to become superheated.

This type of correlation is useful since it predicts a lower bound for the post-dryout temperature and is also applicable to superheated steam cooling.

#### Empirical Correlations

Empirical correlations are listed in Tables 10 and 11 for the liquid-deficient regime and the inverted annular flow regime.

TABLE 9. *Post-Dryout Models: Assumptions<sup>a</sup>*

Reference/Flow Regime	Wall-Vapor Heat Transfer
Laverty and Rohsenow (1967) Liquid dispersed	$Nu_v = 0.023 Re_{v,hom}^{0.8} Pr_v^{0.4}$
Bennett et al. (1967) Liquid dispersed	$Nu_{v,f} = 0.0133 \left( \frac{\rho U D}{\mu} \right)^{0.84} Pr_{v,f}^{0.33}$
Groeneveld (1973) Liquid dispersed	$Nu_v = 0.023 \left( \frac{\rho_v U_v D}{\mu_v} \right)^{0.8} Pr_v^{1/3} \left( \frac{\mu_v}{\mu_w} \right)^{0.14} \left[ 1 + 0.3 \left( \frac{D}{L + D/100} \right)^{0.7} \right]$
Plummer et al. (1976) Liquid dispersed	Taken from Groeneveld (1973)
Saha (1980) Liquid dispersed $K_1$ correlation	Taken from Bennett et al. (1967)
Saha (1980) Liquid dispersed $\delta$ correlation	Taken from Bennett et al. (1967)
Jones and Zuber (1977) Liquid dispersed	$Nu_v = 0.023 \left( \frac{GD}{\mu_v} \frac{\lambda}{\alpha} \right)^{0.8} Pr_v^{0.4}$
Fung (1981) Inverted annular	$T_v = \frac{T_w + T_{sat}}{2}$
Kaufman (1976) Inverted annular	$\frac{h_w - \ell^D}{k_v} = 0.023 Re_{film}^{0.8} Pr_v^{0.4}, Re_{film} = \frac{GD \lambda}{\mu_g}$ for $Re_{film} < 100$ : $h_w - \ell = \frac{k_v}{\delta}$
Elias and Chambré (1981) Inverted annular	$U_v \frac{\partial T}{\partial X} = \frac{k}{\rho C_p} \frac{\partial^2 T}{\partial y^2}; \frac{\partial H}{\partial Y} = 0$ (assumed) conduction across vapor film only
Chan and Yadigaroglu (1980) Inverted annular	$q = \frac{k_v}{\delta} (T_w - T_S) + q_{rad}$ $\delta$ = laminar vapor film thickness

TABLE 9 (Cont'd)

Vapor-Liquid Heat Transfer	Comments, Additional Equations
$h_{v-d} = 0.37 \text{ Re}_d^{0.6}$	$C_D = 0.5$ , $d_{\text{initial}} = 0.1 - 1 \text{ mm}$
$h_{v-d} = \frac{2k_v}{d} \left[ 1 + 0.276 \text{ Re}_d^{0.5} \left\{ \frac{\nu_g R_a}{k_g (\gamma - 1) M} \right\}^{1/3} \right]$	$d_{do} = 0.3 \text{ mm}$ , no droplet breakup, $\frac{dP}{dz} = 0$ , $q_{w-d} = 0$ at dryout point, $U_v - U_d = \text{free fall velocity}$
Taken from Bennett et al. (1967)	$We_c = 6.5$ , $S_{do} = \left( \frac{\rho_l}{\rho_g} \right)^{0.205} \left( \frac{GD}{\mu_l} \right)^{0.16}$ , $q_{w-d} = \frac{k_{vf}}{\delta} (1 - \alpha) (T_w - T_s) \exp \left[ \frac{2D}{Z - Z_{do}} \right]$
See original paper	where $\delta = .025 \text{ mm}$ $We_c = 7.5$ , $\left( U_v - U_d \right)_{do} = \left( g \left( 1 - \frac{\rho_v}{\rho_l} \right) + \frac{4q_{do} U_{ldo}}{\rho_v H_{fg} D} \right)^{1/2} \left( \frac{\rho_l We_c \sigma}{0.75 C_D \rho_v^2} \right)^{1/2}$
$\Gamma a = K_1 [k_v (1 - \alpha) (T_v - T_{sat}) / D^2 H_{fg}]$	$w-d$ taken from Groeneveld (1973)
where $K_1 = 6300 \left( 1 - \frac{P}{P_{cr}} \right)^2 \frac{GX_a}{\alpha} \left( \frac{D}{\rho_v \sigma} \right)^{1/2}$	$q_{w-d} = 0$ for $\Delta T > 222^\circ\text{C}$
$d/d_{do} = \left( \frac{1 - X_a}{1 - X_{do}} \right)^{1/3}$	$j_{g,do}$ from drift flux model
$\frac{d_{do}}{D} = 1.47 \left\{ \frac{\rho_g j_{g,do}^2}{[cg(\rho_l - \rho_v)]^{1/2}} \right\}^{-0.675}$	$N_{sr} = \frac{3}{2} \left( \frac{\pi n}{6} \right)^{2/3} \frac{k_v DH_{fg}}{C_{p,v} q_{do} X_a} \text{Nu}_d (1 - \alpha)^{1/3}$ , $q_{w-d} = 0$
$\Gamma a = \Gamma a_{sr} (X_e - X)$	$n = \text{droplet concentration}$
$\text{Nu}_d = 2 + 0.74 \text{ Re}_d^{1/2} \text{Pr}_w^{1/3}$	$q_{w-d} = 0$ ; $\epsilon = 0.08 U \left( \frac{1}{2} \delta_T \right)$
$q_{i-l} = \rho_l C_{p,l} (\epsilon + \alpha) \frac{dT}{dr}$ , flux to heat subcooled liquid core	$\delta_T = \text{turbulent vapor film thickness}$
$\Gamma a$ from heat balance	At $\alpha = 0.4$ the flow regime becomes dispersed
$q_{i-l}$ : from $\text{Nu}_l = 0.023 \text{ Re}_{l,e}^{0.8} \text{Pr}_{l,e}^{0.4}$	$(U_v - U_l)$ evaluated from momentum balance
$\text{Re}_{l,e} = (U_v - U_l) \rho_v^{1/2} \rho_l^{1/2} (D - 2\delta) \rho_f$	$\delta = \text{vapor film thickness} = \frac{D(1 - \sqrt{1 - \alpha})}{2}$
$q_w - q_{i-l} \left( \frac{D}{D - 2\delta} \right) = q_{\text{evaporation}}$	Requires value of constant vapor film thickness over entrance region
Assumes interface temperature below saturation in entrance region, hence no vapor generation	It is assumed that 20% of the vapor generated will become entrained in the liquid core
$q_{i-l} = h(T_{sat} - T_l) C$	
$h$ from Dittus-Boelter equation	
$C = \text{enhancement factor} = 1.5 - 2.0$	

TABLE 10. *Post-Dryout Correlations*<sup>a</sup>

Equation and Reference	Range of Applicability of Equation			Equation agrees with data from	Comments
	$P$ (MPa)	$G \times 10^3$ (kg m <sup>-2</sup> s <sup>-1</sup> )	$X$	Geometry	
$Nu_f = 0.00136(Re_f)^{0.853} Pr_f^{1/3} \left( \frac{X}{1-X} \right)^{0.147} \left( \frac{\rho_g}{\rho_l} \right)^{2/3}$ Polomik et al. (1961)	5.60-10.2	1.00-2.45	0.40-0.70	Annulus	Polomik et al. (1961)
$Nu_f = 0.416 Re_f^{0.509} Pr_f^{1/3} \left( \frac{\rho_g}{\rho_l} \right)^{0.208} \left( \frac{1-X}{X} \right)^{0.616}$ Polomik et al. (1961)	5.60-10.2	1.00-2.45	0.40-0.70	Annulus	Exponents and coefficients for Eqs. (1)-(3) obtained from least error analysis
$Nu_f = 0.023 Re_f^{1/3} \left( \frac{1-X}{X} \right)^{0.01} \phi^{0.417}$ $\times \left( \frac{\rho_l}{\rho_g} \right)^{0.091}$ $\phi$ in Btu hr ft <sup>-2</sup>	5.60-10.2	1.00-2.45	0.40-0.70	Annulus	Polomik et al. (1961)
$Nu_g = 0.00115(Re_g)^{0.9} Pr_g^{0.3} \left( \frac{T_w}{T_s} - 1 \right)^{-0.15}$ $T$ in °F Polomik (1967)	4.08-10.2	0.70-2.70	0.20-1.00	2-rod	Has additional temperature parameter to allow for property variations at the heater wall $\pm 20\%$ variation with data
$Nu_g = 0.0039 \left\{ Re_g \left[ \frac{\rho_g}{X} + \frac{\rho_l}{1-X} \right] \right\}^{0.9}$ Polomik (1967)	4.08-10.2	0.70-2.70	0.20-1.00	2-rod	$\pm 10\%$ variation with data from Hensch (1964); better than above equation
$\phi \left[ \frac{De^{0.2}}{(GX)^{0.8}} \right] = C(T_w - T_s)^m$ $m = 1.284 - 0.00312 G$ $C = \frac{1}{389} e^{0.01665 G}$ Collier (1962)	7.03	> 1.00	0.15-1.00	Round tubes and annuli	$T_w - T_s$ must be below 200°C Polomik et al. (1961); Bertolotti (1961)

$\phi \left[ \frac{De^{0.2}}{(GX)^{0.8}} \right] = 0.018 (T_w - T_s)^{0.921}$			7.03	see comments	0.15-1.00	Round tubes and annuli	Polomik et al (1961); Bertolotti (1961)	Correlation may be used if either $G < 106$ or $T_w - T_s > 200^\circ\text{C}$
$\text{Nu}_f = 0.0193 \text{Re}_f^{0.8} \text{Pr}_f^{1.23} \left( \frac{\rho}{\rho_f} \right)^{0.068}$ $\times \left[ X + \frac{q}{\rho_f} (1 - X) \right]^{0.68}$			4.08-21.9	0.70-3.40	0.07-1.00	Round tubes	Polomik et al. (1961); Bishop and co-workers (1962, 1964, 1965); Swenson et al. (1961); Miropol'skiy (1963)	
Bishop et al. (1965)								
$\text{Nu}_f = 0.033 \text{Re}_w^{0.8} \text{Pr}_w^{1.25} \left( \frac{\rho}{\rho_f} \right)^{0.197}$ $\times \left[ X + \frac{q}{\rho_f} (1 - X) \right]^{0.738}$			4.08-21.9	0.70-3.40	0.07-1.00	Round tubes	Polomik et al. (1961); Bishop and co-workers (1962, 1964, 1965); Swenson et al. (1961); Miropol'skiy (1963)	
Bishop (1965)								
$\text{Nu}_w = 0.098 \left\{ \text{Re}_w \frac{\rho_w}{\rho_g} \left[ X + \frac{q}{\rho_g} (1 - X) \right] \right\}^{0.8}$ $(\text{Pr}_w)^{0.83} \left( \frac{\rho}{\rho_f} \right)^{0.50}$			16.8-21.9	1.35-3.40	0.10-1.00	Round tubes	Swenson et al. (1961); Bishop et al. (1964); Miropol'skiy (1963)	Based on high-pressure data
Bishop et al. (1964)								
$\text{Nu}_v = 0.055 \left\{ \text{Re}_v \frac{\rho_v}{\rho_g} \left[ X + \frac{q}{\rho_g} (1 - X) \right] \right\}^{0.82}$ $\times (\text{Pr}_v)^{0.96} \left( \frac{\rho}{\rho_f} \right)^{0.34} \left( 1 + \frac{26.9}{L/D} \right)$			16.8-21.9	1.35-3.40	0.10-1.00	Round tubes	Bishop et al. (1964)	
Bishop et al. (1964)								
$\text{Nu}_f = 0.0089 \left( \frac{GxD}{\alpha \mu_f} \right)^{0.84} \left( \frac{C_p}{k} \right)^{1/3} \left( \frac{1 - X_{DO}}{X - X_{DO}} \right)^{1/8}$			7	1.03-2.00	0.45-1.20	Round tubes	4 sets; see Cumo and Urbani (1974)	Error 10-25%
Cumo and Urbani (1974)								
$T_w - T_{\text{sat}} = 1.915 \left\{ \frac{\phi}{G[X + (1 - X/4.15)]} \right\}^2$			14.2-18.2	1.00-4.00	0.30-0.75	Tubes	Lee (1970)	Based on data obtained on 1.3-cm-ID indirectly heated tube
Lee (1970)								

Table 10 (cont'd)

Equation and Reference	Range of Applicability of Equation				Equation agrees with data from	Comments
	P (MPa)	$G \times 10^3$ (kg m <sup>-2</sup> s <sup>-1</sup> )	X	Geometry		
$Nu_g = 0.023 \left\{ Re_g \left[ X + \frac{\rho_g}{\rho_l} (1 - X) \right] \right\}^{0.8} Pr_w^{0.8} Y$ $Y = 1 - 0.1 \left( \frac{\rho_l}{\rho_g} - 1 \right)^{0.4} (1 - X)^{0.4}$	4.05-22.3	0.70-2.00	0.06-1.00	Tubes	Swenson et al. (1961); Miropol'skiy (1963); Schmidt (1960)	Factor Y was determined empirically
Miropol'skiy (1963)						
$Nu_g = 0.0089 \left( Re_g \frac{X}{\alpha} \right)^{0.84} (Pr_f)^{1/3} \left( \frac{1 - X}{X - X_{DO}} \right)^{0.124}$	5.06	0.50-3.00	0.40-1.00	Tubes	Brevi et al. (1969)	
Brevi et al. (1969)						
$Nu = 0.06 \left\{ \left[ Re_w \left( X + \frac{\rho_g}{\rho_l} (1 - X) \right) \right] \left( \frac{\rho_w}{\rho_g} \right) Pr_w \right\}^{0.8}$ $\times \left( \frac{G}{G_o} \right)^{0.4} \left( \frac{P}{P_c} \right)^{2.7}$ $G_o = 10^3 \text{ kg m}^{-2} \text{ s}^{-1}$	14.2-22.3	0.75-4.10	0.10-1.00	Tubes	Herkenrath et al. (1967); Swenson et al. (1961); Bishop et al. (1964)	
Herkenrath et al. (1967)						
$Nu_w = 0.005 \left( \frac{DeU \rho_w}{v_w} \right)^{0.8} (Pr_g)^{0.5}$	> 14.0	> 0.70	< 0.10	Tubes	Bishop and co-workers (1962, 1964)	Design equation; to be used only at low-quality or subcooled conditions
Tong (1965)						
$Nu_g = 1.604 \times 10^{-4} \left[ Re_g \left( X + \frac{\rho_g}{\rho_l} (1 - X) \right) \right]^{0.838}$ $Pr_w^{1.81} \phi^{0.278} \left( \frac{k_g}{k_{crit}} \right)^{-0.508}$ $\phi \text{ in Btu hr}^{-1} \text{ ft}^{-2}$	6.88-20.2	1.05-5.30	0.12-0.90	Tubes	Bennett et al. (1967); Bishop et al. (1965); Bertolotti (1964)	



$$\left\{ \left[ X + \frac{\rho_g}{\rho_l} (1 - X) \right] \right\}^b \text{Pr}_w^c$$
$$Y = 1 - 0.1 \left( \frac{\rho_L}{\rho_g} - 1 \right)^{0.4} (1 - x)^{0.4}$$
$$\begin{array}{ll} a = 1.09 \times 10^{-3} & b = 0.989 \\ c = 1.41 & d = -1.15 \\ e = 0 \end{array}$$
$$\begin{array}{ll} a = 5.20 \times 10^{-2} & b = 0.688 \\ c = 1.26 & d = -1.06 \\ e = 0 \end{array}$$
$$\begin{array}{ll} a = 3.27 \times 10^{-3} & b = 0.901 \\ c = 1.32 & d = -1.50 \\ e = 0 \end{array}$$
$$h = 0.114 \text{ Re}_g^{0.244} \text{ Pr}_{g,w}^{2.54} D_{eq}^{-0.304} k_g^{0.334}$$

<sup>a</sup>For definition and units of all symbols, see Nomenclature.

Bennett and  
co-workers (1964,  
1967); Bishop  
et al. (1964,  
1965); Bertolotti  
(1961, 1964);  
Swenson et al.  
(1951); Schmidt  
(1960); Era et al.  
(1967);  
Groeneveld (1969);  
Polomik (1967)

Groeneveld (1969); RMS error: 17.5%  
Polomik (1967)

TABLE 11. Low-Quality and Subcooled Film Boiling Correlations<sup>a</sup>

References	Equation	Range of Applicability				Comments
		Test Fluid	Geometry	Pressure (MPa)	Flow Rate (kg m <sup>-2</sup> s <sup>-1</sup> )	Subcooling (°C) QR Quality
Bromley et al. (1952, 1953)	$h = h_{FB} = 3/4 \dot{n}_{rad}$	Nitrogen; water; n-pentane; benzene; carbon tetrachloride; ethyl alcohol	Horizontal carbon cylinders; OD: 6.4 mm; 9.5 mm; 12.7 mm	Not given	Pool boiling	Saturated
	$h_{FB} = 0.62 \left[ \frac{k_v g \rho_v (\rho_l - \rho_v) h'_{fg}}{D \mu_v \Delta T_s} \right]^{1/4}$					
	$h_{rad} = \frac{5.67 \times 10^{-8} (T_w^4 - T_s^4)}{\left( \frac{1}{\epsilon_w} + \frac{1}{\epsilon_l} - 1 \right) \Delta T_s}$					
	$h'_{fg} = h_{fg} \left( 1 + \frac{0.4 C_p \Delta T_s^2}{h_{fg}} \right)$					
	$h_{FB} = 0.425 \left\{ \frac{k_v g \rho_v (\rho_l - \rho_v) h'_{fg}}{\mu_v \Delta T_s [\sigma/g(\rho_l - \rho_v)]^{1/2}} \right\}^{1/4}$					
Berenson (1961)			Horizontal surface		Pool boiling	Saturated
						Theory only
Siviour and Ede (1970)	$q_{total} = q_v + q_L$	Water; water plus detergent	Horizontal cylinders; OD: 3.2 mm; 6.4 mm	0.101	Pool boiling	0-90°C
	$q_v = 0.613 \frac{k_v \Delta T_s}{D} \left[ \frac{g \rho_v (\rho_l - \rho_v) h'_{fg}}{\mu_v k \Delta T_s} \right]^{1/4} + q_{rad}$					
	$q_L = 0.57 \frac{k_v \Delta T_{sub}}{D} [Gr Pr^2]$					
	$Gr = g \frac{\beta \Delta T_{sub} D^3}{\nu^2}$					
Andersen (1977)	$h_c = c_1 \left[ \frac{k_v^2 h'_{fg} \rho_v (\rho_l - \rho_v)^4}{\mu_v^4 \Delta T_s^2 \sigma} \right]^{1/11}$				Low flow rates	Saturated
	$0.3321 \leq C_1 \leq 0.5498$					Gives slightly higher heat transfer coefficient than Berenson's equation for $\Delta T_s > 200^\circ\text{C}$ ; theory only

Ellison	$h = \frac{4}{3} \left[ \frac{g \rho_p k_f^2 H}{12 \Delta T_s L \mu_p} \right]^{\frac{1}{4}} + q_{\text{rad}}$	Water	Vertical annulus; OD: 63.5 mm; ID: 6.4 mm length: 76.2 mm	0.11-0.41 (0.336-1.53) x 10 <sup>3</sup>	28-56°C	
Bailey (1972)	$h = \left[ \frac{2k g \rho_p (\rho_f - \rho_g) H f g}{D \mu_g \Delta T_s} \right]^{\frac{1}{4}}$	Theory	Vertical rods		Saturated	D = rod OD
Collier (1980)	$\frac{h(z)z}{k_g} = \left[ \frac{z^3 g \rho_p (\rho_f - \rho_g) H f g}{4 k_g \mu_g \Delta T} \right]^{\frac{1}{4}}$	Theory	Vertical surface			Laminar vapor film
Collier (1980)	$\frac{h(z)z}{k_g} = 0.056 \text{Re}_g^{0.2} [\text{Pr Gr}^*]^{1/3}$		Vertical surface			Turbulent vapor film
	$\text{Gr}^* = \left[ \frac{z^3 g \rho_p (\rho_f - \rho_g)}{\mu_g^2} \right]$					

<sup>a</sup>For definition and units of all symbols, see Nomenclature.

They generally predict a heat transfer coefficient that is based on the temperature difference between wall and saturation. They are simple to use but have a limited range of validity and should not be extrapolated outside their recommended range. If extrapolation is unavoidable, one should check that the predicted temperatures fall between the upper and lower boundaries for the post-dryout temperatures, as discussed elsewhere in this chapter.

Because of the scarcity of water data at low flows, low qualities, and subcooled conditions, some of the correlations proposed in Table II are based on cryogenic or refrigerant film boiling data.

### Phenomenological Correlations

These predictive methods are based on the physical mechanisms governing this type of heat transfer and use  $h_{w-v}$  based on the vapor temperature. For the liquid-deficient regime, phenomenological correlations usually predict the degree of thermal nonequilibrium. Values for the actual vapor temperature  $T_{va}$ , or actual quality  $X_a$ , can be generated from existing post-dryout data, provided the assumption of forced convective cooling only (i.e., no droplet-wall interaction) of the heated wall in the post-dryout region is correct. This approach has been used by Tong and Young (1974), Plummer et al. (1976), Groeneweld-Delorme (1976a) Chen et al. (1979), and Shah (1980).

Table 12 presents a summary of recent nonequilibrium correlations. In general, these correlations are a significant improvement over the empirical post-CHF correlations. They can be given the correct asymptotic trends to let them smoothly converge with the single-phase superheated-steam cooling correlations. Several of the nonequilibrium correlations are questionable, e.g., Plummer et al.'s (1976) assumption that the nonequilibrium in quality,  $X_a - X_{do}$ , is directly proportional to  $X_e - X_{do}$  or length in a uniformly heated test section and Tong and Young's (1974) incorrect use of Bennett et al.'s (1967) data at low superheat and its narrow data base range ( $P = 7$  MPa only).

Attempts have also been made to develop phenomenological correlations for the inverted annular regime (Dougall and Rohsenow, 1963; Kalinin, 1969, 1970) and the slug flow film boiling regime (Chi, 1967; Kalinin et al., 1970). Due to a limited data base, they have not yet been verified.

### Pool Film Boiling Correlations

Pool film boiling correlations are applicable in pool boiling and low mass velocities. They are summarized in Table 11. Most of these correlations basically have the form

$$h_c = A \left[ \frac{g k_v^3 \rho_v (\rho_l - \rho_v) H_{fg}}{\mu_v \Delta T_s} \right]^{\frac{1}{4}} f(U, \lambda) + h_{rad}$$

which was originally derived by Bromley (1950) from Nusselt's classical analysis of filmwise condensation. The latent heat  $H_{fg}$  is usually modified to include the vapor superheat, while the

TABLE 12. Nonequilibrium Post-Dryout Correlations<sup>a</sup>

References	Nonequilibrium Equation	To be Used in Conjunction with	Comments
Chen et al. (1979)	$\frac{X_e - X_a}{X_e} = \frac{0.26}{1.15 - \left(\frac{P}{P_c}\right)^{0.65}} \frac{T_{ba} - T_{sat}}{T_w - T_{ba}}$	$h_{w-v} = \frac{f}{2} G X_a C_{p,vf} Pr_v^{-2/3}$ $f = 0.037 \left[ \frac{DG}{\mu_v} \left( X_a - \frac{\rho_v}{\rho_x} (1 - X_a) \right) \right]^{-0.17}$	Underpredicts $T_{ba}$ measured by Nijhawan et al. (1980)
Groeneveld and Fung (1976)	$\frac{H_{ba} - H_{ve}}{H_{fg}} = \exp(-\tan \psi)$ $\psi = a_1 Pr_{ve}^{a_2} Re_{hom}^{a_3} \left( \frac{qDC_{pve}}{k_{ve} H_{fg}} \right)^{a_4} \sum_{i=0}^i b_i (X_e)^i$ (if $\psi < 0 \pm \psi = 0$ , if $\psi > \pi/2 \pm \psi = \pi/2$ ) $Re_{hom} = GD X_{1/ve}^{a_{hom}} X_1 = \min(X_e, 1)$	$Nu_{vf} = 0.008348 \left[ \frac{GD}{\mu_{vf}} \left( X_a + \frac{\rho_v}{\rho_x} (1 - X_a) \right) \right]^{0.8774} Pr_f^{0.6112}$ $a_1 = 0.13864 \quad b_0 = 1.3072$ $a_2 = 0.2031 \quad b_1 = -1.0833$ $a_3 = 0.20006 \quad b_2 = 0.8455$ $a_4 = -0.09232$	Overpredicts $T_{ba}$ measured by Nijhawan et al. (1980) $X_a = \max$ (predicted value, $X_{do}$ ) i.e., just downstream of dryout $X_a = X_{do}$ until $T_{ba}$ reaches predicted value
Tong and Young (1974)	$\frac{X_a}{X_e} = 1 + aB^{-0.12} \left[ X_e - \exp(bB^{0.8}) \right]$ $B = 0.05 + G/1350$ $G < 945 \text{ kg/m}^2 \quad a = -0.49, b = -0.26$ $1080 < G < 3375 \quad a = -0.29, b = -0.57$ $945 < G < 1080 \quad \text{interpolate}$	$q = q_{TB} + q_{FB} \quad q_{TB} = q_{NB} \exp[f(\Delta T, X_e, q)]$ $q_{FB} \text{ from:}$ $Nu_v = 0.023 \left\{ \frac{GD}{\mu_v} \left[ \frac{X_a \rho_v / \rho_g + S(1 - X_a) \rho_v / \rho_f}{X_a + S(1 - X_a)} \right] \right\}^{0.8} Pr_v^{0.4}$	Nonequilibrium is assumed to disappear for $\Delta T < 110^\circ\text{C}$ or $G > 3375 \text{ kg m}^{-2} \text{ s}^{-1}$
Shah (1980)	for $\frac{q}{H_{fg}} > 4.5 \times 10^{-4} \quad X_a = f(X_{do}, X_e, Fr_x)$ $Fr_x = G^2 / (\rho_g g D); f = \text{graphical}$ relationship may also be obtained from table	$q = F_{DC} h_{w-v} (T_w - T_{ba})$ $h_{w-v} \text{ evaluated as by Groeneveld and Fung (1976) if } Pr^* > 0.8 \text{ and } X_a > X_{do} + 0.3 \rightarrow F_{DC} = 1.5 X_a^{0.14}, \text{ else } F_{DC} = 1.0$	$F_{DC} = \text{droplet cooling factor}$
Plummer et al. (1976)	$\frac{X_a - X_{do}}{X_e - X_{do}} = K = 0.07 \ln \left[ G(1 - X_{do})^{5\sqrt{D}} \right] + 0.4$	$q = h_{w-v} (T_w - T_v) + h_{w-d} (T_w - T_{sat})$ $h_{w-v} \text{ from:}$ $Nu_v = 0.023 \left( \frac{GX^D}{\mu_a} \right)^{0.8} Pr_v^{1/3} \left( \frac{\mu_v}{\mu_w} \right)^{0.14} \left[ 1 + 0.3 \left( \frac{D}{0.01 D + L_{FB}} \right)^{0.7} \right]$ $h_{w-d} = \frac{k_{vf}}{d} (1 - \alpha) \exp \left( \frac{-2D}{L_{FB}} \right); d = 1.22 \times 10^{-4} \text{ m}$	To evaluate the slip ratio $S$ , use an iterative procedure $S = f(S_{do}, K, X_e, X_{do})$

<sup>a</sup>For definition and units of all symbols, see Nomenclature

velocity effect is included theoretically or empirically through  $f(U, \lambda)$  where  $\lambda$  is either equal to the diameter, the critical wavelength, or the most unstable wavelength.

### Miscellaneous

More recently, Shah (1980) proposed a graphical technique for predicting the actual quality  $X_a$ , which is combined with an equation for droplet cooling. This technique is reported to be valid for a number of fluids and is fairly simple to use.

In addition to the above prediction methods, one can also assume that in the liquid deficient regime no evaporation will take place, i.e., the wall heat flux is used only for superheating of the vapor and  $X_a$  remains constant. Here the predicted wall temperature is very high since the vapor becomes progressively more superheated. This prediction is pessimistic except at lower flows (Bennett et al., 1967). It is, however, useful as an upper boundary for the heated surface temperature.

## 7.3 Comparison with Experimental Data

### 7.3.1 Available Data

In reviewing the available post-CHF data, Groeneveld (1977) showed that film boiling data were virtually nonexistent at low flows, low pressures, and low qualities. This is not surprising since surface temperatures at these conditions are usually excessive. This gap in the data is gradually being filled with data obtained at the Chalk River Nuclear Laboratories (Fung et al., 1979; Stewart, 1981) and Lehigh University (Nijhawan et al., 1980) using the hot-patch technique developed at Chalk River (Groeneveld and Gardiner, 1978). Fung (1978) and Groeneveld and Gardiner (1977) have summarized the available post-dryout sources; Fig. 17 presents an overview of the ranges covered by film boiling data obtained in tubes.

The experimental data from various sources were examined and compared. Although occasionally the data are inconsistent, the general trends are those shown in Table 13 and Fig. 11. These trends are in agreement with our current understanding of the physical mechanisms.

### 7.3.2 Comparison with Tube Data

#### Inverted Annular Flow Regime and Pool Film Boiling

The pool film boiling case has been well researched, and one can predict the heat transfer coefficient with reasonable accuracy using Bromley's (1950) or Berenson's (1961) equations, provided the liquid is near the saturation temperature. For subcooled water, an increase in the film boiling heat transfer coefficient of approximately 2.5%/°C has been observed.

No satisfactory correlation is currently available for subcooled or low-quality convective film boiling of water. A comparison of subcooled flow film boiling data with several correlations was made by Stewart (1981). For low flows and  $X_e = 0$ , Berenson's (1961) correlation approximately agrees with

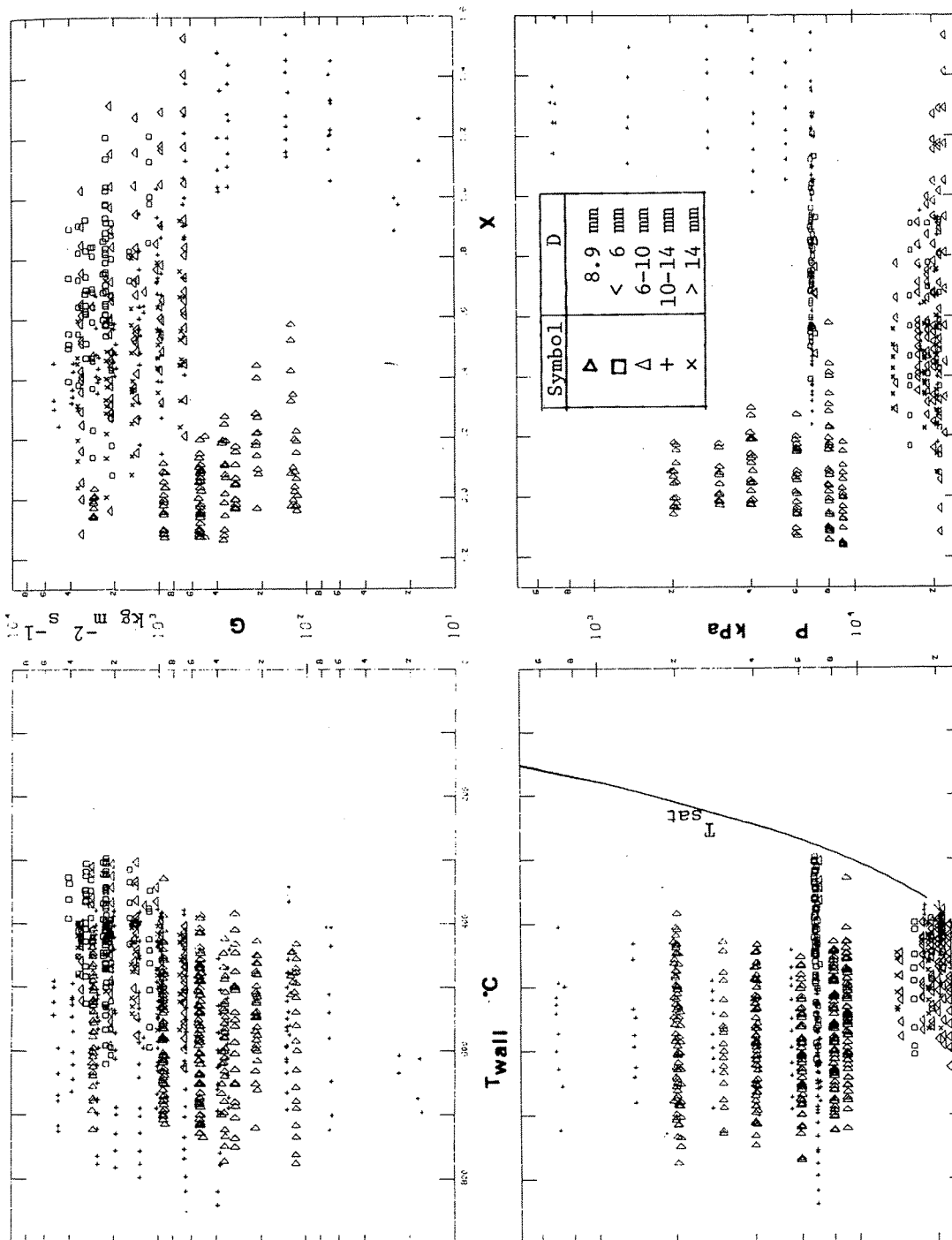


Fig. 17. Range of post-dryout data [ $D = 8.9$  mm data obtained by Stewart and Groeneveld (1982)]

Table 13. *Trends of Post-CHF Data*

Parametric Trend	Corresponding Physical Mechanism
Increase in wall heat flux increases $h$ .	Higher wall heat flux means a higher heat flux from the vapor to the droplets or liquid core. Since the vapor-liquid heat transfer coefficient remains constant, the vapor superheat must become larger.
Increase in $G$ improves $h$ (except at subcooled conditions where conduction dominates).	Higher $G$ will result in greater slip velocities. This will result in (1) an increased ventilation factor and thus an improved heat transfer coefficient between vapor and droplets; (2) more droplet breakup, hence more interfacial area; and, most important of all, (3) an increased vapor velocity that improves $h$ between wall and vapor. The first two also reduce the vapor superheat required to transfer the same amount of heat to the droplets.
Increase in $P$ improves $h$ ; near the critical pressure the nonequilibrium disappears.	Heat transfer properties of the vapor improve with an increase in $P$ . Also $\sigma$ decreases with $P$ resulting in smaller droplets and more interfacial area which reduces vapor superheat. Near the critical point $\sigma$ and $H_{fg}$ both approach zero and the flow becomes homogeneous.
Nonequilibrium gradually disappears for $X_e > 1.0$ .	For $X_e \gg 1.0$ , the vapor temperature is much greater than $T_{sat}$ and the thermal driving force for vapor-droplet heat transfer will increase until all liquid is evaporated.
Increase in $h$ with increase in local subcooling ( $X_e < 0$ ) (inverted annular flow regime).	Vapor blanket thickness depends on subcooling of the liquid. High subcoolings result in very thin vapor blankets and very efficient heat transfer by conduction across the vapor blanket.
Increase in $h$ for increase in quality ( $G > 1000 \text{ kg m}^{-2} \text{ s}^{-1}$ ).	A higher quality increases the vapor velocity at a given mass flow and hence increases the wall-vapor heat transfer coefficient. This will result in an increase in $h$ since the vapor superheat is expected to be small at high mass flows.
Decrease in $h$ for an increase in quality at low $G$ values ( $G < 250 \text{ kg m}^{-2} \text{ s}^{-1}$ ).	At low $G$ values, most of the wall heat flux is used to superheat the vapor in the dispersed flow region. This will result in a continually increasing vapor superheat with $X$ and can offset the previously discussed positive effect of $X$ on $h$ .



Stewart's data. For subcooled conditions, however, a factor similar to that observed in pool film boiling is required, i.e.,  $h_{\text{subc}} = h_{x=0} (1 + 0.025 \Delta T_{\text{sub}})$ . Fung (1981) reported that his model for inverted annular flow was in reasonable agreement with Stewart and Groeneveld's (1982) high-pressure data and Fung et al.'s (1981, 1979) atmospheric pressure data. It should be noted that the comparison was very limited and that the model's predictions are based partially on empirically derived constants.

### Liquid Deficient Regime

During the past 15 years, much progress has been made in understanding the physical mechanisms governing liquid-deficient heat transfer. Post-dryout models such as those by Bennett et al. (1967), Groeneveld (1973), and Plummer et al. (1976) have been reasonably successful in predicting the post-dryout temperature distribution. These models, however, require accurate values of the dryout quality; they are generally considered useful especially for predictions outside the data base (provided the assumed physical mechanisms are still valid).

Of the prediction methods discussed in the previous section, the phenomenological correlations are considered the most accurate. They tend to satisfy the data trends of Table 13; hence, they have a much wider range of applicability than the empirical post-dryout correlations of Table 10, but they are generally more difficult to use. Figure 18 shows schematically the relative temperature predictions of the four prediction methods. Note that curve A, based on the "thermal equilibrium after dryout" assumption, represents a lower boundary, while curve B, based on the "no evaporation after dryout" assumption, represents an upper boundary for the post-dryout temperature.

Most correlations of Table 10 are based on only a few sets of data covering a fairly narrow range of experimental data. The data sets (Groeneveld, 1977) contain much data that are not reliable. The errors in the data tend to result in reported post-dryout temperatures that are lower than what these authors consider to be fully developed film boiling. In the derivation of Groeneveld's post-dryout correlations, care was taken that the data subject to possible errors were not included. This could be the reason why Groeneveld's correlation seems conservative compared with some other post-dryout correlations (Slaughterbeck et al., 1973).

### 7.3.3 Comparison with Rod Bundle Data

Most post-CHF experiments have been carried out on simple geometries such as tubes or annuli (Groeneveld and Gardiner, 1977; Fung, 1978). Experimentation in bundle geometries is much more cumbersome because of large and expensive loop facilities, extensive instrumentation of the bundle, and increased likelihood of heater failure. Direct application of tube post-CHF predictive methods to bundle geometries is commonly practiced. It is warranted if enthalpy and flow imbalances are small or can be predicted with confidence. However, present subchannel code predictions of post-dryout conditions are unreliable because of a complete lack of verification data.

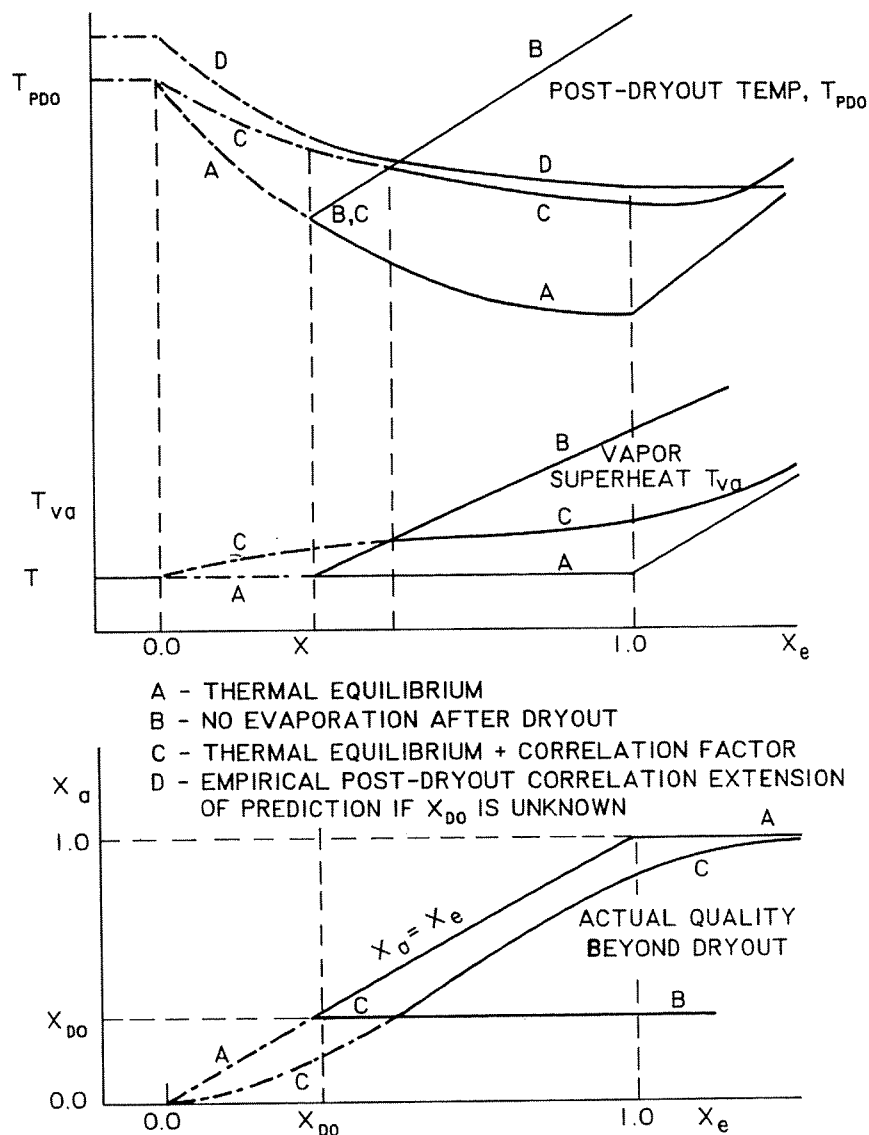


Fig. 18. Various predictions of post-dryout parameters.

Virtually all post-CHF correlations are based on steady-state data. Frequently these correlations are applied to transient conditions. Post-CHF heat transfer is expected to be somewhat higher during fast transient blowdown as compared with steady-state conditions because of the higher CHF, more intense mixing, and, hence, lower vapor superheat. For the slower transient reflooding situations, correlations based on steady-state data maybe used; Hsu (1975), for example, has shown that Bromley's correlation, augmented by an empirical transition boiling term, gave reasonable agreement with the FLECHT data. This correlation showed a significant contribution of the transition boiling term at temperatures as high as 700°C.

Other post-CHF experiments in a PWR-type bundle (17 x 17 array) under mildly transient conditions, high pressure, and a wide range of qualities were carried out by Morries et al. (unpublished Oak Ridge National Laboratory Report). He noted that thermal equilibrium correlations, such as the Dougall-Rohsenow

correlation (Dougall, 1963) vastly overpredict the post-CHF heat transfer, while the empirical post-CHF correlations of the type described in Sec. 7.2.2 ("phenomenological correlations") resulted in much better predictions.

Predictive methods based on tube data have frequently been found to overestimate sheath temperatures in fuel bundles. This is not surprising since

1. Bundles always contain unheated walls, which collect a liquid film, thus forming a heat sink. Tong and Young's (1974) correction for the cold wall has resulted in a prediction of a higher heat transfer coefficient.
2. Tubes do not contain rod-spacing devices (warts, grid spacers), which usually result in improved downstream heat transfer (e.g., Era et al., 1967; Groeneveld and Yousef, 1980). Frequent grid spacers (short spacer pitch) also prevent high vapor superheats, thus reducing sheath temperatures.
3. Partially dry bundles could result in a subchannel-type oscillation due to large differences in friction pressure gradients in wet and dry subchannels (e.g., Groeneveld, 1973a).
4. Film boiling experiments in bundles are often terminated at a power level just above the dryout power to reduce the chance of heater failure. At such low-power levels, film boiling heat transfer is not yet fully developed (Groeneveld and McPherson, 1973).

#### 7.3.4 Miscellaneous

Ralph et al. (1977) and Snoek and Laperrière (unpublished Chalk River Nuclear Laboratories report) observed significant reductions in post-dryout heat transfer coefficient for downflow compared with upflow for the same cross-section average conditions. For low flow rates, downflow tends to result in lower slip ratios and hence lower vapor velocities and lower values of  $h_{w-v}$ . In addition, the lower slip ratios reduce the interfacial area and heat transfer, resulting in a higher vapor superheat and a lower vapor mass flow rate. All these factors have a negative effect on the post-dryout heat transfer.

A number of other effects have been quantified for superheated steam correlations, as discussed in Sect. 2. These effects are expected to apply also to the wall-vapor component of the film boiling models.

#### 7.4 Final Remarks

Post-CHF heat transfer correlations developed for the liquid-deficient regime can be used with reasonable confidence within their data base range. The correlations derived by Groeneveld (1969), Groeneveld and Fung (1976), and Condie [as reported by Morries et al. (unpublished Oak Ridge National Laboratory Report)] tend to be the most reliable because of their large and wide-ranging data base. Caution should be exercised in using these correlations at low flows and pressures since here the data base is scarce.

Correlations for the low-quality or subcooled film boiling region are questionable because of the lack of a reliable data base and the difficulty in accounting for the various physical mechanisms in a single correlation.

To remove the uncertainty in the prediction of post-CHF heat transfer, the following studies need to be done: measurement of vapor superheat or degree of nonequilibrium during film boiling in tubes; measurement of liquid temperature during subcooled and low-quality film boiling in tubes; and removal of empiricisms in current analytical heat transfer models for the inverted annular flow regime.

A limitation of some of the correlations is their dependence on steam property equations. During a LOCA, sheath temperatures well in excess of 800°C are frequently postulated to occur. Several heat transfer correlations require evaluation of steam properties at the sheath temperature. Current ASME steam property equations are valid only up to 800°C.

## 8 SUMMARY OF CONCLUSIONS AND FINAL REMARKS

Empirical heat transfer correlations may be used with reasonable confidence for most flow regimes and boiling modes, except for the inverted annular, stratified, and slug flow regimes and the transition boiling mode. Reliable CHF and post-CHF correlations are not yet available for low flows and low pressures.

The lack of success in developing realistic analytical models for the various boiling modes (with the exception of the CHF in annular flow, and liquid-dispersed film boiling) has limited the full utilization of the two- and three-fluid model features of current advanced reactor safety codes.

Most heat transfer correlations are based on tube data. Extrapolation of tube correlations to bundle geometries equipped with flow-obstructing spacers is common practice in reactor safety analysis, as is extrapolation outside the range of the data base. Justification is usually absent.

Heat transfer during single-phase cooling and pre-CHF boiling has been extensively studied and may be predicted at most conditions with reasonable accuracy. Any errors in prediction are expected to have only a minor effect on the maximum fuel temperature during a LOCA.

No single CHF correlation can ever be expected to have a very wide range of applications since the mechanisms governing the boiling crisis change with the flow regime. The most promising approach is the CHF table look-up technique.

Of all the heat transfer modes considered, the transition boiling regime is the least understood. Many transition boiling correlations have been suggested in the literature. All of them are unreliable even within their recommended ranges.

Most heat transfer correlations are functions only of the fluid properties. Surface effects are usually ignored. The

minimum film boiling temperature, however, can be strongly affected by the presence of a surface oxide layer.

#### ACKNOWLEDGMENTS

The authors wish to thank Miss E. Gehlert, Mrs. I. McGandy, and Mr. E. Lindeman for their assistance in the preparation of the manuscript. Part of this review was performed by the first author during his attachment to CEN, Grenoble.

#### NOMENCLATURE

$A$	flow area, normal to flow, $m^2$
$Bo$	boiling number $(= \frac{q}{GH_{fg}})$ , (-)
$C_p$	specific heat at constant pressure, $kJ\ kg^{-1}\ K^{-1}$
$CHF$	critical heat flux, $kW\ m^{-2}$
$d$	rod diameter; droplet diameter, $m$
$D$	tube diameter, $m$
$De$	hydraulic equivalent diameter, $m$
$D_{he}$	heated equivalent diameter, $m$
$D_{hy}$	hydraulic equivalent diameter, $m$
$Fr$	Froude number $(= \frac{G^2}{\rho_l g D_{hy}})$ , (-)
$g$	acceleration due to gravity, $m\ s^{-2}$
$G$	mass flux, $kg\ m^{-2}\ s^{-1}$
$Gr$	Grashof number $[= D_{hy}^3 \rho^2 g \beta (T_w - T_b) / \mu^2]$
$h$	heat transfer coefficient, $kW\ m^{-2}\ K^{-1}$
$h_l^*$	single-phase liquid heat transfer coefficient, based on superficial velocity, $kW\ m^{-2}\ K^{-1}$
$h_m$	heat transfer coefficient at CHF, $kW\ m^{-2}\ K^{-1}$
$H$	enthalpy, $kJ\ kg^{-1}$
$I$	correction factor defined in Sec. 2.4, (-)
$J$	correction factor defined in Sec. 2.4, (-)
$J_g$	volumetric vapor flux $(= GX / \rho_g)$ , $m\ s^{-1}$
$k$	thermal conductivity, $kW\ m^{-1}\ K^{-1}$
$L$	length, $m$
$L_h$	heated length, $m$
$L_{sp}$	axial distance between spacer planes, $m$
$M$	molecular weight, $kg\ kmol^{-1}$
$n$	Droplet density, $m^{-3}$ , number of rods
$N$	Power, $kW$
$N_{sr}$	defined in Table 9, (-)

Nu	Nusselt number ( $= \frac{h D_{hy}}{k}$ ), (-)
$p$	pitch, m
$P$	Pressure, kPa
$P^+$	reduced pressure, $\frac{P}{P_c}$ , (-)
Pr	Prandtl number ( $= \frac{\mu C_p}{k}$ ), (-)
$q$	surface heat flux, kW m <sup>-2</sup>
$R$	gas constant, J kg <sup>-1</sup> K <sup>-1</sup>
$Ra$	universal gas constant, kN m kmol <sup>-1</sup>
Re	Reynolds number ( $= \frac{\rho U D_{hy}}{\mu}$ ), (-)
$Re_d$	droplet Reynolds number $= \frac{\rho_v (U_v - U_d) d}{\mu_v}$ , (-)
$S$	slip ratio ( $= \frac{U_v}{U_l}$ ), (-)
$S$	suppression factor defined graphically by Chen (1963), (-)
$T$	temperature, °C
$T^*$	absolute temperature, K
$T^+$	reduced temperature, $\frac{T}{T_c}$ , (-)
$U$	velocity, m s <sup>-1</sup>
$v$	specific volume, m <sup>3</sup> kg <sup>-1</sup>
$W$	total mass flow rate, kg s <sup>-1</sup>
$X$	flow quality (vapor weight fraction), (-)
$X_{tt}$	Martinelli parameter $\left[ = \left( \frac{1-x}{x} \right)^{0.9} \left( \frac{\rho_g}{\rho_f} \right)^{0.5} \left( \frac{\mu_f}{\mu_g} \right)^{0.1} \right]$ , (-)
$Z$	axial distance from inlet, m
$z$	vertical elevation, m

**Abbreviations** (may also be used as subscripts)

AFD	axial flux distribution
CHF	critical heat flux
C/S	cross section
DO	dryout
ECCS	emergency core cooling system
FB	film boiling
LP	liquid phase
MFB	minimum film boiling
NB	nucleate boiling
ONB	onset of nucleate boiling

PB pool boiling  
 RFD radial flux distribution  
 RPF radial power factor, defined in Condie and Bengston (1978)

**Greek**

$\alpha$  void fraction, (-)  
 $\alpha$  thermal diffusivity,  $\text{m}^2 \text{s}^{-1}$   
 $\beta$  volumetric expansion coefficient,  $\text{K}^{-1}$   
 $\gamma$  coefficient for isentropic expansion, (-)  
 $\Gamma$  volumetric vapor generation rate,  $\text{kg m}^{-3} \text{s}^{-1}$   
 $\delta$  vapor film thickness, m  
 $\Delta H$  local subcooling,  $\text{kJ kg}^{-1}$   
 $\Delta T$  temperature difference (usually with respect to saturation), K  
 $\epsilon$  Eddy diffusivity,  $\text{m}^2 \text{s}^{-1}$   
 $\epsilon$  fraction of flow area occupied by flow obstruction, (-)  
 $\theta$  inclination with respect to vertical upflow, rad  
 $\mu$  viscosity,  $\text{kg m}^{-1} \text{s}^{-1}$   
 $\rho$  density,  $\text{kg m}^{-3}$   
 $\sigma$  surface tension,  $\text{N m}^{-1}$   
 $\phi$  surface heat flux,  $\text{kW m}^{-2}$   
 $\psi_0$  nondimensional parameter in Shah's (1976) correlation reported in Table 2

**Subscripts**

$a$  actual  
 $avg$  average  
 $b$  bulk  
 $BLA$  boiling length average  
 $conv$  convective  
 $c$  critical  
 $d$  droplet  
 $do$  value pertaining to onset of dryout condition  
 $e$  equilibrium  
 $f$  film temperature, average of wall and bulk temperature  
 $f$  saturated liquid  
 $fg$  difference between saturated liquid and saturated vapor  
 $g$  saturated vapor  
 $in$  inlet  
 $i-l$  interface-subcooled liquid  
 $l$  liquid (may be subcooled)  
 $max$  maximum

meas measured  
min minimum film boiling value  
o reference  
pred predicted  
Q apparent quench temperature  
rad radiation  
ref reference, undisturbed  
s,sat saturated  
sc subchannel  
sp flux spike  
sub subcooling  
TP two-phase (pre-CHF) region  
v vapor  
v-d vapor-droplet  
w heated wall  
w-l wall-liquid  
w-v wall-vapor

#### Superscripts

\* superficial value, based on superficial velocity; also absolute value  
+ reduced value

#### REFERENCES

Addoms, J. N. 1948, Heat Transfer at High Rates to Water Boiling Outside Cylinders, D.Sc. thesis, Massachusetts Institute of Technology, Cambridge.

Andersen, J. G. M. 1977, Low Flow Film Boiling Heat Transfer on Vertical Surfaces I. Theoretical Model, AIChE Symp. Ser. vol. 73, no. 73, pp. 2-6.

Bailey, N. A. 1972, The Interaction of Droplet and Forced Convection in Post-Dryout Heat Transfer at High Subcritical Pressures, European Two-Phase Flow Group Meeting, Rome.

Barnett, P. G. 1966, A Correlation for Burnout Data for Uniformly Heated Annuli and Its Use for Predicting Burnout in Uniformly Heated Rod Bundles, Atomic Energy Establishment Winfrith Report AEEW-R-463.

Barnett, P. G. 1968, A Comparison of the Accuracy of Some Correlations for Burnout Annuli and Rod Bundles, Atomic Energy Establishment Winfrith Report AEEW-R-558.

Baumeister, K. J., and F. F. Simon 1973, Leidenfrost Temperature - Its Correlation for Liquid Metals, Cryogenics, Hydrocarbons, and Water, *J. Heat Transfer* vol. 95, pp. 166-173.



Becker, K. M. 1967, An Analytical and Experimental Study of Burnout Conditions in Vertical Round Ducts, *Nukleonik* vol. 9, no. 6, pp. 257-270.

Becker, K.M., and G. Hernborg 1964, Measurements of the Effects of Spacers on the Burnout Conditions for Flow of Boiling Water in a Vertical Annulus and a Vertical 7-Rod Cluster, Atom Energi (Stockholm) Report AE-165.

Becker, K. M., J. Bager, and D. Djursing 1972, Burnout Correlations in Simple Geometries: Most Recent Assessments, Invited lecture presented at the *Seminar of Two-Phase Flow Thermohydraulics*, Rome, Italy, Report KTH-NEL-18.

Becker, K. M., J. Flinta, and O. Nylund 1967, Dynamic and Static Burnout Studies for the Full-Scale Marviken Fuel Elements in the 8-MW Loop FRIGG, *Proceedings of Symposium on Two-Phase Flow Dynamics*, Eindhoven, Netherlands, vol. 1, pp. 461-474. Published by Euratom, Brussels.

Bell, K. J. 1967, The Leidenfrost Phenomenon: A Survey, *Chem. Eng. Prog. Symp. Ser.* vol. 63, no. 79, pp. 73-82.

Bennett, A. W., H. A. Kearsley, and R. K. F. Keays 1964, Heat Transfer to Mixtures of High-Pressure Steam and Water in an Annulus, Part VI, Atomic Energy Research Establishment Report AERE-R-4352.

Bennett, A. W., G. F. Hewitt, H. A. Kearsley, and R. K. F. Keays 1966, The Wetting of Hot Surfaces by Water in a Steam Environment at High Pressures, Atomic Energy Research Establishment Report AERE-R-5146.

Bennett, A. W., G. F. Hewitt, H. A. Kearsley, and R. K. F. Keays 1967, Heat Transfer to Steam-Water Mixtures Flowing in Uniformly Heated Tubes in Which the Critical Heat Flux Has Been Exceeded, Atomic Energy Research Establishment Report AERE-R-5373.

Berenson, P. J. 1960, Transition Boiling Heat Transfer from a Horizontal Surface, Massachusetts Institute of Technology MIT Technical Report No. 17.

Berenson, P. J. 1961, Film Boiling Heat Transfer from a Horizontal Surface, *J. Heat Transfer* vol. 83, pp. 351-358.

Bergles, A. E. 1977, Burnout in Boiling Heat Transfer. II. Subcooled and Low-Quality Forced Convective Systems, *Nucl. Saf.* vol. 18, no. 2, pp. 154-167.

Bergles, A. E. 1979, Burnout in Boiling Heat Transfer. III. High-Quality Forced Convective Systems, *Nucl. Saf.* vol. 20, no. 6, pp. 671-689.

Bertoletti, S. 1961, Heat Transfer and Pressure Drop with Steam-Water Spray, Centro Informazioni - Studi Esperienze, Milano CISE R-36.

Bertoletti, S. 1964, Heat Transfer to Steam-Water Mixtures, Centro Informazioni - Studi Esperienze, Milano CISE R-78.

Biasi, L., G. C. Clerici, S. Garribba, R. Sala, and A. Tozzi 1967, Studies on Burnout: Part 3, *Energ. Nucl. Milan* vol. 14, pp. 530-536.

Bishop, A. A., L. E. Efferding, and L. S. Tong 1962, A Review of Heat Transfer and Fluid Flow of Water in the Supercritical Region and during "Once-Thru" Operation, Westinghouse Canada Atomic Power Report WCAP-2040.

Bishop, A. A., R. O. Sandberg, and L. S. Tong 1964, High-temperature Supercritical Pressure Water Loop. V. Forced Convection Heat Transfer to Water after the Critical Heat Flux at High Supercritical Pressures, Westinghouse Canada Atomic Power Report WCAP-2056 (Part 5).

Bishop, A. A., R. O. Sandberg, and L. S. Tong 1965, Forced Convection Heat Transfer at High Pressure after the Critical Heat Flux, American Society of Mechanical Engineering ASME-65-HT-31.

Bjornard, T. A., and P. Griffith 1977, PWR Blowdown Heat Transfer, *Proceedings of ASME Topical Meeting on Thermal and Hydraulic Aspects of Nuclear Reactor Safety*, Atlanta, Georgia, vol. 1, pp. 17-41, O. C. Jones, Jr. and S. G. Bankoff, eds. Published by ASME, New York.

Bowring, R. W. 1972, A Simple but Accurate Round Tube; Uniform Heat Flux Dryout Correlation over the Pressure Range 0.7-17.0 MN/m<sup>2</sup>, Atomic Energy Establishment Winfrith Report AEEW-R-789.

Bowring, R. W. 1977, A New Mixed-Flow Cluster Dryout Correlation for Pressures in the Range 0.6-15.5 MN/m<sup>2</sup> for Use in Transient Blowdown Code, *Proceedings of IME Meeting on Reactor Safety*, Manchester, Paper C217/77.

Bradfield, W. S. 1967, On the Effect of Subcooling on the Wall Superheat in Pool Boiling, *J. Heat Transfer* vol. 89, pp. 269-270.

Brevi, R., M. Cumo, A. Palmieri, and D. Pitimada 1969, Heat Transfer Coefficient in Post Dryout Two-Phase Mixtures, European Two-Phase Group Meeting, Karlsruhe.

Bromley, L. A. 1950, Heat Transfer in Stable Film Boiling, *Chem. Eng. Prog.* vol. 46, pp. 221-227.

Bromley, L. A. 1952, Effect of Heat Capacity on Condensate, *Ind. Eng. Chem.* vol. 44, pp. 2966-2969.

Bromley, L. A., N. R. LeRoy, and J. A. Robbers 1953, Heat Transfer in Forced Convective Film Boiling, *Ind. Eng. Chem.* vol. 45, pp. 2639-2646.

Butterworth, D., and R. G. Owen 1975, The Quenching of Hot Surfaces by Top and Bottom Flooding: A Review, Atomic Energy Research Establishment AERE-R-7992.

Butterworth, D., and R. A. W. Shock 1975, The Design of Vertical Thermosyphon Reboilers, Atomic Energy Research Establishment AERE-R-8053.

Chan, K. C., and G. Yadigaroglu 1980, Calculations of Film Boiling

6. Heat Transfer above the Quench Front During Reflooding, *Experimental and Analytical Modelling of LWR Safety Experiment*, American Society of Mechanical Engineers ASME Publ. HTD-Vol. 7.

Chen, J. C. 1963, A Correlation for Boiling Heat Transfer to Saturated Fluids in Convective Flow, American Society of Mechanical Engineers ASME 63-HT-34.

Chen, J. C., F. T. Ozkaynak, and R. K. Sundaram 1979, Vapor Heat Transfer in the Post-CHF Region Including the Effect of Thermodynamic Nonequilibrium, *Nucl. Eng. Des.* vol. 51, pp. 143-155.

Cheng, S. C., W. W. L. Ng, and K. T. Heng 1978, Measurements of Boiling Curves of Subcooled Water Under Forced Convective Conditions, *Int. J. Heat Mass Transfer* vol. 21, pp. 1385-1392.

Cheng, S. C., K. T. Poon, P. Lau, and W. W. L. Ng 1981, Transition Boiling Heat Transfer in Forced Vertical Flow (Measurements of Quench Temperature), University of Ottawa 20th Quarterly Progress Report, Oct.-Dec. 1981, Argonne National Laboratories Contract 31-109-38-5503.

Chi, J. W. H. 1967, Slug Flow and Film Boiling of Hydrogen, *J. Spacecr. Rockets* vol. 4, pp. 1329-1332.

Clément, P., R. Deruaz, M. Lambert, and P. Pic 1979, Refroidissement de secours des reacteurs à eau légère; Essais de renouage en géométrie tubulaire, Centre D'Etudes Nucléaires de Grenoble Report TT-156.

Clerici, G. C., S. Garriba, R. Sala, and A. Tozzi 1965, A Catalogue of Burnout Correlations for Forced Convection in the Quality Region, Euratom Report EUR-3300.e.

Colburn, A. P. 1933, Method of Correlating Forced Convective Heat Transfer Data and a Comparison with Fluid Friction, *Trans. Am. Inst. Chem. Eng.* vol. 29, pp. 174-210.

Collier, J. G. 1962, Heat Transfer and Fluid Dynamic Research as Applied to Fog-Cooled Reactors, Atomic Energy of Canada Limited, Chalk River, Ontario, Report AECL-1631.

Collier, J. G. 1980, *Convective Boiling and Condensation*, Second Edition, London: McGraw-Hill.

Condie, K. G., and S. J. Bengston 1978, Development of the MOD 7 CHF Correlation, E.G.&G. Idaho Inc., Idaho Falls, Idaho, Report PN-181-78.

Cooper, M. G. 1982, Correlations for Nucleate Boiling - Formulation Using Reduced Properties, *Physico Chemical Hydrodynamics* vol. 3, no. 2, pp. 89-111.

Cumo, M., and G. C. Urbani 1971, Anomalies in Post-Dryout Heat Transfer at High Pressures, *Trans. Am. Nucl. Soc.* vol. 14, pp. 245-246.

Cumo, M., and G. C. Urbani 1974, Post-Burnout Heat Transfer (Attainable Precision Limits of the Measured Coefficient),

Comitato Nazionale Energia Nucleare CNEN/RT/ING(74)24.

Dengler, C. E., and J. N. Addoms 1956, Heat Transfer Mechanisms for Vaporization of Water in a Vertical Tube, *Chem. Eng. Prog. Symp. Ser.* vol. 52, no. 18, pp. 95-103.

Dhir, V. K., R. B. Duffey, and I. Cotton 1981, Quenching Studies on a Zircaloy Rod Bundle, *J. Heat Transfer* vol. 103, pp. 293-299.

Dittus, F. W., and L. M. K. Boelter 1930, Heat Transfer in Automobile Radiators of the Tubular Type, University of California Publications, vol. 2, pp. 443-461.

Doroshchuk, V. E., and F. P. Lantsman 1970, Selecting Magnitudes of Critical Heat Fluxes with Water Boiling in Vertical Uniformly Heated Tubes, *Therm. Eng. (USSR)* vol. 17, no. 12, pp. 18-21.

Doroshchuk, V. E., L. L. Levitan, and F. P. Lantzman 1975, Investigations into Burnout in Uniformly Heated Tubes, American Society of Mechanical Engineers ASME 75-WA/HT-22.

Dougall, R. S., and W. M. Rohsenow 1963, Film Boiling on the Inside of Vertical Tubes with Upward Flow of the Fluid at Low Qualities, Massachusetts Institute of Technology Report No. 9079-26.

Elias, E., and P. Chambré 1981, Inverted Annular Film Boiling Heat Transfer from Vertical Surfaces, *Nucl. Eng. Des.* vol. 64, pp. 249-257.

Ellion, M. E. 1954, A Study of the Mechanism of Boiling Heat Transfer, California Institute of Technology Report JPL-MEMO-20-88.

Era, A., G. P. Gaspari, A. Hassid, A. Milani, and R. Zavattarelli 1967, Heat Transfer Data in the Liquid Deficient Region for Steam-Water Mixtures at 70 kg/cm<sup>2</sup> Flowing in Tubular and Annular Conduits, Centro Informazioni-Studi Esperienze, Milano CISE R-184.

Forster, K., and R. Greif 1959, Heat Transfer to a Boiling Liquid; Mechanism and Correlation, *J. Heat Transfer* vol. 81C, pp. 43-53.

Fung, K. K. 1977, Forced Convective Transition Boiling, M.Sc. thesis, University of Toronto.

Fung, K. K. 1978, Post-CHF Heat Transfer during Steady-State and Transient Conditions, Report NUREG/CR-0195, Argonne National Laboratories ANL-78-55.

Fung, K. K. 1981, Subcooled and Low-Quality Film Boiling of Water in Vertical Flow at Atmospheric Pressure, Ph.D. thesis, University of Ottawa.

Fung, K. K., S. R. M. Gardiner, and D. C. Groeneveld 1979, Subcooled and Low-Quality Flow Film Boiling of Water at Atmospheric Pressure, *nucl. Eng. Des.* vol. 55, pp. 51-57.

Gasc, B. 1966, Repartition des coefficients d'echange dans une grappe, *EAES Heat Transfer Symposium on Superheated Steam or Gas*, Berne, Aug. 31-Sept. 3.

- Gaspari, G. P., A. Hassid, R. Ravetta, L. Rubiera 1968, Heat Transfer Crisis and Pressure Drop with Steam-Water Mixtures: Further Experimental Data with Seven-Rod Bundles, Centro Informazioni Informazioni-Studi Esperienze, Milano Report R-208.
- Gaspari, G. P., A. Hassid, and C. Vanoli 1969, An Experimental Investigation on the Influence of Radial Power Distribution on Critical Heat Flux in a Nuclear Rod Cluster, *European Two-Phase Flow Group Meeting*, Karlsruhe.
- Gaspari, G. P., R. Ravetta, L. Rubiera, G. Vanoli 1970, Heat Transfer Crisis and Pressure Drop Measurements with Steam-Water Mixtures in Nineteen-Rod Clusters, Centro Informazioni-Studi Esperienze, Milano Report R-294.
- Gellerstedt, J. S., R. A. Lee, W. J. Oberjohn, R. H. Wilson, and L. J. Stanek 1969, Correlation of Critical Heat Flux in a Bundle Cooled by Pressurized Water, *Two-Phase Flow and Heat Transfer in Rod Bundles*, American Society of Mechanical Engineers Winter Annual Meeting, Los Angeles, pp. 63-71.
- Ginoux, J. J. 1978, *Two-Phase Flows and Heat Transfer with Application to Nuclear Reactor Design Problems*, New York: McGraw-Hill, pp. 375-381.
- Griffel, J., and C. F. Bonilla 1965, Forced Convection Boiling Burnout for Water in Uniformly Heated Tubular Test Sections, *Nucl. Struct. Eng.* vol. 2, pp. 1-35.
- Griffiths, P., J. F. Pearson, and R. J. Lepkowski 1977, Critical Heat Flux during a Loss-of-Coolant Accident, *Nucl. Saf.* vol. 18, no. 3, pp. 298-305.
- Groeneveld, D. C. 1969, An Investigation of Heat Transfer in the Liquid-Deficient Regime, Atomic Energy of Canada Limited, Chalk River, Ontario, Report AECL-3281.
- Groeneveld, D. C. 1972, The Thermal Behaviour of a Heated Surface at and Beyond Dryout, Atomic Energy of Canada Limited, Chalk River, Ontario, Report AECL-4309.
- Groeneveld, D. C. 1973, Forced Convective Heat Transfer to Superheated Steam in Rod Bundles, Atomic Energy of Canada Limited, Chalk River, Ontario, Report AECL-4450.
- Groeneveld, D. C. 1975, The Effect of Short Flux Spikes on the Dryout Power, Atomic Energy of Canada Limited, Chalk River, Ontario, Report AECL-4927.
- Groeneveld, D. C. 1981a, Heat Transfer Phenomena Related to the Boiling Crisis, Atomic Energy of Canada Limited, Chalk River, Ontario, Report AECL-7239.
- Groeneveld, D. C. 1982, A General CHF Prediction Method for Water Suitable for Reactor Accident Analysis, Centre D'Etudes Nucléaires de Grenoble, Report DRE/STT/SETRE/82-2.
- Groeneveld, D. C., and A. S. Borodin 1980, Occurrence of Slow Dryout in Forced Convective Flow, *Multiphase Transport; Fundamentals*

*and Reactor Safety Applications*, Washington, D.C.: Hemisphere, vol. 2, pp. 583-600.

Groeneveld, D. C., and K. K. Fung 1976, Forced Convective Transition Boiling: Review of Literature and Comparison of Predictive Methods, Atomic Energy of Canada Limited, Chalk River, Ontario, Report AECL-5543.

Groeneveld, D. C., and G. G. J. Delorme 1976, Predictions of Thermal Nonequilibrium in the Post-Dryout Regime, *Nucl. Eng. Des.* vol. 36, pp. 17-26.

Groeneveld, D. C., and S. R. M. Gardiner 1977, Post-CHF Heat Transfer under Forced Convective Conditions, *ASME Symposium on the Thermal and Hydraulic Aspects of Nuclear Reactor Safety*, vol. 1, pp. 43-73, O. C. Jones and S. G. Bankoff, eds.

Groeneveld, D. C., and S. R. M. Gardiner 1978, A Method of Obtaining Flow Film Boiling Data for Subcooled Water, *Int. J. Heat Mass Transfer* vol. 21, pp. 664-665.

Groeneveld, D. C. and G. D. McPherson 1973, In-Reactor Post-Dryout Experiments with 36-Element Fuel Bundles, Atomic Energy of Canada Limited, Chalk River Ontario, Report AECL-4705.

Groeneveld, D. C., and J. C. Rousseau 1983, CHF and Post-CHF Heat Transfer: An Assessment of Prediction Methods and Recommendations for Reactor Safety Codes, *Proceedings NATO Meeting on Advances in Two-Phase Flow and Heat Transfer*, vol. I, pp. 209-239, (NATO ASI Series, Series E, No. 63), Nijhoff, The Hague.

Groeneveld, D. C. and J. C. Stewart 1982, The Minimum Film Boiling Temperature for Water during Film Boiling Collapse, *7th Int. Heat Transfer Conf.*, Munich.

Groeneveld, D. C., and W. W. Yousef 1980, Spacing Devices for Nuclear Fuel Bundles: A Survey of Their Effect on CHF, Post-CHF Heat Transfer, and Pressure Drop, *Proceedings of the ANS/ASME/NRC International Topical Meeting on Nuclear Reactor Thermal-Hydraulics*, Saratoga Springs, NY, NUREG/CP-0014, vol. 2, pp. 1111-1130.

Guglielmini, G., E. Nannei, and C. Pisoni 1978, Comparative Analysis of Heat Transfer Correlations for Forced Convective Boiling, *Comitato Nazionale Energia Nucleare RT/ING(78)18*.

Guglielmini, G., E. Nannei, and C. Pisoni 1980, Survey of Heat Transfer Correlations in Forced Convective Boiling, *Wärme und Stoffübertragung* vol. 13, pp. 177-185.

Hadaller, G., and S. Banerjee 1969, Heat Transfer to Superheated Steam in Round Tubes, Atomic Energy of Canada Limited, Pinawa, Manitoba, Internal Report WDI-147.

Heineman, J. B. 1960, An Experimental Investigation of Heat Transfer to Superheated Steam in Round and Rectangular Channels, Argonne National Laboratories ANL-6213.

Hench, J. E. 1964, Forced Flow Transition Boiling Experiments in a Two-Rod Test Section at High Pressure, American Society of

Mechanical Engineers ASME 64-WA/HT-44.

Henry, R. E. 1974, A Correlation for the Minimum Boiling Temperature, *AIChE Symp. Ser.* vol. 70, no. 138, pp. 81-90.

Herkenrath, H., P. Mörk-Mörkenstein, U. Jung and F.-J. Weckermann 1967, Wärmeübergang an Wasser bei Erzwungener Strömung im Druckbereich von 140 bis 250 bar, Euratom report EUR-3658d.

Hewitt, G. F. 1978, Critical Heat Flux in Flow Boiling, *Proceedings of Sixth International Heat Transfer Conference*, Toronto, Canada, vol. 6, pp. 143-172, Hemisphere Publishing Corp., Washington.

Hewitt, G. F., and N. S. Hall-Taylor 1970, *Annular Two Phase Flow*, Oxford: Pergamon.

Hoffman, H. W. 1970, Experimental Studies of the Heat Transfer and Fluid Dynamic Characteristics of Rod-Cluster-Type Nuclear Reactor Fuel Elements, Oak Ridge National Laboratories ORNL-4356, pp. 74-118.

Howard, P. A. 1976, An Experimental and Analytical Study of the Sputtering Phenomenon, Argonne National Laboratories ANL-76-41.

Howard, P. A., J. H. Lineman, and M. A. Grolmes 1975, Experimental Study of the Stationary Boiling Front in Liquid Film Cooling of a Vertical Heated Rod, *CJChE/CSME-75-HT-14*, 15th National Heat Transfer Conference, San Francisco.

Hsu, Y. Y. 1975, A Tentative Correlation for the Regime of Transition Boiling and Film Boiling During Reflood, Paper presented at the 3rd Water Reactor Safety Review Information Meeting, United States Nuclear Regulatory Commission, Washington, D.C.

Hsu, Y. Y., and W. D. Beckner 1977, Correlation for the Onset of Transient CHF, cited in Tong, L. S., and G. L. Bennett, NRC Water Reactor Safety Research Program, *Nucl. Saf.* vol. 18, no. 1, pp. 1-44.

Iloeje, O. C., D. N. Plummer, W. M. Rohsenow, and P. Griffith 1974, A Study of Wall Rewet and Heat Transfer in Dispersed Vertical Flow, Massachusetts Institute of Technology, Cambridge, MIT Technical Report 72718-92.

Ivey, H. J., and D. J. Morris 1962, On the Relevance of the Vapour-Liquid Exchange Mechanism for Subcooled Boiling Heat Transfer at High Pressures, Atomic Energy Establishment Winfrith AEEW-R-137.

Janssen, E., F. A. Schraub, R. B. Nixon, B. Matzner, and J. F. Casterline 1969, Sixteen-Rod Heat Flux Investigation, Steam-Water at 600 to 1250 psi, *Two-Phase Flow and Heat Transfer in Rod Bundles*, American Society of Mechanical Engineering Winter Annual Meeting, pp. 81-88.

Jens, W. H., and P. A. Lottes 1951, Analysis of Heat Transfer Burnout, Pressure Drop, and Density Data for High-Pressure Water, Argonne National Laboratories ANL-4627.

- Jones, O. C., Jr., and N. Zuber 1977, Post-CHF Heat Transfer: A Nonequilibrium Relaxation Model, American Society of Mechanical Engineering ASME 77-HT-79.
- Kalinin, E. K. 1969, Investigation of the Crisis of Film Boiling in Channels, *Two-Phase Flow and Heat Transfer in Rod Bundles*, American Society of Mechanical Engineering Winter Annual Meeting, Los Angeles, pp. 89-94.
- Kalinin, E. K., V. K. Koshkin, S. R. Yarkho, I. I. Berlin, Y. S. Kochelaev, V. V. Kostyuk, A. L. Korolev, and G. N. Sdobnov 1970, Investigation of Film Boiling in Tubes with Subcooled Nitrogen Flow, *Fourth International Heat Transfer Conference*, B4.5, Paris.
- Kalinin, E. K., V. K. Koshkin, S. A. Yarkho, I. I. Berlin, V. V. Kostyuk, and Yu. S. Kochelaev 1969, Heat Transfer in Tubes with Rod Regime in the Case of Flow Boiling of a Subcooled Liquid, *Cocurrent Gas-Liquid Flow*, New York: Plenum, pp. 497-525.
- Katto, Y 1978, A Generalized Correlation of Critical Heat Flux for the Forced Convection Boiling in Vertical Uniformly Heated Round Tubes, *Int. J. Heat Mass Transfer* vol. 21, pp. 1527-1542.
- Katto, Y. 1979a, A Generalized Correlation of Critical Heat Flux for the Forced Convection Boiling in Vertical Uniformly Heated Round Tubes - A Supplementary Report, *Int. J. Heat Mass Transfer* vol. 22, pp. 783-794.
- Katto, Y. 1979b, An Analysis of the Effect of Inlet Subcooling on Critical Heat Flux of Forced Convection Boiling in Vertical Uniformly Heated Tubes, *Int. J. Heat Mass Transfer* vol. 22, pp. 1567-1575.
- Katto, Y. 1980, General Features of CHF of Forced Convection Boiling in Uniformly Heated Vertical Tubes with Zero Inlet Subcooling, *Int. J. Heat Mass Transfer* vol. 23, pp. 493-504.
- Kaufman, J. M. 1976, Post-Critical Heat Flux Heat Transfer to Water in a Vertical Tube, M.Sc. thesis, Massachusetts Institute of Technology, Cambridge.
- Kidd, G. J., W. J. Stelzman, and H. W. Hoffman 1968, The Temperature Structure and Heat Transfer Characteristics of an Electrically Heated Model of a Seven-Rod Cluster Fuel Element, American Society of Mechanical Engineering 68-WA/HT-33.
- Kim, A. K., and Y. Lee 1979, A Correlation of Rewetting Temperature, *Lett. Heat Mass Transfer* vol. 6, pp. 117-123.
- Kobori, T. 1976, Critical Heat Flux Measurements in a Full-Scale Rod Cluster, *Bull. JSME* vol. 19, no. 131, pp. 540-546.
- Koram, K. K., and E. M. Sparrow 1978, Turbulent Heat Transfer Downstream of an Unsymmetric Blockage in a Tube, *J. Heat Transfer* vol. 100, pp. 588-594.
- Krall, K. M., and E. M. Sparrow 1966, Turbulent Heat Transfer in the Separated, Reattached, and Redevelopment Regions of a Circular



Tube, J. *Heat Transfer* vol. 88, pp. 131-136.

Kutateladze, S. S., and V. M. Borishanskii 1966, *A Concise Encyclopedia of Heat Transfer*, Oxford: Pergamon.

Laperrière, A. 1983, An Analytical and Experimental Investigation of Forced Convective Film Boiling, M.A.Sc. thesis, Department of Mechanical Engineering, University of Ottawa.

Lauer, H., and W. Hufschmidt 1976, Heat Transfer and Surface Rewet During Quenching, *Two-Phase Flow and Heat Transfer*, vol. III (proceedings of NATO Advanced Study Institute, Istanbul, Turkey), Washington, D.C.: Hemisphere, pp. 1309-1326.

Laverty, W. F., and W. M. Rohsenow 1967, Film Boiling of Saturated Liquid Nitrogen Flowing in a Vertical Tube, *J. Heat Transfer* vol. 89, pp. 90-98.

Lee, D. H. 1970, Studies of Heat Transfer and Pressure Drop Relevant to Subcritical Once-Through Evaporators, IAEA-SM-130/56, *IAEA Symposium on Progress in Sodium-Cooled Fast-Reactor Engineering*, Monaco, published by International Atomic Energy Authority, Vienna.

Lee, Y., W. J. Chen, and D. C. Groeneveld 1978, Rewetting of Very Hot Vertical and Horizontal Channels by Flooding, *Proceedings of 6th Int. Heat Transfer Conference*, Toronto, Hemisphere Publishing Corp., Washington, D.C., vol. 5, pp. 95-100.

Leung, J. C. M. 1978, Critical Heat Flux under Transient Conditions: A Literature Survey, Argonne National Laboratories Report NUREG/CR-0056; Argonne National Laboratories 78-39.

Leung, J. C. M. 1980, Transient Critical Heat Flux and Blowdown Heat Transfer Studies, Argonne National Laboratories Report NUREG/CR-1559; Argonne National Laboratories 80-53.

Levitan, L. L., and F. P. Lantsman 1977, Critical Heat Fluxes in Internally Heated Annular Channels, *Therm. Eng. (USSR)* vol. 24, no. 4, pp. 16-21.

Macbeth, R. V. 1963, Burnout Analysis, Part 4: Application of a Local Conditions Hypothesis to World Data for Uniformly Heated Tubes and Rectangular Channels, Atomic Energy Establishment Winfrith AEEW-R-267.

Mattson, R. J., K. G. Condie, S. J. Bengston, and C. F. Obenchain 1974, Regression Analysis of Post-CHF Flow Boiling Data, *Fifth Int. Heat Transfer Conf.* vol. IV, B3.8, Tokyo.

McAdams, W. H. 1954, *Heat Transmission*, New York: McGraw-Hill.

McAdams, W. H., W. E. Kennel, C. S. Minden, R. Carl, P. M. Picornell, and J. E. Dew 1949, Heat Transfer at High Rates to Water with Surface Boiling, *Inst. Chem. Eng.*, vol. 41, pp. 1945-1955.

McDonough, J. B., W. Milich, and E. C. King 1961, An Experimental Study of Partial Film Boiling Region with Water at Elevated Pressures in a Round Vertical Tube, *Chem. Eng. Prog. Symp. Ser.* vol. 57, no. 32, pp. 197-208.

- McPherson, G. D. 1971, The Use of Enthalpy Imbalance in Evaluating the Dryout Performance of Fuel Bundles, Atomic Energy of Canada Limited, Chalk River, Ontario, Report AECL-3968.
- Merte, H., and J. A. Clark 1961, Boiling Heat Transfer Data for Liquid Nitrogen at Standard and Near-Zero Gravity, *Adv. Cryog. Eng.* vol. 7, pp. 246-250.
- Miropol'skiy, Z. L. 1963, Heat Transfer in Film Boiling of a Steam-Water Mixture in Steam Generating Tubes, *Teploenergetika* vol. 10, pp. 49-53.
- Mueller, R. E. 1967, Film Boiling Heat Transfer Measurements in a Tubular Test Section, Euratom Atomic Energy Commission EURAEC-1871/General Electric Atomic Power GEAP-5423.
- Nelson, R. A. 1980, Forced Convective Post-CHF Heat Transfer and Quenching, American Society of Mechanical Engineering Winter Annual Meeting, 80-WA/HT-69, Chicago.
- Nijhawan, S., J. C. Chen, R. K. Sundaram, and E. J. London 1980, Measurement of Vapour Superheat in Post-Critical Heat Flux Boiling, *J. Heat Transfer* vol. 102, pp. 450-470.
- Nishio, S., and M. Hirata 1978, Direct-Contact Phenomenon between a Liquid Droplet and High-Temperature Solid Surface, *6th Int. Heat Transfer Conference* vol. I, pp. 245-250, Toronto.
- Nobel, L. 1970, The Heat Transfer Coefficient as a Function of Steam Quality for High-Pressure Once-Through Flow Boiling, with Determination of the Transition Points between the Regions of Particular Heat Transfer, Euratom report EUR-4561.
- Norman, W. S., and V. McIntyre 1960, Heat Transfer to a Liquid Film on a Vertical Surface, *Trans. Inst. Chem. Eng.* vol. 38, pp. 301-307.
- Peterson, W. C., M. M. Aboul Fetouh, and M. G. Zaalouk 1973, Boiling Curve Measurements from a Controlled Forced Convection Process, *Proc. Brit. Nucl. Eng. Society, Conference on Boiler Dynamics and Control in Nuclear Power Stations*, London.
- Plummer, D. N., P. Griffith, and W. M. Rohsenow 1976, Post-Critical Heat Transfer to Flowing Liquid in a Vertical Tube, *16th National Heat Transfer Conference*, 76-CSME/ChE-13, St. Louis, Missouri.
- Plummer, D. N., O. C. Iloeje, P. Griffith, and W. M. Rohsenow 1973, A Study of Post-Critical Heat Flux Heat Transfer in a Forced Convection System, Massachusetts Institute of Technology Report No. 73645-80.
- Polomik, E. E. 1967, Transition Boiling, Heat Transfer Program, Final Summary Report on Program for Feb. 63-Oct. 67, General Electric Atomic Power Report 5563.
- Polomik, E. E., S. Levy, and S. G. Sawochka 1961, Heat Transfer Coefficients with Annular Flow during Once-Through Boiling of Water to 100% Quality at 800, 1000, and 1400 psi, General Electric Atomic Power Report 3703.

Quinn, E. P. 1965, Forced Flow Transition Boiling Heat Transfer from Smooth and Finned Surfaces, General Electric Atomic Power Report 4786.

Quinn, E. P. 1966, Physical Model of Heat Transfer Beyond the Critical Heat Flux, General Electric Atomic Power Report 5093.

Ragheb, H. S., S. C. Cheng, and D. C. Groeneveld 1981, Observations in Transition Boiling of Subcooled Water under Forced Convective Conditions *Int. J. Heat Mass Transfer* vol. 24, no. 7, pp. 1127-1137.

Ralph, J. C., S. Sanderson, and J. A. Ward 1977, Post-Dryout Heat Transfer under Low-Flow and Low-Quality Conditions, American Society of Mechanical Engineering Winter Annual Meeting, Atlanta, Georgia.

Ramu, K., and J. Weisman 1974, A Method for the Correlation of Transition Boiling Heat Transfer Data, *Proceedings of the Fifth International Heat Transfer Conference*, Tokyo, vol. IV, B4.4.

Rohsenow, W. M. 1952, A Method of Correlating Heat Transfer Data for Surface Boiling Liquids, *Trans. American Soc. of Mech. Eng.* vol. 74, p. 969.

Rohsenow, W. M., and H. Choi 1961, *Heat, Mass, and Momentum Transfer*, Englewood Cliffs, NJ: Prentice-Hall.

Rohsenow, W. M., and J. P. Hartnett 1973, *Handbook of Heat Transfer*, New York: McGraw-Hill.

Saha, P. 1980, A Nonequilibrium Heat Transfer Model for Dispersed Droplet Post-Dryout Regime, *Int. J. Heat Mass Transfer* vol. 23, pp. 438-492.

Schmidt, K. R. 1960, Thermodynamic Investigations of Highly Loaded Boiler Heating Surfaces, Atomic Energy of Canada report AEC-TR-4033.

Schrock, V. E., and L. M. Grossman 1959, Forced Convection Boiling Studies; Final Report on Forced Convection Vaporization Project, USAEC Report Technical Information Department 14632.

Shah, M. M. 1976, A New Correlation for Heat Transfer during Boiling Flow through Pipes, *ASHRAE Trans.* vol. 82, Part 2, pp. 66-86.

Shah, M. M. 1977, A General Correlation for Heat Transfer during Subcooled Boiling in Pipes, *ASHRAE Trans.* vol. 83, Part 1, pp. 202-217.

Shah, M. M. 1979, A Generalized Graphical Method for Predicting CHF in Uniformly Heated Vertical Tubes, *Int. J. Heat Mass Transfer* vol. 22, pp. 557-568.

Shah, M. M. 1980, A General Predictive Technique for Heat Transfer during Saturated Film Boiling in Tubes, *Heat Transfer Eng.* vol. 2, pp. 51-62.

Shah, M. M. 1981, Generalized Prediction of Heat Transfer during Two Component Gas-Liquid Flow in Tubes and their Channels, *AIChE Symp. Ser.* vol. 77, no. 208, pp. 140-151.

Shah, M. M. 1982, CHART Correlation for Saturated Boiling Heat

Transfer: Equations and Further Study, *ASHRAE Trans.* vol. 88, Part 1, pp. 185-196.

Shires, G. L., A. R. Pickering, and R. T. Blacker 1964, Film Cooling of Vertical Fuel Rods, Atomic Energy Research Establishment report AERE-R-343.

Sieder, E. N., and G. E. Tate 1936, Heat Transfer and Pressure Drop of Liquids in Tubes, *Ind. Eng. Chem.* vol. 28, pp. 1429-1436.

Simon, F. F., and R. J. Simoneau 1969, Transition from Film to Nucleate Boiling in Vertical Forced Flow, American Society of Mechanical Engineering report ASME 69-HT-26.

Siviour, J. B., and A. J. Ede 1970, Heat Transfer in Subcooled Pool Film Boiling, *Fourth Int. Heat Transfer Conf.*, Paris, B3.12.

Slaughterbeck, D. C., L. J. Ybarrondo, and C. F. Obenchain 1973, Flow Film Boiling Heat Transfer Correlations: A Parametric Study with Data Comparisons, American Society of Mechanical Engineering report ASME 73-HT-50

Smolin V. N., and V. K. Polyakov 1978, Coolant Boiling Crisis in Rod Assemblies, *Sixth Int. Heat Transfer Conf.*, Toronto, vol. 5, pp. 47-52.

Snoek, C. W. 1972, The Influence of Pressure on the Leidenfrost Point, M.E.Sc. Thesis, The University of Western Ontario.

Spiegler, P., J. Hopenfeld, M. Silberberg, C. F. Bumpus, and A. Norman 1963, Onset of Stable Film Boiling and Foam Limit, *Int. J. Heat Mass Transfer* vol. 6, pp. 987-994.

Stewart, J. C. 1981, Low-Quality Film Boiling at Intermediate and Elevated Pressures, M.A.Sc. thesis, University of Ottawa.

Stewart, J. C., and D. C. Groeneveld 1982, Low-Quality and Subcooled Film Boiling at Elevated Pressures, *Nucl. Eng. Des.* vol. 67, pp. 259-272.

Swenson, H. S., J. R. Carver, and G. Szoeko 1961, The Effects of Nucleate Boiling versus Film Boiling on Heat Transfer in Power Boiler Tubes, American Society of Mechanical Engineering report ASME 61-WA-201.

Tahir, A., and M. B. Carver 1982, ASSERT and COBRA Predictions of Flow Distribution in Vertical Bundles, *CNS/ANS International Conference on Numerical Methods in Nuclear Engineering*, Montreal.

Thom, J. R. S., W. M. Walker, T. A. Fallon, and G. F. S. Reising 1966, Boiling in Subcooled Water during Flow up Heated Tubes or Annuli, *Proc. Inst. Mech. Eng.* vol. 180, Part 3C, pp. 226-246.

Thompson, T. S. 1973, On the Process of Rewetting a Hot Surface by a Falling Liquid Film, *Nucl. Eng. Des.* vol. 31, pp. 234-245; also Atomic Energy of Canada Limited, Chalk River, Ontario Report AECL-4516.

Thompson, T. S. 1974, Rewetting of a Hot Surface, *Proceedings 5th Int. Heat Transfer Conf.*, Tokyo, B3.13; also Atomic Energy of

Canada Limited, Report AECL-5060.

Todreas, N. E., and W. M. Rohsenow 1965, The Effect of Nonuniform Axial Heat Flux Distribution, Massachusetts Institute of Technology Department of Mechanical Engineering, Report 9843-37.

Tolubinskiy, V. I., Y. D. Domashev, A. K. Litoshenko, and A. S. Matorin 1977, Boiling Crisis in Concentric and Eccentric Annuli, *Heat Transfer Sov. Res.* vol. 9, no. 1, pp. 132-139.

Tong, L. S. 1965, *Boiling Heat Transfer and Two Phase Flow*, New York: Wiley.

Tong, L. S. 1967, Prediction of Departure from Nucleate Boiling for an Axially Nonuniform Heat Flux Distribution, *J. Nucl. Energy* vol. 21, pp. 241-248.

Tong, L. S. 1969, Critical Heat Fluxes in Rod Bundles, *Two-Phase Flow and Heat Transfer in Rod Bundles*, American Society of Mechanical Engineering Winter Annual Meeting, Los Angeles, pp. 31-46.

Tong, L. S. 1972a, Boiling Crisis and Critical Heat Flux, United States Atomic Energy Commission Report Technical Information Department 25887.

Tong, L. S. 1972b, Heat Transfer Mechanisms in Nucleate and Film Boiling, *Nucl. Eng. Des.* vol. 21, pp. 1-25.

Tong, L. S. 1975, A Phenomenological Study of Critical Heat Flux, American Society of Mechanical Engineering Report ASME 75-HT-68.

Tong, L. S. and G. F. Hewitt 1972, Overall Viewpoint of Flow Boiling CHF Mechanisms, American Society of Mechanical Engineering Report ASME 72-HT-54.

Tong, L. S., and J. Weisman 1979, *Thermal Analysis of Pressurized Water Reactors*, Second edition, American Nuclear Society, La Grange Park, Illinois.

Tong, L. S., and J. D. Young 1974, A Phenomenological Transition and Film Boiling Heat Transfer Correlation, *Fifth Int. Heat Transfer Conf.*, Tokyo, vol. IV, B3.9.

Weisman, J., and R. W. Bowring 1975, Methods for Detailed Thermal and Hydraulic Analysis of Water-Cooled Reactors, *Nucl. Sci. Eng.* vol. 57, pp. 255-276.

Whalley, P. B. 1974, The Calculation of Dryout in a Heated Annulus, Atomic Energy Research Establishment report AERE-M-266.

Whalley, P. B. 1978, The Calculation of Dryout in a Rod Bundle - A Comparison of Experimental and Calculated Results, Atomic Energy Research Establishment Report AERE-R-8977.

Whalley, P. B., P. Hutchinson, and G. F. Hewitt 1975, Prediction of Annular Flow Parameters for Transient Conditions and for Complex Geometries, *European Two-Phase Flow Group Meeting*, Haifa, Israel.

Whalley, P. B., P. Hutchinson, and P. W. James 1978, The Calculation of Critical Heat Flux in Complex Situations Using an Annular Flow Model, *6th Int. Heat Transfer Conf.*, Toronto, vol. 5, pp. 65-70.

Wright, R. M. 1961, Downflow Forced Convection Boiling of Water in Uniformly Heated Tubes, United States Atomic Energy Commission University of California Radiation Laboratory Report 9744.

Yamanouchi, A. 1968, Effect of Core Spray Cooling in Transient State After Loss of Coolant Accident, *J. Nucl. Sci. Tech.* vol. 5, p. 547.

Yao, S. C., and R. E. Henry 1978, An Investigation of the Minimum Film Boiling Temperature on Horizontal Surfaces, *J. Heat Transfer* vol. 100, pp. 260-267.

Yao, S. C., L. E. Hochreiter, and W. J. Leech 1982, Heat Transfer Augmentation in Rod Bundles Near Grid Spacers, *J. Heat Transfer* vol. 104, pp. 76-81.

Zuber, N., M. Tribus, and J. W. Westwater 1961, The Hydrodynamic Crisis in Pool Boiling of Saturated and Subcooled Liquids, *International Developments in Heat Transfer*, Part II, No. 27, Int. Heat Transfer Conf., Boulder, Colorado, published by American Society of Mechanical Engineers, New York, pp. 230-236.

# MULTIPHASE SCIENCE AND TECHNOLOGY

## Volume 2

*Edited by*

**G. F. Hewitt**

Thermal Hydraulics Division  
U.K. Atomic Energy Authority  
Harwell Laboratory, England  
and

Department of Chemical Engineering and Chemical Technology  
Imperial College of Science and Technology  
London, England

**J. M. Delhay**

Centre d'Etudes Nucléaires de Grenoble  
Service des Transferts Thermiques  
Grenoble, France

**N. Zuber**

Division of Reactor Safety Research  
U.S. Nuclear Regulatory Commission  
Washington, D.C., U.S.A.

● **HEMISPHERE PUBLISHING CORPORATION**

A subsidiary of Harper & Row, Publishers, Inc.

Washington    New York    London

**DISTRIBUTION OUTSIDE NORTH AMERICA**

**SPRINGER-VERLAG**

Berlin    Heidelberg    New York    Tokyo

## **MULTIPHASE SCIENCE AND TECHNOLOGY, Volume 2**

Copyright © 1986 by Hemisphere Publishing Corporation. All rights reserved. Printed in the United States of America. Except as permitted under the United States Copyright Act of 1976, no part of this publication may be reproduced or distributed in any form or by any means, or stored in a data base or retrieval system, without the prior written permission of the publisher.

1 2 3 4 5 6 7 8 9 0 B C B C 8 9 8 7 6

### **Library of Congress Cataloging in Publication Data**

(Revised for volume 2)

Main entry under title:

Multiphase science and technology.

Includes bibliographies and indexes.

1. Vapor-liquid equilibrium—Addresses, essays, lectures.
2. Ebullition—Addresses, essays, lectures.
3. Cooling—Addresses, essays, lectures. I. Hewitt, G. F. (Geoffrey Frederick) II. Delhay, J. M. date. III. Zuber, N.

TP156.E65M84 660.2'96 81-4527

ISBN 0-89116-283-8 (v. 2) Hemisphere Publishing Corporation

ISSN 0276-1459

### **DISTRIBUTION OUTSIDE NORTH AMERICA:**

ISBN 3-540-16408-1 Springer-Verlag Berlin